T.R.
GEBZE TECHNICAL UNIVERSITY
GRADUATE SCHOOL OF NATURAL AND APPLIED SCIENCES

STYRENE-BASED STAR-SHAPED POLYMERS: SYNTHESIS AND APPLICATIONS AS FLUORESCENT PROBES

ENİS TAŞCI
A THESIS SUBMITTED FOR THE DEGREE OF
DOCTOR OF PHILOSOPHY
DEPARTMENT OF CHEMISTRY

GEBZE
2018

T.R.

GEBZE TECHNICAL UNIVERSITY

GRADUATE SCHOOL OF NATURAL AND APPLIED SCIENCES

STYRENE-BASED STAR-SHAPED POLYMERS: SYNTHESIS AND APPLICATIONS AS FLUORESCENT PROBES

ENİS TAŞCI

A THESIS SUBMITTED FOR THE DEGREE OF DOCTOR OF PHILOSOPHY

DEPARTMENT OF CHEMISTRY

THESIS SUPERVISOR

PROF. DR. AYŞE GÜL GÜREK

II. THESIS SUPERVISOR

ASSOC. PROF. DR. MEHMET ATİLLA TAŞDELEN

GEBZE

2018

T.C.
GEBZE TEKNİK ÜNİVERSİTESİ
FEN BİLİMLERİ ENSTİTÜSÜ

STİREN-TABANLI YILDIZ-ŞEKİLLİ POLİMERLER: FLORESANS PROB OLARAK SENTEZ VE UYGULAMALARI

ENİS TAŞCI

DOKTORA TEZİ
KİMYA ANABİLİM DALI

DANIŞMANI
PROF. DR. AYŞE GÜL GÜREK

II. DANIŞMAN
DOÇ. DR. MEHMET ATİLLA TAŞDELEN

GEBZE
2018

GEBZE TEKNİK ÜNİVERSİTESİ	DOKTORA JÜRİ ONAY FORMU

GTÜ Fen Bilimleri Enstitüsü Yönetim Kurulu'nun 03/01/2018 tarih ve 2018/02 sayılı kararıyla oluşturulan jüri tarafından 22/01/2018 tarihinde tez savunma sınavı yapılan Enis TAŞCI 'nın tez çalışması Kimya Anabilim Dalında DOKTORA tezi olarak kabul edilmiştir.

JÜRİ

ÜYE (TEZ DANIŞMANI)	: Prof. Dr. Ayşe Gül GÜREK
ÜYE	: Prof. Dr. Hayal Bülbül SÖNMEZ
ÜYE	: Doç. Dr. Hakan DURMAZ
ÜYE	: Yrd. Doç. Dr. İlke ANAÇ
ÜYE	: Yrd. Doç. Dr. Erdinç DOĞANCI

ONAY

Gebze Teknik Üniversitesi Fen Bilimleri Enstitüsü Yönetim Kurulu'nun

...../...../..... tarih ve ...../..... sayılı kararı.

SUMMARY

In this thesis, it is intended that synthesis of star-shaped styrene copolymers with different amounts of pyrene side groups and use as chemical probes towards nitroaromatic compounds. In addition, it is aim that synthesis of linear styrene copolymers with pyrene side groups for topology effect investigation in the optical sensor application towards to nitroaromatic compounds.

For this purpose, firstly novel alkoxyamine compounds (**2**,**4** and **6**) that are to be used as unimolecular initiators in nitroxy mediated radical polymerization (NMP) method which is a controlled polymerization method, were synthesized. Then, in the presence of unimolecular initiator compounds, star-shaped polymers with chloride side groups were synthesized by the NMP of styrene and vinylbenzyl chloride monomers with different monomer feed ratios. Chloride functional units of the obtained star polymers were converted into azide functional groups. Finally, styrene star-shaped copolymers with pyrene side groups were synthesized using "click" chemistry technique, which is a very effective functionalization method. Also, linear styrenic copolymers were synthesized using the same synthesis strategy like star-shaped ones to study the differences in optical chemical sensor applications against nitroaromatic compounds. The obtained styrene polymers were used as a chemical probe towards to nitroaromatic compounds.

The chemical structures of the synthesized polymers were analyzed by FTIR and ^{1}H NMR spectroscopy. Their thermal properties were also investigated by the differential scanning calorimeter (DSC) and thermogravimetric analysis (TGA) experiments. The average molecular weight of the polymers was determined by gel permeation chromatography (GPC) technique. Moreover, the fluorescence sensor properties of the polymers were examined by the fluorescence spectrophotometer.

Key Words: Click Chemistry, Pyrene, Nitroaromatic Compounds, Fluorescence sensing, Star-shaped polymers, Nitroxide Mediated Radical Polymerization.

ÖZET

Bu tez çalışmasında farklı oranlarda piren yan gruplarına sahip yıldız-şekilli stirenik kopolimerlerin sentezlemesi ve nitroaromatik bileşiklere karşı optik kimyasal sensör uygulamalarında kullanılması amaçlanmaktadır. Ayrıca, nitroaromatik bileşiklere karşı optik kimyasal sensör uygulamalarında topoloji etkisini incelemek için piren yan gruplarına sahip lineer stiren kopolimerlerinin de sentezlenmesi amaçlanmaktadır.

Bu amaçla tüm polimerler için öncelikle kontrollü bir polimerleşme yöntemi olan Nitroksit Aracılı Radikal Polimerizasyonunda (NMP) unimoleküler başlatıcı olarak kullanılacak alkoksiamin bileşikleri (**2**,**4** ve **6**) sentezlendi. Sonrasında, stiren ve vinilbenzil klorür monomerleri kullanılarak NMP yöntemi ile klorür (-Cl) yan gruplarına sahip stiren polimeri sentezlendi. Elde edilen polimerlerin klorür yan grupları sodyum azidür ile azidür ($-N_3$) gruplarına dönüştürüldü. Son adımda ise azidür yan gruplarına sahip stiren polimerleri 1-etinil piren kullanılarak oldukça etkili bir fonksiyonlandırma yöntemi olan tıkla (click) kimyası tekniğiyle piren grupları ile fonksiyonlandırıldı ve piren yan gruplarına sahip stiren yıldız-şekilli kopolimerleri elde edildi. Yine aynı strateji kullanılarak nitroaromatik bileşiklere karşı optik kimyasal sensör uygulamalarında topoloji farkını incelemek için yeni bir NMP başlatıcısı ile lineer stiren kopolimerleri sentezlendi. Elde edilen stiren polimerleri nitroaromatik bileşiklere karşı optik kimyasal sensör uygulamalarında kullanıldı.

Sentezlenen polimerlerin yapıları FTIR ve ^{1}H NMR spektroskopisi ile aydınlatıldı. Termal özellikleri diferansiyel taramalı kalorimetre (DSC) ve termogravimetrik analiz (TGA) ile tespit edildi. Polimerlerin ortalama molekül ağırlıkları jel geçirgenlik kromatografisi (GPC) teknikleri ile belirlendi. Ayrıca, polimerlerin floresans sönsör özellikleri floresans spektrofotometre ile incelendi.

Anahtar Kelimeler: Click Kimyası, Floresans Sensör, Piren, Nitroaromatik Bileşikler, Yıldız-şekilli polimerler, Nitroksit Aracılı Radikal Polimerizasyonu.

ACKNOWLEDGEMENTS

I am truly grateful to those who provided me with assistance during my PhD studies. I would like to sincerely and gratefully thank my supervisors for his guidance and patience in my research. I am also grateful to the other members of my PhD committee, and the Chemistry Department Lab mates for their helpful suggestions.

I would like thank the Scientific and Technological Research Council of Turkey (TUBITAK) for financial support which enabled me to carry out this work (Grant number:115Z742).

Finally, I am grateful to my wife for during all stages involved in the preparation of this thesis. I also acknowledge my mother, father and sister for their encouragement and support throughout my education. This accomplishment would not have been possible without their unconditional love, support and prayers.

TABLE of CONTENTS

LIST of ABBREVIATIONS and ACRONYMS

Abbreviations and Acronyms		**Explanations**
NMP	:	Nitroxide Mediated Polymerization
BPO	:	Benzoyl Peroxide
AIBN	:	Azobisisobutyronitrile
NAC	:	Nitroaromatic Compound
TNT	:	2,4,6-Trinitrotoluene
PA	:	Picric Acid
DNT	:	2,4-Trinitrotoluene
NT	:	4-Nitrotoluene
DNP	:	2,4-Dinitrophenol
TNP		2,4,6-Trinitrophenol
NP	:	4-Nitrophenol
CH_2Cl_2	:	Dichloromethane
CuBr	:	Copper Bromide
$CDCl_3$	:	Chloroform
DCM	:	Dichloromethane
THF	:	Tetrahydrofuran
DMSO-d_6	:	Dimethyl sulfoxide-d6
MeOH	:	Methanol
FTIR	:	Fourier Transform Infrared Spectroscopy
NMR	:	Nuclear Magnetic Resonance Spectroscopy
TGA	:	Thermogravimetric Analysis
DSC	:	Differential Scanning Calorimetry
GPC	:	Gel Permeation Chromatography
ESI-MS	:	Electron Spray Ionization Mass Spectroscopy
HR-MS	:	High Resolution Mass Spectroscopy
LC-MS		Liquid Chromatography Mass Spectroscopy
HCl	:	Hydrochloric acid
$MgSO_4$	:	Magnesium Sulfate
TEMPO	:	2,2,6,6-tetramethyl-1-piperidinyloxy

CLRP	:	Controlled Living Radicalic Polymerization
DMF	:	*N*,*N*-Dimetilformamide
NaN_3	:	Sodium azide
$NaHCO_3$	:	Sodium bicarbonate
$NaCO_3$	:	Sodiumicarbonate
K_2CO_3	:	Potassium carbonate
St	:	Styrene
VBC	:	4-Vinylbenzyl chloride
TEA	:	Triethylamine
PMDETA	:	N,N,N′,N″,N″- Pentamethyldiethylenetriamine
Tg	:	Glass Transition Temperature

LIST of FIGURES

LIST of TABLES

1. INTRODUCTION

1.1. Thesis Overview

Production of polymers with the desired molecular architecture and molecular weight distribution has been one of the most important issues of macromolecular chemistry. Nitroxide mediated radical polymerization (NMP) is a prominent technique among controlled/living radical polymerization (CLRP) techniques and still stays attractive for the researchers at the present time. This polymerization method does not require metal catalysts which are very difficult to get rid of them. Besides, it is tolerant to variety of functional groups and allows easy purification of the polymerization products. NMP method can be carried out in two ways as uni- and bimolecular. In the bimolecular way, in order to ensure controlled progression of the polymerization, free stable nitroxide counter radical (co-radical) derivatives are used together with radical initiators (BPO, AIBN and etc.). On the other hand, in the unimolecular way, thermally homolitic cleavage of alkoxyamine groups is to provide carbon radical and nitroxide counter radical in order to initiate polymerization. The unimolecular method is more preferred due to lack of side reactions (between nitroxide radical and initiator) which may affect the nitroxide and initiator concentrations as it happens in the bimolecular way. Thereby, the unimolecular way offers better control over the polymerization. Styrene and styrene derivatives can be polymerized easily with NMP [1-12].

The nitroaromatic compounds (NACs) contain both nitro group and aromatic ring. The fast and selectively detection of the nitroaromatic compounds has enormous importance due to their explosive properties. The NACs have been widely employed to produce various explosives to be used in military operations, mining and construction industry [13-18]. 2,4,6-Trinitrotoluene (TNT) has been the most commonly used NAC as an explosive. Although picric acid (PA) has comparable explosive properties to TNT, rather, it has been widely used in the manufacturing of dyes, rocket fuels, pharmaceuticals, and firework [19-21]. Because of its widespread use and solubility in water, PA is a major contaminant for ground water, soil, biological species [22]. Exposure to PA, due to its nitro and phenol functional units, has been known to result in skin and eye irritation, dizziness, nausea, gastritis, liver malfunction, anaemia, cancer and cyanosis [19-21,23]. Therefore, simple, cheap,

selective and sensitive detection of PA is of crucial importance in terms of prevention of environmental pollution and security concerns [24-25]. Also, the nitroaromatic compounds are known as environmental pollutant. The nitroaromatic compounds are often used in either construction industry or military field. Their use causes accumulation in the environment by time. Thus, the pollution in such environment and the contamination of nearby water sources can arise. The US Environmental Protection Agency has set the maximum level of trinitrotoluene (TNT) for drinking water at 2 ppb [26]. In return, the concentration can rise up to 500 ppb in the water and 1000-5000 ppm in the earth. Since PA is highly soluble in water, it can easily contaminate soil and ground water. Therefore, detection or recognition of PA with help of fluorescent chemosensors is highly significant [21,27].

The fluorescense chemosensors are more advantageous than other kind of sensors owing to their fast response time, high sensitivity, selectivity and allowing real time measurements. Among those, the macromolecules including pyrene attract great attention as fluorescence probes owing to their long fluorescence lifetime and well characterized fluorescence spectrums [28-30].

In this thesis, star-shaped styrene copolymers with different amounts of pyrene side groups were synthesized and used as chemical probes towards nitroaromatic compounds. For this purpose, firstly alkoxyamine compound that was to be used as unimolecular initiator in NMP was synthesized. Then, in the presence of unimolecular initiator compound, star-shaped polymers with chloride side groups was synthesized by the NMP of styrene and vinylbenzyl chloride monomers with different monomer feed ratios. Chloride functional units of the obtained star polymers was converted into azide functional groups. Finally, styrenic star-shaped copolymers with pyrene side groups was synthesized by 1,3-dipolar cycloaddition (click) reaction between azide functional groups of the precursor polymer and 1-ethynyl pyrene. Linear styrenic copolymers was synthesized using the same synthesis strategy like star-shaped ones to study the differences in optical chemical sensor applications against nitroaromatic compounds.

The chemical structures of the synthesized polymers were analyzed by FTIR and ^{1}H NMR. Their thermal properties were investigated by the differential scanning calorimeter (DSC) and thermogravimetric analysis (TGA) experiments. The average molecular weights of the polymers were determined by gel permeation

chromatography (GPC) technique. Moreover, the fluorescence sensor properties of the polymers were examined by the fluorescence spectrophotometer.

2. THEORETICAL PART

2.1. Fluorescence Spectroscopy

Fluorescence spectroscopy is one of the oldest analytical methods. This technique can be used in medicine, pharmaceutics, biology and chemistry. The method of determination based on the fluorescence property of substance is called fluorescence spectroscopy. With this method, many substances can be determined with a precision under one millionth [31-32].

Fluorescence spectroscopy has many advantages to the other analytical methods related to sensitivity, selectivity, and response time [33-34]. Therefore, fluorescence chemosensors were used for the detection of various analytes such as cations, anions, nitroaromatics, biological entities, etc [35].

Absorption of light by a molecule causes the excitation of an electron. The electron moves from a ground state to an excited state. Each of these electronic states may include a number of different vibrational levels. Absorption of light is from the lowest electronic vibrational state to a number of vibrational levels in the excited electronic state. After the electron has been excited, it rapidly relaxes from the highest vibrational states to the lowest vibrational state of the excited electronic state. The rate for this relaxation is on the order of picoseconds. After returning to the lowest vibrational state of the excited electronic state, the electron in the excited state can pass the ground state by a number of different processes. The system can loose the energy by internal conversion (heat), quenching (external conversion), emission of photon (fluorescence), or intersystem crossing (phosphorescence) [32].

Fluorescence occurs generally in aromatic molecules which have conjugated π electrons in their structures. To investigate the spectroscopy of a molecule, emission spectrum of it is plotted by fluorescence intensity versus wavelength (nm) or wavenumber (cm-1). Emission spectra change with the chemical structure of the molecules and the solvent used for solvation [36].

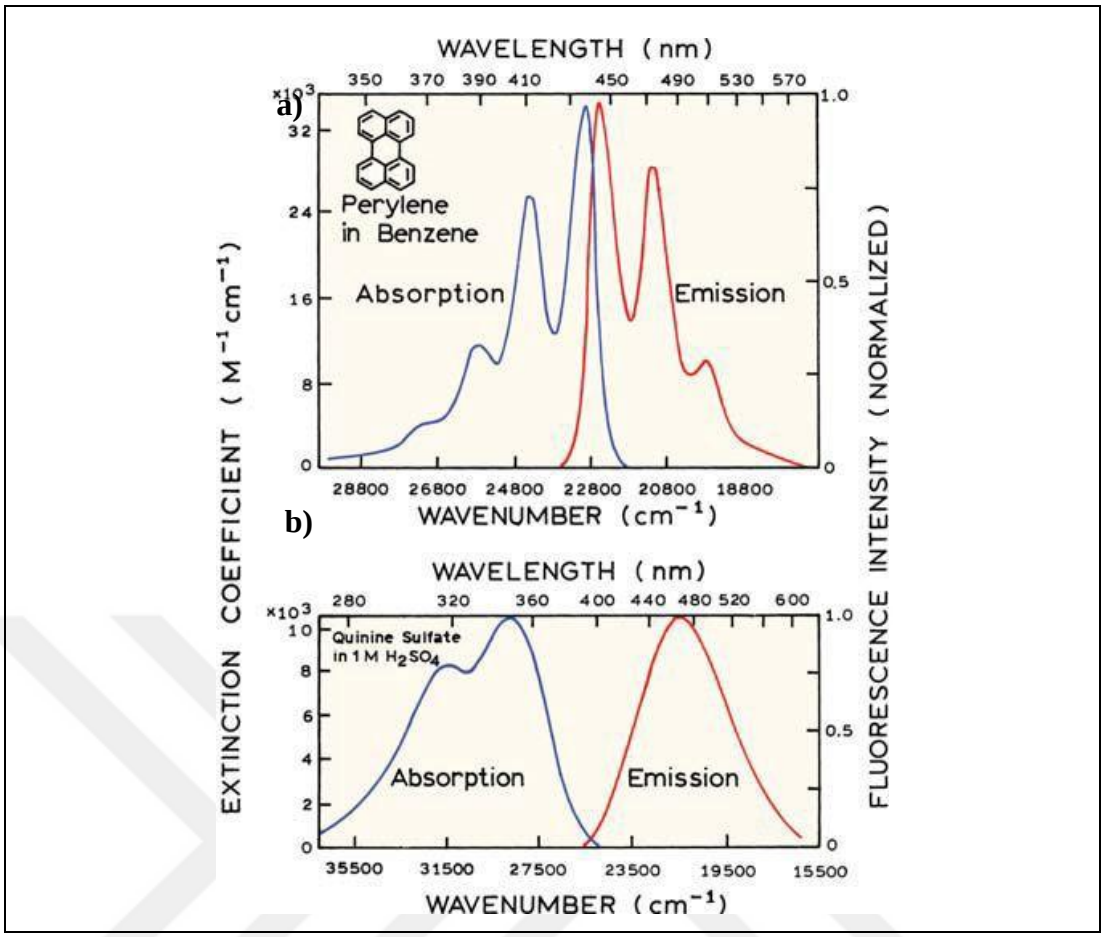

Figure 2.1: Absorption and fluorescence emission spectra of a) perylene, b) quinine sulfate.

2.2. Limunescence

Luminescence is the emission of ultraviolet, visible or infrared light from the electronically excited states. The word luminescence, which comes from the Latin (lumen = light) was first introduced as luminescenz by the physicist and science historian Eilhardt Wiedemann in 1888, to describe "all those phenomena of light which are not solely conditioned by the rise in temperature," as opposed to incandescence. Luminescence is often considered as cold light whereas incandescence is hot light. Different excitation modes correspond to different types of luminescence (Table 2.1).

Table 2.1: The various types of luminescence.

Phenomenon	Mode of Excition
Photoluminescence (fluorescence, phosphorescence, delayed fluorescence)	Absorption of light (photons)
Radioluminescence	Ionizing radiation (X-rays, α, β, γ)
Cathodoluminescence	Cathode rays (electron beams)
Electroluminescence	Electric field
Thermoluminescence	Heating after prior storage of energy (e.g., radioactive irradiation)
Chemiluminescence	Chemical reaction (e.g., oxidation)
Bioluminescence	In vivo biochemical reaction
Triboluminescence	Frictional and electrostatic forces
Sonoluminescence	Ultrasound

Luminescence is more precisely defined as follows: spontaneous emission of radiation from an electronically excited species or from a vibrationally excited species not in thermal equilibrium with its environment [37]. The various types of luminescence are classified according to the mode of excitation (see Table 2.1).

Luminescent compounds can be of very different kinds:

Organic compounds: aromatic hydrocarbons (naphthalene, anthracene, phenanthrene, pyrene, perylene, porphyrins, phtalocyanins, etc.) and derivatives, dyes (fluorescein, rhodamines, coumarins, oxazines), polyenes, diphenylpolyenes, some amino acids (tryptophan, tyrosine, phenylalanine), etc.

Inorganic compounds: uranyl ion (UO_2^+), lanthanide ions (e.g., Eu_3^+, Tb_3^+), doped glasses (e.g., with Nd, Mn, Ce, Sn, Cu, Ag), crystals (ZnS, CdS, ZnSe, CdSe, GaS, GaP, Al_2O_3/Cr_3^+ (ruby)), semiconductor nanocrystals (e.g., CdSe), metal clusters, carbon nanotubes and some fullerenes, etc.

Organometallic compounds: porphyrin metal complexes, ruthenium complexes (e.g., $Ru(bpy)_3^{2+}$), copper complexes, complexes with lanthanide ions, complexes with fluorogenic chelating agents (e.g., 8-hydroxy-quinoline, also called oxine), etc.

Fluorescence and phosphorescence are particular cases of luminescence (Table 2.1). The mode of excitation is absorption of one or more photons, which brings the absorbing species into an electronic excited state. The spontaneous emission of

photons accompanying de-excitation is then called photoluminescence which is one of the possible physical effects resulting from interaction of light with matter, as shown in Figure 2.2. Stimulated emission of photons can also ocur under certain conditions. Additional processes, not shown, can take place for extremely high intensities of radiation, but are not relevant for luminescence studies.

If the excitation is occurred with the absorption of light, the process is called photoluminescence. Once a molecule is excited to an electronic state by absorption of a photon, it can return to the ground state with emission of light, which is one of the possible physical effects resulting from interaction of light with matter, as shown in Figure 2.2.

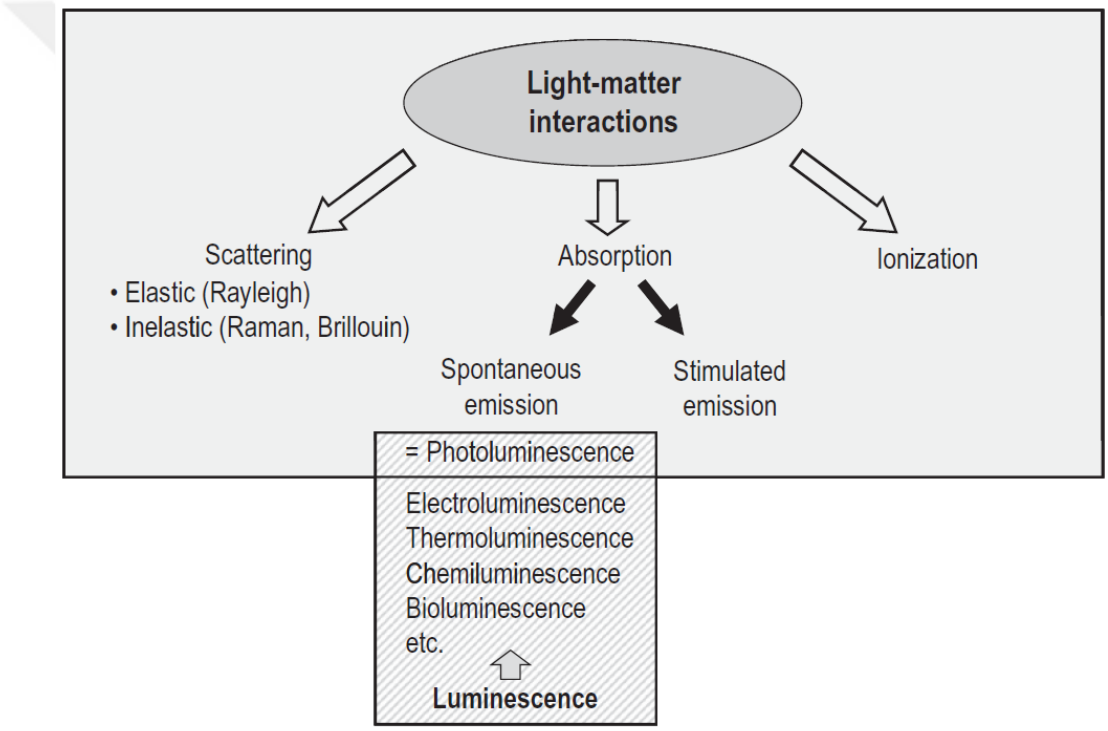

Figure 2.2: Position of photoluminescence in the frame of light–matter interactions.

Luminescence is the term to describe the process in which electronically excited molecules emit a light. Depending on the nature of the excited state, it is divided into two categories, fluorescence and phosphorescence. If the excited electron is paired to the second electron which is in the ground state orbital by opposite spin, molecules emit a photon when returning to the ground state. This process is called as fluorescence and typical fluorescence lifetime is near 10 ns (10^{-9} s). In phosphorescence mechanism, light emission occurs from excited triplet state. In this excited state, electron is paired

to the second electron by same spin. Unlike the fluorescence mechanism, transitions to the ground state are forbidden and because of that emission related to that, lifetimes are longer than the former one, they are typically milliseconds to seconds. Schematic representations of ground state, excited singlet state and excited triplet state are given in Figure 2.3.

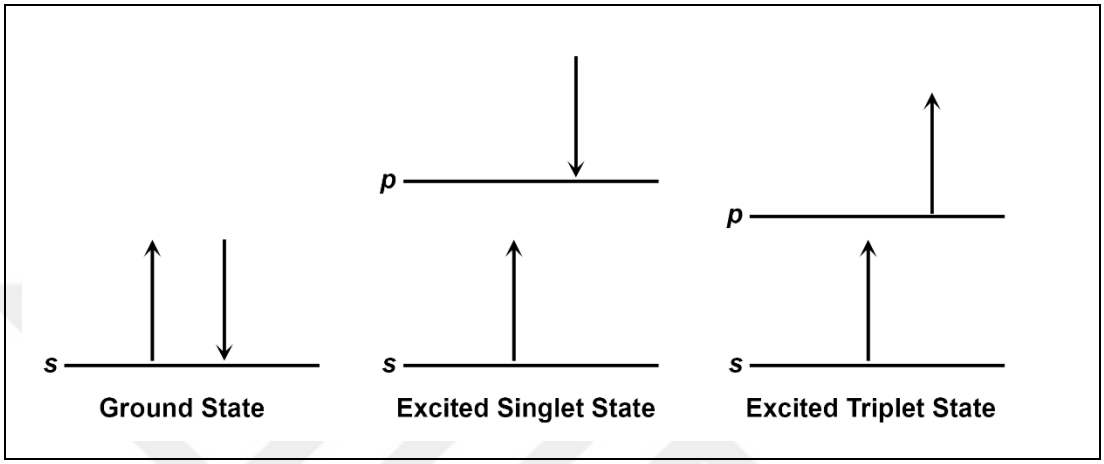

Figure 2.3: Schematic represantations of ground state, excited singlet state and excited triplet state.

2.3. Various De-Excitation Processes of Excited Molecules

Once a molecule is excited by absorption of a photon, it can return to the ground state with emission of fluorescence, or phosphorescence after intersystem crossing, but it can also undergo intramolecular charge transfer and conformational change. Interactions in the excited state with other molecules may also compete with de-excitation: electron transfer, proton transfer, energy transfer, excimer or exciplex formation (Figure 2.4). These de-excitation pathways may compete with fluorescence emission if they take place on a time-scale comparable with the average time (lifetime) during which the molecules stay in the excited state. This average time represents the experimental time window for observation of dynamic processes. The characteristics of fluorescence (spectrum, quantum yield and lifetime), which are affected by any excited-state process involving interactions of the excited molecule with its close environment, can then provide information on such a microenvironment. It should be noted that some excited-state processes (conformational change, electron transfer, proton transfer, energy transfer, excimer or exciplex formation) may lead to a

fluorescent species whose emission can superimpose that of the initially excited molecule. Such an emission should be distinguished from the "primary" fluorescence arising from the excited molecule. The success of fluorescence as an investigative tool in studying the structure and dynamics of matter or living systems arises from the high sensitivity of fluorometric techniques, the specificity of fluorescence characteristics due to the microenvironment of the emitting molecule, and the ability of the latter to provide spatial and temporal information. Figure 2.5 shows the physical and chemical parameters that characterize the microenvironment and can thus affect the fluorescence characteristics of a molecule.

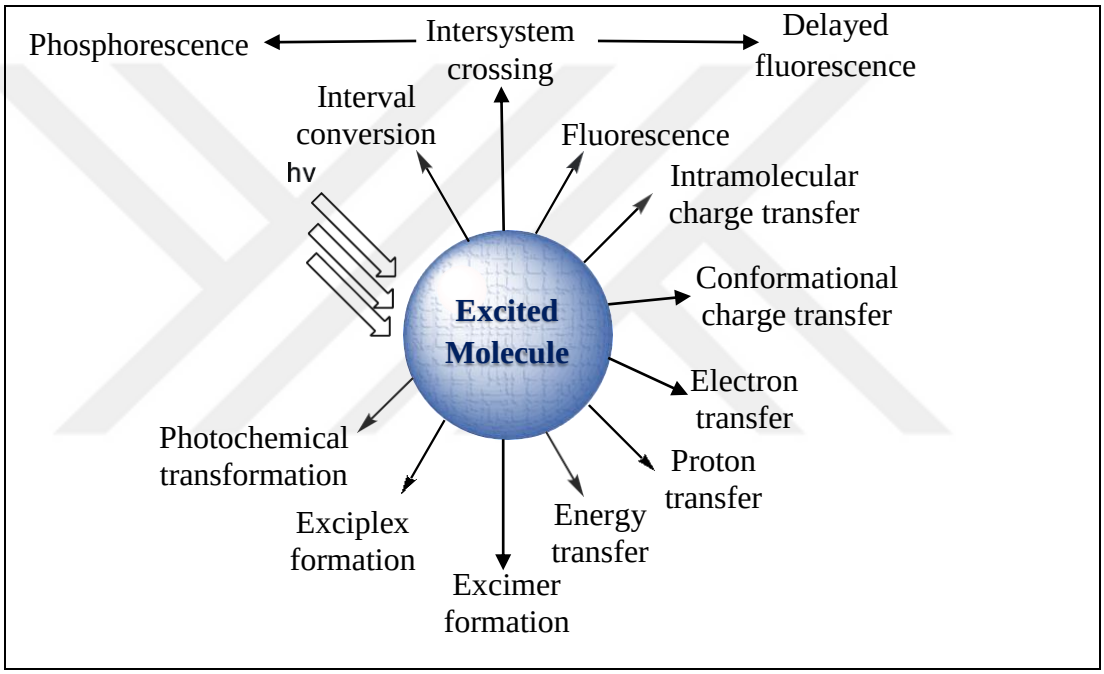

Figure 2.4: Possible de-excitation pathways of excited molecules.

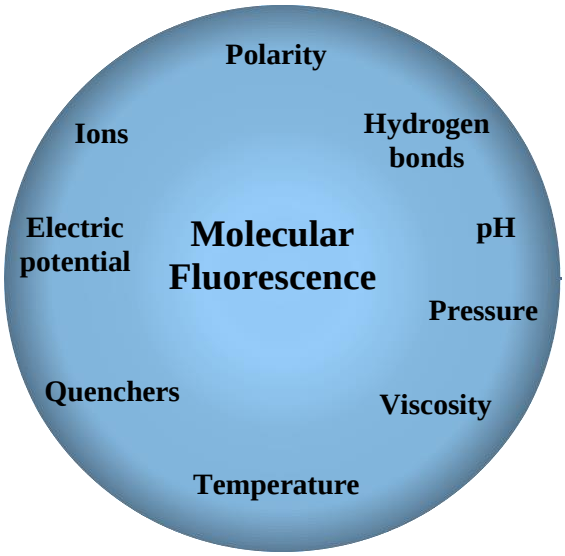

Figure 2.5: Various parameters influencing the emission of fluorescence.

2.4. Jablonski Diagram

Jablonski Diagrams, which are named after Professor Alexander Jablonski, demonstrate the processes that occur between the absorption and emission of light. To illustrate absorption and emission processes, a typical Jablonski diagram which is given in Figure 2.6 is used. It represents the processes that can occur in the excited state. S0, S1, and S2 represent the ground, first and second electronic states, respectively. These electronic states include some vibrational levels numbered like 0, 1, 2, etc. Vertical lines show the transitions between states. An upward arrow means that the atom absorbed light and a downward arrow means that light is emitted from the atom [36].

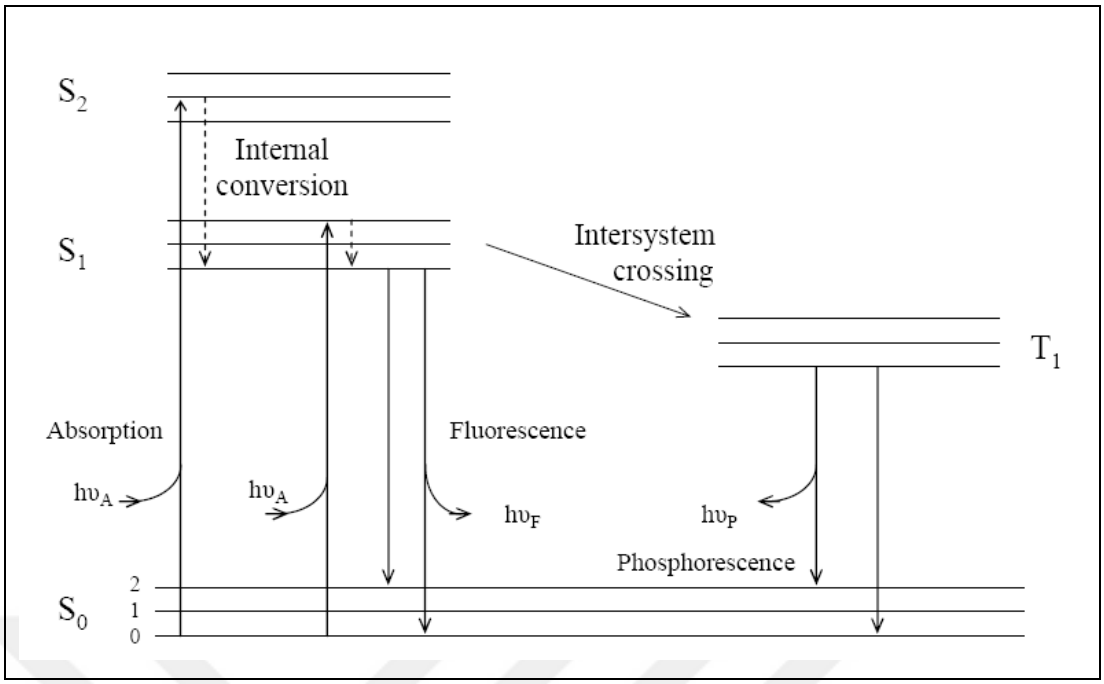

Figure 2.6: One form of a Jablonski diagram.

After the absorption of light, there occurs different processes. The electrons are excited to S_1 or S_2 states however in most cases the electron in S_2 state quickly passes to vibrational S_1 state. This process is called internal conversion and generally occurs within 10^{-12} s which is less than typical fluorescence lifetime, 10^{-8} s after turning back to S_1 state, the electrons can follow two steps. Firstly, the electron can directly pass to a higher excited vibrational ground state at the level of S_0 state and emits a photon. This is the fluorescence process. Secondly, instead of immediately turning back to S_0 state, it goes to the first triplet state T_1 providing a spin conversion and turns back to the S_0 state. This transition from S_1 to T_1 is called intersystem crossing. Emission from T_1 is called phosphorescence, and phosphorescence produces longer wavelenghts compared to the fluorescence [38].

Also Figure 2.7 showed in detail Jablonski diagram and illustration of the relative positions of absorption, fluorescence, and phosphorescence spectra. Jablonski diagram is convenient for visualizing in a simple way the possible processes: photon absorption, internal conversion, fluorescence, intersystem crossing, phosphorescence, delayed fluorescence, and triplet–triplet transitions. The singlet electronic states are denoted by S_0 (fundamental electronic state), S_1, S_2, . . . and the triplet states, T_1, T_2, … Vibrational levels are associated with each electronic state. It is important to note that absorption is very fast ($\approx 10^{-15}$ s) with respect to all other processes. The vertical

arrows corresponding to absorption start from the 0 (lowest) vibrational energy level of S_0 because the majority of molecules are in this level at room temperature. Absorption of a photon can bring a molecule to one of the vibrational levels of S_1, S_2, … The subsequent possible de-excitation processes will now be examined. However, it should be noted that most fluorescent molecules exhibit broad and structureless absorption and emission bands, which means that each electronic state consists of an almost continuous manifold of vibrational levels. If the energy difference between the 0 and 1 vibrational levels of S_0 (and S_1) is, for instance, only about 500 cm^{-1}, the ratio N_1/N_0 becomes about 0.09. Consequently, excitation can then occur from a vibrationally excited level of the S_0 state. This explains why the absorption spectrum can partially overlap the fluorescence spectrum [39].

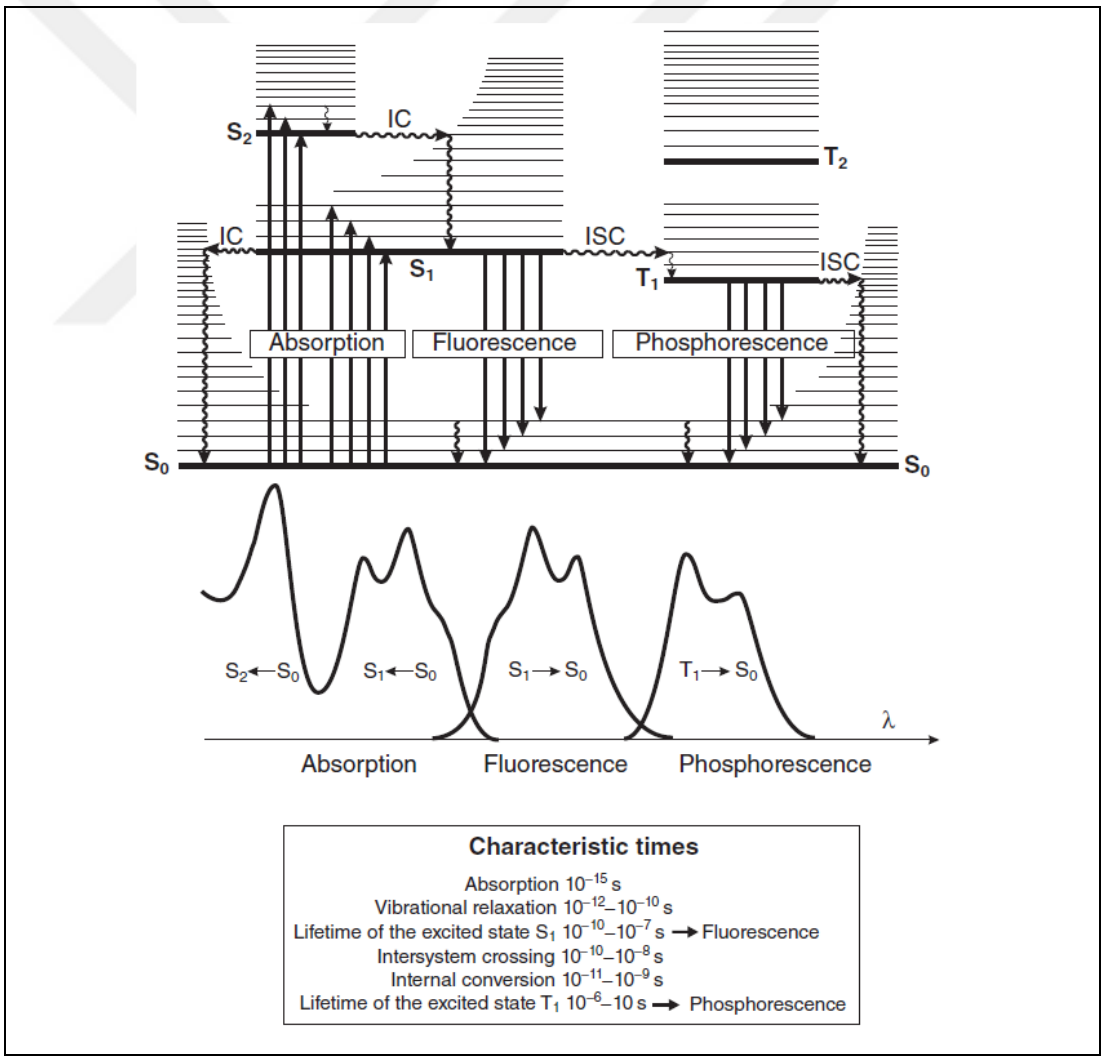

Figure 2.7: Jablonski diagram and illustration of the relative positions of absorption, fluorescence, and phosphorescence spectra.

2.5. Molecular Sensor and Pyrene

Pyrene (Figure 2.8) and its derivatives, with their high quantum yield and chemical stability, are well-studied fluorophores for molecular labeling and fluorescent sensing applications [40-41]. Pyrene has two main emission bands; first one is the emission of pyrene monomers (i.e., distance between molecules is larger than ∼1 nm) between 370 and 400 nm and second is the emission of pyrene excimers (i.e., distance is smaller than ∼1 nm) at around 470 nm [42]. The bright and visible emission of pyrene excimers is particularly interesting because it is very sensitive to the micro-environmental conditions such as temperature, pressure or pH [40]. In addition, the excimer emission can be affected by guest molecules and accordingly it can be used to detect various classes of chemicals including gases, organic molecules and metal ions [43-44]. In particular, pyrene excimer emission can be rapidly quenched via exposure to nitroaromatic explosives and compounds based on electron-transfer between π-π* stacked pyrene molecules and nitroaromatic molecules [45].

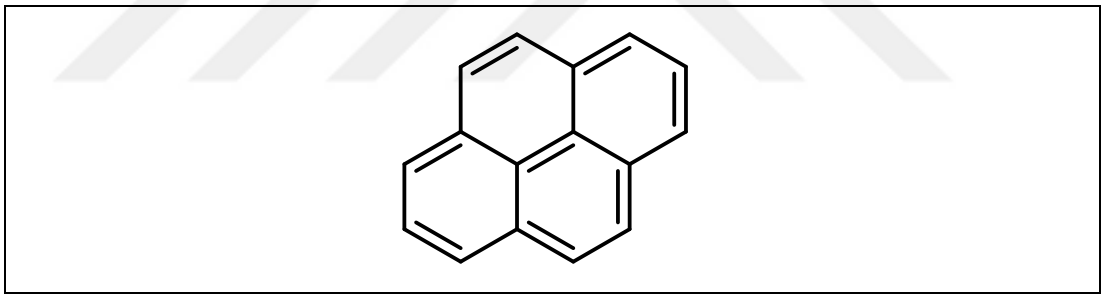

Figure 2.8: Structure of Pyrene.

Pyrene is a fluorescent, polycyclic aromatic hydrocarbon compound. It has been an attractive sensing and probing molecule for an expanded range of application since it has long lifetime and high quantum efficiency. When two pyrene molecules interact via π-π* stacking which is a non-covalent interaction occurring between aromatic molecules, an excimer forms. Pyrene excimers demonstrate high sensitivity to microenvironmental changes [46].

The fluorescence spectrum of pyrene was demonstrated in Figure 2.9. The fluorescence of a singlet excited pyrene molecule is observed at 374, 384 and 394 nm in the spectrum. The interaction of the singlet excited pyrene with an unexcited

pyrene yields an excited dimer. The relaxation of the excited dimer radiates light at a broad wavelength range centered around 470 nm [47]. Pyrene excimers give fast fluorescence response to the molecular changes. Pyrene based aromatic molecules exhibit interesting fluorescence properties because of the efficient excimer formation [48-49].

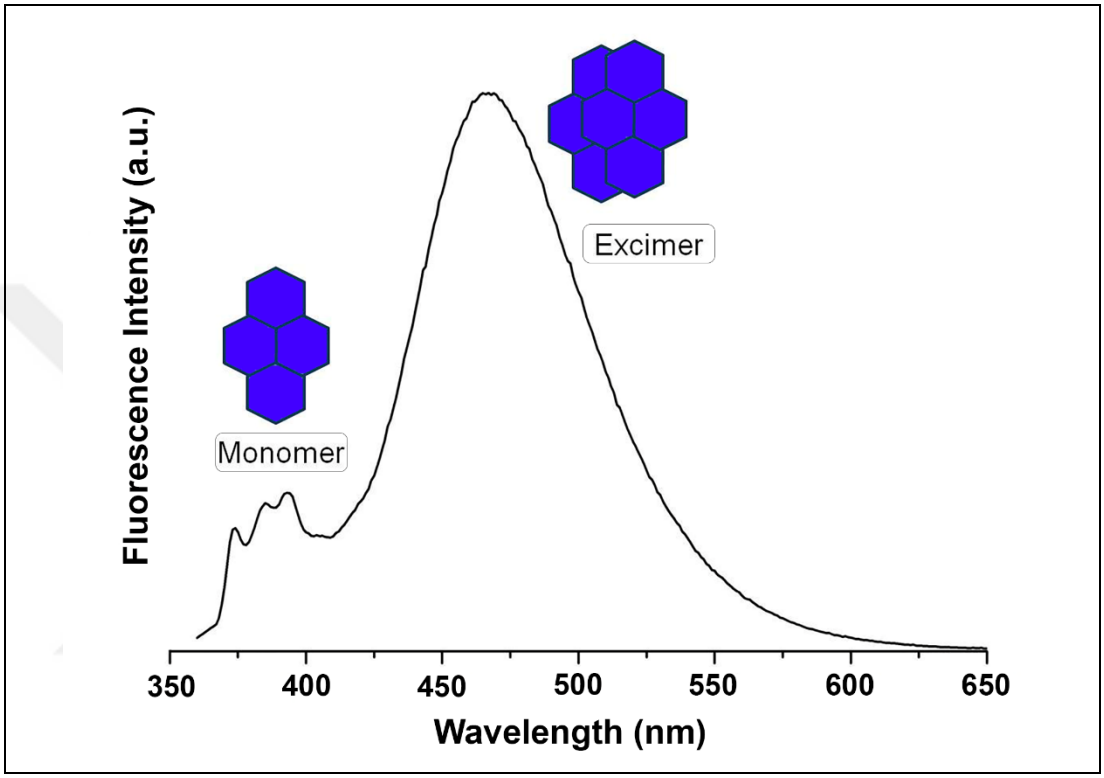

Figure 2.9: Fluorescence spectrum of pyrene showing the monomer and excimer emission of pyrene molecules.

Pyrene-containing macromolecular structures have attracted a great deal of attention to be employed in fluorescent probes [50-53] due to their long fluorescence lifetime and a well defined fluorescence spectrum, which is sensitive to the polarity of the environment [54]. Besides, pyrene and its derivatives have been at the focus of scientific attention in the fields of biomedicine to obtain fluorescence-labeled biomolecules [55], opto-electronics (i.e. light-emitting diodes and solar cells) [40] and organic field effect transistors [56] to improve hole transporting ability.

The pyrene molecules could be linked onto the surface of the star-shaped dendrimer-like copolymer by covalent bond. The pyrene-containing star-shaped dendrimer-like copolymer presented unique spherical structure and had advantage over small molecules (pyrene compounds) or linear polymer in avoiding molecular

aggregation. Therefore, the pyrene-containing star-shaped dendrimer-like copolymer is expected to present different thermal and fluorescent properties from those of pyrene compounds or linear polymer [57].

Pyrene attached polymers are prepared for nitroaromatic explosives sensing. As pyrene excimers can interact with nitroaromatic explosives via π-π* stacking and give electron to the electron deficient nitroaromatic explosives such as trinitrotoluene (TNT), fluorescence of pyrene excimer is quenched in the presence of nitroaromatics. The pyrene excimer emission is known to be rapidly quenched by its exposure to NACs based on electron-transfer between pyrene molecules and NAC molecules [24,58].

Pyrene is a very important PAH compound and have been the most frequently used fluorophore to prepare fluorescently labeled polymers [59] due to its outstanding photophysical properties, such as well-defined fluorescence profiles, relatively long emission lifetime (up to τ = 400 ns in non-polar media), [60] environment-sensitive monomer or excimer emissions [54]. Demirel et al. reported a rapid and facile method for the production of fluorescent active pyrene-doped polyethersulfone (Py-PES) thin film and employed in the detection of NACs in vapor phase [45]. On the other hand, the use of fluorescent nanofibers from electrospinning of pyrene/polymer blends, such as pyrene/polyethersulfone [53] and pyrene/polystyrene [52], for the detection of NACs gave very promising results in terms of sensitivity and selectivity due to their high surface area. Senthamizhan et al. prepared highly fluorescent nanofibers from polystyrene copolymer with covalently attached pyrene units and reported that the obtained polymeric nanofiber mat gave selective and sensitive responses towards TNT in in aqueous media, even in the presence of higher concentrations of various heavy metal pollutants, such as Cd^{2+}, Co^{2+}, Cu^{2+}, and Hg^{2+} [61]. He et al. synthesized two poly(pyrene-co-phenyleneethynylene) conjugated polymers with different compositions and prepared casted thin films of these polymers on pretreated glass plate surfaces. Then, they showed that these thin films responded much more sensitively and selectively to the presence of TNT in aqueous phase than the parent polymer (poly(phenyleneethynylene)) did. The enhanced sensitivity of these pyrene-containing conjugated polymers was attributed to more proper matching of the LUMOs (lowest unoccupied molecular orbital) of these polymers with that of TNT molecules [51]. Burattini et al. synthesized a pyrene-pendant copolymer through very facile imidization reaction of poly(maleic anhydride-alt-1-octadecene) with 1-

pyrenemethylamine and reported that its thin films casted on a quartz plate gave very rapid responses to the vapor of 2,5-dinitrobenzonitrile (selected as a model for TNT) and 50% of the initial fluorescence intensity of the film was quenched in almost 15 seconds [50]. Besides, pyrene and its derivatives have been at the focus of scientific attention in the fields of biomedicine to obtain fluorescence-labeled biomolecules [55], opto-electronics (i.e. light-emitting diodes and solar cells) [40] and organic field effect transistors [56] to improve hole transporting ability.

2.6. Luminescence-Based Methods for Explosives Detection

Fluorescence- or luminescence-based methods for explosives detection offer many benefits over other common techniques. For example, fluorescence methods are typically one to three orders of magnitude more sensitive than absorbance-based methods. Although mass-spectral techniques are also common for explosives detection, instruments with the required sensitivity have not been developed as field-ready and user-friendly. Fluorescence methods require only a source and detector, both of which can be incorporated easily into a handheld device for field detection of explosives. Unfortunately, many explosive compounds are not inherently fluorescent. Explosives such as nitramines, nitrate esters, and peroxides have nonconjugated structures that allow efficient vibrational relaxation. Nitroaromatic explosives (Figure 2.10), despite having aromatic structure, don’t fluoresce as a result of the strong electron-withdrawing nature of the nitro substituents. This lack of native fluorescence notwithstanding, many techniques have been proposed in recent years for explosives detection using luminescence-based methods. Several direct techniques have been investigated, such as high-energy excitation methods including gamma resonance technology and x-ray fluorescence.

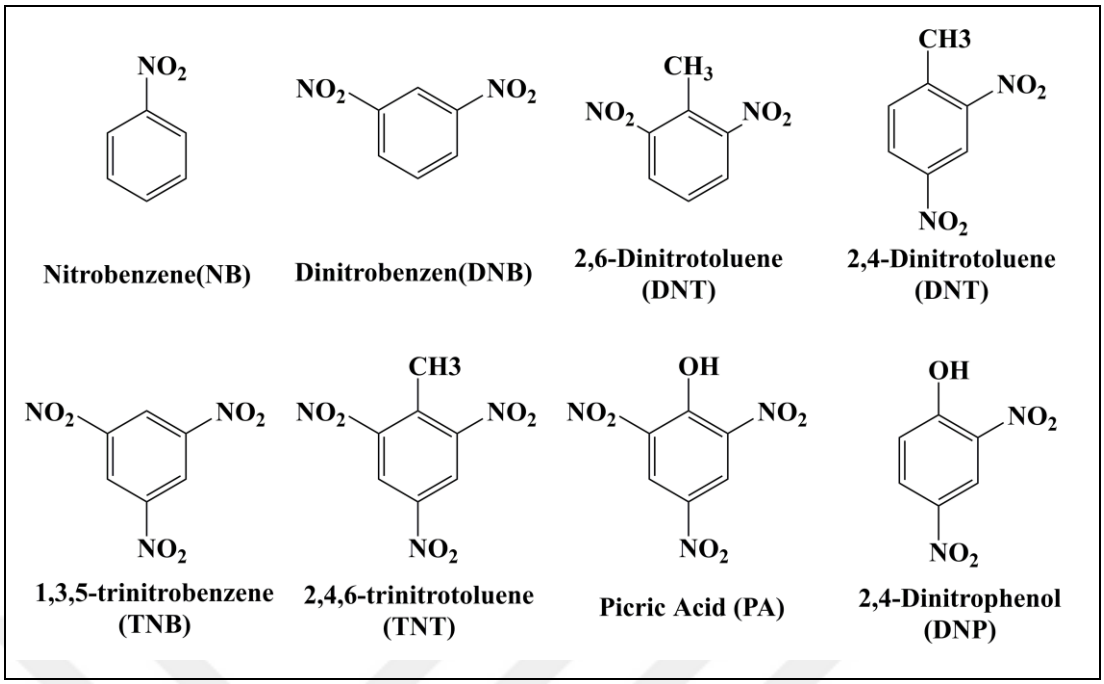

Figure 2.10: Various nitroaromatic compounds.

Other direct methods involve reactions to form fluorescent and chemiluminescent products. Indirect methods have also been used in which the fluorescence of a secondary species is quenched by the explosive. Quenching methods have been utilized with solution-phase, immobilized, and solid-state fluorophores.

A variety of inorganic and organic fluorophores have been studied in the solution phase for fluorescence quenching detection of nitrated explosives. Quenching of pyrene is used as a detection method explosive. Pyrene is a unique fluorophore that exhibits distinct monomer (λ_{mono} = 370−400 nm) and excimer fluorescence (λ_{exc} = 420−600 nm) depending on the distance (d > 1 nm and 0.4 nm < d < 1 nm, respectively) between two pyrene moieties [62]. Many pyrene and pyrene-based molecules and polymers have shown good selectivity and sensitivity for the detection of NACs [25]. The pyrene excimer emission is known to be rapidly quenched by its exposure to NACs based on electron-transfer between pyrene molecules and NAC molecules [24]. Pyrene containing polymers received interest because of their potential use as fluorescent probes [63].

2.7. Nitroxide Mediated Radical Polymerization (NMP)

Nitroxide mediated radical polymerization (NMP) is a prominent technique among controlled/living radical polymerization (CLRP) techniques [64] and still stays attractive for the researchers at the present time. NMP technique that enables the design of well-defined, functional and complex macromolecular architectures [9]. This polymerization method does not require metal catalysts which are very difficult to get rid of. Besides, it is tolerant to variety of functional groups and allows easy purification of the polymerization products. NMP method can be carried out in two ways as uni- and bimolecular. In the bimolecular way, in order to ensure controlled progression of the polymerization, free stable nitroxide counter radical (co-radical) derivatives are used together with radical initiators (BPO, AIBN and etc.). On the other hand, in the unimolecular way, thermally homolitic cleavage of alkoxyamine groups is to provide carbon radical and nitroxide counter radical in order to initiate polymerization. The unimolecular method is more preferred due to lack of side reactions (between nitroxide radical and initiator) which may affect the nitroxide and initiator concentrations as it happens in the bimolecular way. Thereby, the unimolecular way offers better control over the polymerization. Styrene and styrene derivatives can be polymerized easily with NMP [65].

There are several specific cases where NMP has advantages over other CLRP methods. The polymerization of styrene with a radical source and TEMPO is perhaps the simplest way to prepare polystyrene (PS) with a narrow molecular weight distribution, having even been adapted for undergraduate laboratories [66] though the commercial availability of suitable reversible addition-fragmentation chain transfer (RAFT) agents now provides an equally simple alternative. NMP is preferable to atom transfer radical polymerization (ATRP) for systems where the monomer being polymerized can interact with the metal catalyst or when the polymers being prepared must not show any contamination with traces of metal (i.e., in metal-sensitive electronic or biological applications). NMP systems, comprising radical initiator/nitroxide or alkoxyamine with or without additional nitroxide, are also typically simpler initiating systems compared to ATRP initiating systems, which require at minimum activated halide, metal halide, and ligand, but often include other

additives to facilitate the polymerization. In contrast with RAFT polymerization, NMP does not require the use of sometimes unpleasant sulfur chemistry [7].

In this method, a free radical initiator and a stable nitroxy radical as (2,2,6,6-tetramethyl-1-piperidinyloxy) (TEMPO) are used. The TEMPO keeps polymer chain growth under control and acts as a catalyst. However, it does not start the reaction by itself. TEMPO is bound to the polymer end after added each monomer to radical in order to ensure a controlled growth. In this way, monodisperse polymers are obtained. The structure with the TEMPO end group undergoes homolytic fragmentation to give polymeric radical and stable free radical reversibly. The propagation step continues until monomer consumed in the medium. The chemical structure of TEMPO is shown in Figure 2.11.

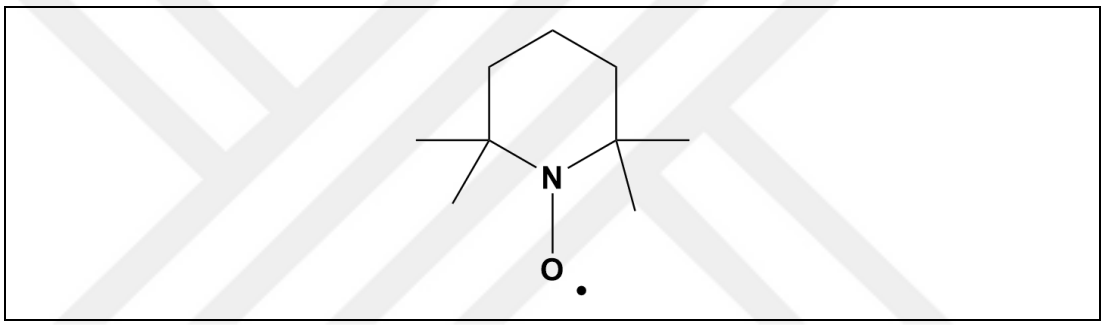

Figure 2.11: The chemical structure of TEMPO.

2.7.1. Basic Mechanism

TEMPO and its derivatives form a strong covalent bond in alkoxyamines. The equilibrium constant (kd (dissociation rate constant) / kc (cross-coupling/association rate constant)) is usually very small, in the presence of excess TEMPO. The equilibrium is strongly shifted towards the dormant species and dramatically reduces the polymerization rate. Controlled/living radical polymerization method with TEMPO is successful at controlling the polymerization of styrene monomers but not successful for acrylate and methacrylate monomers for this reason. A general mechanism for the NMP is shown in Figure 2.12 [67].

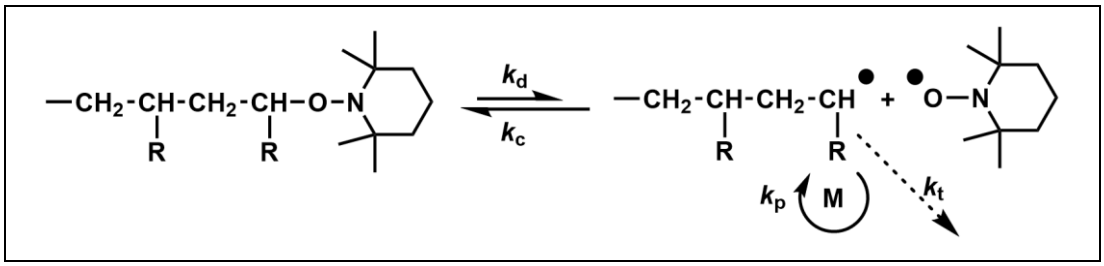

Figure 2.12: Dynamic equilibration for nitroxide mediated radical polymerization (NMP).

Nitroxide-mediated radical polymerization (NMP) reactions can be carried out under homogeneous conditions (bulk or solution polymerization) and under heterogeneous conditions (suspension and emulsion polymerization). The viscosity of the medium is low and the purification of the obtained products is quite easy [68].

2.8. Copper(I)-catalyzed Azide-Alkyne Cycloaddition "Click" Chemistry

It is important to be converted of functional groups in high yield after completion of the polymer reaction successfully. In this regard, "click" chemistry technique is used, due to its high efficiency and ease of reaction conditions [69].

1,3-dipolar cycloaddition reaction, which is performed applying heat from alkyne and azide groups found by Huisgen, is the precursor reaction of the "click chemistry". Additionally, Huisgen type cycloaddition reactions generally give 1,4- and 1,5-triazole isomers (about 1:1) [70]. This method was developed by Sharpless and the non-activated reaction between azide and alkyne groups is carried out in very high yield using Cu(I) salt catalyst under mild conditions and 1,4-triazole formation was performed with high selectivity (Figure 2.13) [71]. Also, Sharpless type "click reactions" have high tolerance for many different functional groups and are carried out in many solvents and solvent mixtures without compromising yield [69].

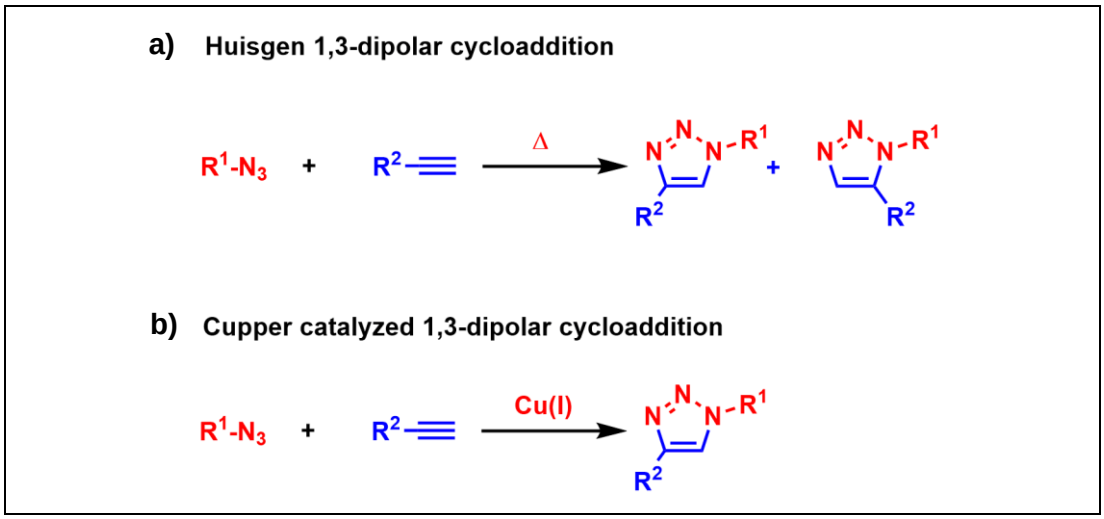

Figure 2.13: Synthesis of 1,2,3-triazoles via 1,3-dipolar cycloaddition of azides and terminal alkynes; a) Huisgen and b) Copper-catalyzed cycloaddition reactions.

3. MATERIAL AND METHOD

3.1. Chemical and Reagents

The chemicals and their properties used in this study are listed in Table 3.1.

Table 3.1: The chemicals and reagents used in synthesis, separation and purification processes.

Name	Company	CAS Number	Assay
Cupper(I) bromide (CuBr)	Sigma-Aldrich	7787-70-4	98%
Dichloromethane (DCM)	Sigma-Aldrich	75-09-2	99.8%
Methanol	Sigma-Aldrich	67-56-1	99.8%
Magnesium sulfate ($MgSO_4$)	Sigma-Aldrich	7487-88-9	99.5%
N,N,N′,N″,N″-Pentamethyldiethylenetriamine (PMDETA)	Aldrich	3030-47-5	99%
N,*N*-Dimetilformamide (DMF)	Sigma-Aldrich	68-12-2	99.8%
Sodium azide (NaN_3)	Aldrich	26628-22-8	99%
Sodium bicarbonate ($NaHCO_3$)	Sigma-Aldrich	144-55-8	99.7%
Sodiumicarbonate ($NaCO_3$)	Sigma-Aldrich	497-19-8	99.5%
Potassium carbonate (K_2CO_3)	Sigma-Aldrich	584-08-7	99%
Sodium chloride	Alfa-Aesar	7647-14-5	99%
Styrene	Aldrich	100-42-5	99%
Triethylamine (TEA)	Sigma-Aldrich	121-44-8	99%
4-Vinylbenzyl chloride	Sigma-Aldrich	1592-20-7	90%
1-ethynylpyrene	Sigma-Aldrich	34993-56-1	96%
Pentaerythritol	Aldrich	115-77-5	98%
Ethylene glycol	Acros	107-21-1	99.8%
2,2,6,6- Tetramethyl-1-piperidinyloxy (TEMPO)	Acros	2564-83-2	98%
1,1,1-Tris(hydroxyl methyl propane)	Sigma-Aldrich	77-99-6	98%

Table: 3.1. Continuation of the table.

2-bromoisobutyryl bromide	Sigma-Aldrich	20769-85-1	98%
Tetrahydrofuran (THF)	Sigma-Aldrich	109-99-9	99.9%
Nitrobenzen	Merck	98-95-3	99%
1,2 Dinitrobenzen	Aldrich	528-29-0	99%
Pikrik asit	Aldrich	88-89-1	98%
4-Nitrotoluen	Aldrich	99-99-0	99%
2,4-Dinitrotoluen	Aldrich	121-14-2	97%
Chloroform	Sigma-Aldrich	67-66-3	99.9%

3.2. Equipments

Chemical structures of the synthesized small molecular compounds, polymers were investigated via;

- Fourier Transform Infrared Spectroscopy (FTIR)

Fourier transform infrared (FTIR) spectra measurement were recorded in transmission mode with a Perkin Elmer Spectrum Two™ Spectrometer equipped with UATR accessory and the results were used any corrections.

- Liquid Chromatography Mass Spectrometry (LC-MS)

Electrospray ionization (ESI) high-resolution mass spectra measurements were obtained on an Agilent 6230A LC–MS Spectrometer.

- Ultraviolet Visible Spectroscopy (UV)

UV-Visible spectral data of polymer were obtained on Shimadzu 2600 UV-Visible Spectrophotometer in the 700–200 nm region by dissolving the sample in DMF.

- Fluoresecence Spectroscopy

Fluorescence spectra were measured using quartz cuvettes (1 cm path length) on a Agilent Cary Eclipse spectrophotometer.

- Nuclear Magnetic Resonance (NMR)

Proton and carbon nuclear magnetic resonance (^{1}H and ^{13}C NMR) spectra were recorded on a Bruker Avance III HD 400 MHz Spectrometer in deuterated chloroform ($CDCl_3$) and non-euterated solvent residues were used as internal reference.

- Thermal Gravimetric Analyzer (TGA)

The thermal stability was determined by thermogravimetric analysis (TGA, Perkin Elmer Instruments model, STA 6000). The TGA thermograms were recorded for 5-10 mg of powder sample at a heating rate of 10 ^{0}C min. in the temperature range of 30 ^{0}C-700 ^{0}C under nitrogen atmosphere**.**

- Differential Scanning Calorimetry (DSC)

Glass transition temperatures (T_g) of the star copolymers was investigated on a Perkin Elmer DSC 8500 double-furnace differential scanning calorimeter (DSC) under nitrogen flow (20 mL min^{-1}) at a heating rate of 200 °C min^{-1}.

- Gel Permeation Chromatography (GPC)

Average molecular weights and molecular weight distributions of the polymers were estimated on an Agilent 1260 Infinity GPC/SEC instrument consisting of a pump, a refractive index detector and two columns (Agilent PLgel 5 μm MIXED-C, 7.5 × 300 mm) which was calibrated using linear polystyrene standards. THF was used as the eluent at a flow rate of 0.5 mL/min at 40 ^{0}C.

4. EXPERIMENTAL

4.1. General Procedure

The reactions were performed in inert atmosphere (dry argon atmosphere) in order to prevent chemicals from influence of oxygen and moisture in the air. The glassware used in the reactions were dried in the burner flame, argon was passed through them and used after filling with argon by cooling.

4.1.1. Preperation of Dry Styrene and Vinyl Benzyl Chloride Monomers

Styrene and vinyl benzyl chloride monomers were dried by passing neutral/basic Al_2O_3 under argon atmosphere. The dried products were stored in the refrigerator.

4.1.2. Preperation of Dry *N, N*-Dimetilformamide (DMF)

DMF was stirred overnight by adding CaH_2 and then distilled under vacuum. Dry DMF, was kept under argon in the presence of molecular sieves (4A°).

4.1.3. Drying of the Synthesized Polymers

The synthesized polymers were precipitated in appropriate solvents (methanol), filtered through a G4 sintered filter and weighed on a precision balance. Polymers were allowed to dry at room temperature under reduced pressure by recording the weighing results. Then, weight of the polymer was measured periodically and the same value of the last three measurements showed that polymer was dry.

4.1.4. Gravimetric Determination of the Monomer Conversion

The ratio of the dry polymer weight to the total weight of initiator and the monomer was used for gravimetric monomer conversion.

4.2. Experiments

The thesis project includes the synthesis of styrenic star-shaped and linear copolymers with pyrene side groups, their characterization of structures and the use of the resulting polymers in optical sensor applications towards to nitroaromatic compounds. In order to obtain uniformly distributed polymers, we tried to optimize the parameters such as the molecular weights of the polymers and the ratios between repeating units (styrene / 4-vinylbenzyl chloride) and the TEMPO ratio in the polymer. The data for polymers synthesized in the optimization are not included in the report.

Within the scope of the thesis, initially, initiator compounds were synthesized. (**1-6**). Subsequently, linear and star-shaped styrene copolymers with styrene:4-vinylbenzyl chloride monomer feed ratios were synthesized with 100:5, 100:10 and 100:15 per arm (St:VBC) with chloride, azide and pyrene side groups. Different codes were given to the polymers. For example, P1-a represents P1 polymer having chloride side groups in this coding system. The codes were used such as P1-a and P1-b to distinguish P1 polymers at different reaction conditions (such as different styrene:4-vinylbenzyl chloride ratio). The encodings of all synthesized polymers are presented in Table 4.1.

Tablo 4.1: Codings used in the synthesis of polymers.

Polymers	**Feed Ratio (St:VBCl)**	**Chlorinated Polymer**	**Azide Polymer**	**Pyrene Func. Final Product**
Star-Shaped (Tetra-func.)	100:5	P1-a	P2-a	P3-a
	100:10	P1-b	P2-b	P3-b
	100:15	P1-c	P2-c	P3-c
Star-Shaped (Tri-func.)	100:5	P4-a	P5-a	P6-a
	100:10	P4-b	P5-b	P6-b
	100:15	P4-c	P5-c	P6-c
Linear	100:5	P7-a	P8-a	P9-a
	100:10	P7-b	P8-b	P9-b
	100:15	P7-c	P8-c	P9-c

4.2.1. Synthesis of Pyrene Functional Tetra-Armed Star-Shaped Styrene Copolymers (P3-(a-c))

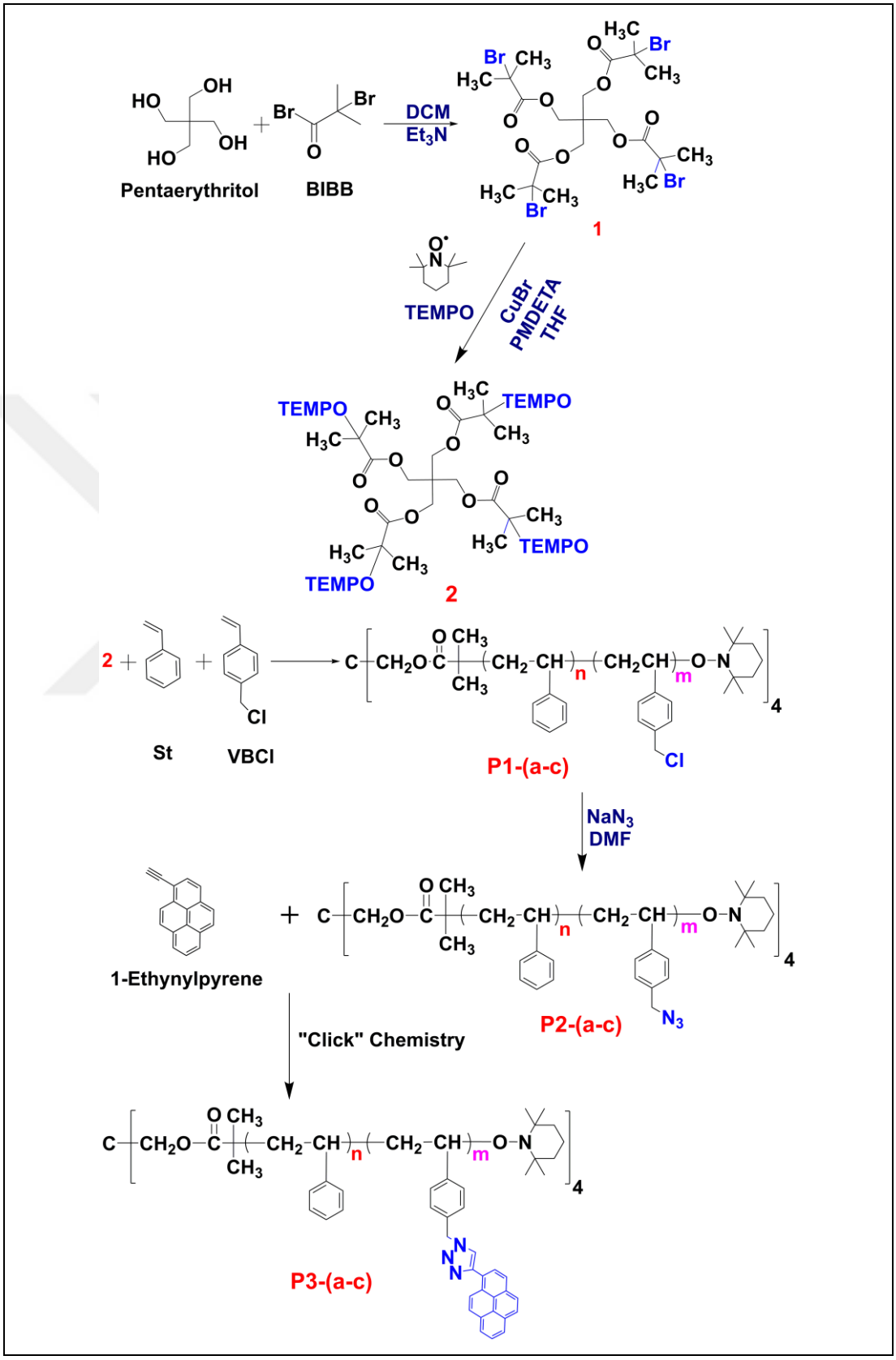

Figure 4.1: Synthetic procedure for the preparation of tetra-armed poly **P3-(a-c)**.

4.2.1.1. Synthesis of Tetrafunctional Initiators (1 and 2)

4.2.1.1.1. Synthesis of Tetrabromo-Functionalized Initiator (1)

Pentaerythritol tetrakis(2-bromoisobutyrate) (**1**) was synthesized according to the literature with minor modifications [72]. Pentaerythritol (1 g, 7.34 mmol, 1 eq.) and TEA (3.64 g, 32.32 mmol, 4.9 eq.) were dissolved in DCM (10 mL) under argon atmosphere and the mixture was cooled to 0 °C with ice-salt mixture. BIBB (14.86 g, 64.63 mmol, 4.4 eq) dissolved in DCM (5 mL) was added dropwise in 30 minutes and then the mixture was left stirring for 12 h at room temperature. The obtained solution was transferred to separatory flask and washed with a 20 mL Na_2CO_3 (%10, w/v) aqueous solution. The organic phase was dried over anhydrous $MgSO_4$, the solvent was evaporated, and finally, compound **1** was obtained after recrystallization with methanol.

Yield: 4.28 g (80%). m.p: 133-135 °C. HRMS (ESI, m/z): 754.87 $[M + Na]^+$, MW_{theo}: 731.88 g mol^{-1}. FTIR (ATR, cm^{-1}): 3000 and 2850 (-CH), 1729 (C=O). ^1H NMR (400 MHz, $CDCl_3$, δ, ppm): 4.35 (s, 8H; C***H***$_2$OCO), 1.96 (s, 24H; (C***H***$_3$)$_2$CBr). ^{13}C NMR (100 MHz, $CDCl_3$, δ, ppm): 30.64 (s, -***C***H_3), 43.67 (s, ***C***-$CH_2O)_4$), 55.19 (s, ***C***-$(CH_3)_2$), 62.90 (s, -***C***H_2O), 170.91 (s, ***C***=O).

4.2.1.1.2. Synthesis of Tetra TEMPO-Capped Alkoxyamine/NMP Initiator (2)

Compound **1** (0.9 g, 1.23 mmol, 1 eq.) and TEMPO (1.84 g, 11.80 mmol, 9.6 eq.) was dissolved in THF (20 mL) in a 50 mL one-necked round bottom flask under argon atmosphere. Then, CuBr (0.72 g, 5.04 mmol, 4.1 eq.) was added and the mixture was deaerated with three freeze-pump-thaw cycles. After the addition of PMDETA (1.75 g, 10.08 mmol, 8.2 eq.), the color of the solution turned to dark green and the reaction mixture was left stirring at room temperature for 48 h. Upon completing the reaction, solvent was removed via rotary evaporator, the crude product was dissolved in DCM and purified by precipitating into cold methanol:water (1:4) mixture. Finally, compound **2** was collected as a white powdery product by filtering through a sintered glass filter (G4) and dried under vacuum at room temperature.

Yield: 1.22 (95%). m.p: 157-160 °C. HRMS (ESI, m/z): 1037.76 $[M+H]^+$, M_{Wtheo}: 1036.77 g/mol. FTIR (ATR, cm^{-1}): 3000 and 2850 (-CH), 1730 (C=O), 1360 (N-O), 1130 (C-O). ^{1}H NMR (400 MHz, $CDCl_3$, δ, ppm): 1.00 and 1.14 (s, 48H; C***H***$_3$ (TEMPO)), 1.47 (s, 24H; CC***H***$_3$), 1.40-1.70 (m, 24H; C***H***$_2$), 4.24 (s, 8H; CC***H***$_2$). ^{13}C NMR (100 MHz, $CDCl_3$, δ, ppm): 17.04 (s, CH_2***C***HCH_2), 20.52 and 24.63 (s, C***H***$_3$ (TEMPO)), 33.51 (s, OC***C***H_3), 40.50 (s, ***C***H_2CH_2***C***H_2), 42.39 (s, ***C***-$CH_2O)_4$), 59.60 (s, -**C**H_2O), 62.68 (s, N-***C***-$(CH_3)_2$), 81.26 (s, ***C***-$(CH_3)_2$), 175.23 (s, ***C***=O).

4.2.1.2. Synthesis of Chloride Side-Functional Styrenic Star Copolymers (P1)

Chloride side-functional styrenic star copolymers (**P1-a**, **P1-b**, and **P1-c**) were synthesized in the same manner via unimolecular nitroxide-mediated radical polymerization (NMP) of styrene (St) and 4-vinylbenzyl chloride (VBCl) at different monomer feed ratios. Therefore, the synthesis of **P1-a** was given as the representative for the chloride side-functional styrenic star copolymers (Please see Table 4.2 for the synthesis of **P1-b** and **P1-c**).

Compound **2** (0.046 g, 0.04 mmol), St (1.85 g, 17.74 mmol), VBCl (0.14 g, 0.89 mmol), and TEMPO (0.083 g, 0.53 mmol) were placed into a 25 mL Schlenk flask under argon and freeze-thaw degassed three times. The flask was dipped into an oil-bath, which was thermostated at 120 °C, the reaction mixture was stirred for 48 h and then polymerization was quenched by fast cooling in a water-ice bath. The obtained crude polymerization product was dissolved in DCM (20 mL) and purified by precipitating twice in cold methanol. **P1-a** was separated on a sintered glass filter (G4) by vacuum filtration and dried under reduced pressure at 35 °C until constant weight was attained.

Yield: 1.57 g (77%). $M_{n,\ GPC}$: 15 300 g/mol; M_w/M_n: 1.46. **FTIR** (cm^{-1}): 3026−3080 (CH stretching, aromatic); 2848−2920 (CH stretching, aliphatic); 1601, 1493 and 1452 (C=C stretching, aromatic). **^{1}H NMR** (400 MHz, $CDCl_3$, δ, ppm): 6.47− 7.11 (C_6***H***$_4$ and C_6***H***$_5$); 4.52 (C_6H_4C***H***$_2Cl$); 1.44−2.05 (polymer backbone).

Tablo 4.2: P1-(a-c) Polymers Experimental Data.

Polymer	Feed Ratio (St:VBCl)	Initiator (2)(mmol)	Styrene (mmol)	VBCl (mmol)	TEMPO (mmol)	Yield (%)	$Mn_{,GPC}$	PDI
P1-a	100:5	0.04	17.74	0.89	0.53	77	15300	1.46
P1-b	100:10	0.04	17.74	1.77	0.53	50	14800	1.57
P1-c	100:15	0.04	17.74	2.66	0.53	35	13700	1.49

4.2.1.3. Synthesis of Azide Side-Functional Styrenic Star Copolymers (P2)

The synthesis of **P2-a** was given as the representative for the azide side-functional styrenic star copolymers (Please see Table 4.3 for the synthesis of **P2-b** and **P2-c**).

P1-a (0.8 g, $M_{n,NMR}$: 36 383 g/mol, contains 0.65 mmol of Cl units) was dissolved in anhydrous DMF (40 mL) in a single-necked round bottom flask under argon. NaN_3 (0.430 g, 6.615 mmol) was added in one portion, the mixture was purged gently with Ar for 5 min and left stirring for two days at 60 °C. After the reaction was completed, the raw polymerization product was transferred to a separating funnel with DCM (100 mL), the organic layer was washed with brine (2x50 mL) and deionized water (50 mL). The solvent was evaporated to ~5 mL and azide functional star-shaped styrene copolymer was precipitated in cold methanol. **P2-a** was separated by vacuum filtration on a sintered glass filter (G4) and dried under reduced pressure at 40 °C until constant weight was attained.

Yield: 0.76 g (94.6%). $M_{n,GPC}$: 15 600 g/mol; Mw/Mn: 1.46. FTIR (cm^{-1}): 3026−3080 (CH stretching, aromatic); 2848−2920 (CH stretching, aliphatic); 1601, 1493 and 1452 (C=C stretching, aromatic). ^{1}H NMR (400 MHz, $CDCl_3$, δ, ppm): 6.47−7.11 ($C_6\boldsymbol{H}_4$ and $C_6\boldsymbol{H}_5$); 4.21 ($C_6H_4C\boldsymbol{H}_2N_3$); 1.44−2.05 (polymer backbone).

Table 4.3: P2-(a-c) Polymers Experimental Data.

Polymer	Precursor Polymer	Pre. Polymer (-Cl / mmol)	NaN_3 (mmol)	Yield (%)	$Mn_{,GPC}$	PDI
P2-a	P1-a	0.35	3.5	94.6	15600	1.46
P2-b	P1-b	0.65	6.5	94.5	15000	1.58
P2-c	P1-c	0.81	8.1	91	14100	1.57

4.2.1.4. Synthesis of Pyrene Side-Functional Styrenic Star Copolymers (P3)

The synthesis of **P3-a** was given as the representative for the pyrene side-functional styrenic star copolymers (Please see Table 4.4 for the synthesis of **P3-b** and **P3-c**).

P2-a (0.5 g, $M_{n,NMR}$: 36 576 g/mol, contains 0.40 mmol of N_3 unit), 1-ethynylpyrene (0.27 g, 1.21 mmol), and PMDETA (0.84 g, 4.86 mmol) were dissolved in DMF (20 mL) and the resulting solution was degassed by gently purging argon for 5 min. After the addition of CuBr (0.70 g, 4.86 mmol) in one portion, the mixture was degassed again with argon for 5 min and left stirring at room temperature for 48 h. Then, the solvent was removed by rotary evaporator, the residue was dissolved in DCM (100 mL) and washed with water (2 × 100 mL). The obtained organic phases were dried over $MgSO_4$, concentrated to 10 mL by a rotary evaporator, and then **P3-a** was purified by precipitating in cold methanol. **P3-a** was collected on a sintered glass filter (G4) by vacuum filtration as a yellow product and dried under reduced pressure at ambient temperature until constant weight was attained.

Yield: 0.45 g (76%). $M_{n,GPC}$: 15 900 g/mol; M_w/M_n: 1.45. FTIR (cm^{-1}): 3026−3080 (CH stretching, aromatic); 2848−2920 (CH stretching, aliphatic); 1601, 1493 and 1452 (C=C stretching, aromatic). ^{1}H NMR (400 MHz, $CDCl_3$, δ, ppm): 7.68−8.70 (C***H***, pyrene); 6.51− 7.11 (C_6***H***$_4$ and C_6***H***$_5$); 5.47 (C_6H_4C***H***$_2N_3$); 1.44−2.05 (polymer backbone).

Table 4.4: P3-(a-c) Polymers Experimental Data.

Polymer	Precursor Polymer	Pre. Polymer (-N_3 / mmol)	Ethynyl Pyr. (mmol)	Yield (%)	Mn,GPC	PDI
P3-a	P2-a	0.40	1.21	76	15900	1.45
P3-b	P2-b	0.69	2.07	78	15300	1.49
P3-c	P2-c	1.65	4.95	80	14400	1.38

4.3.1. Synthesis of Pyrene Functional Three-Armed Star-Shaped Styrene Copolymers (P6-(a-c))

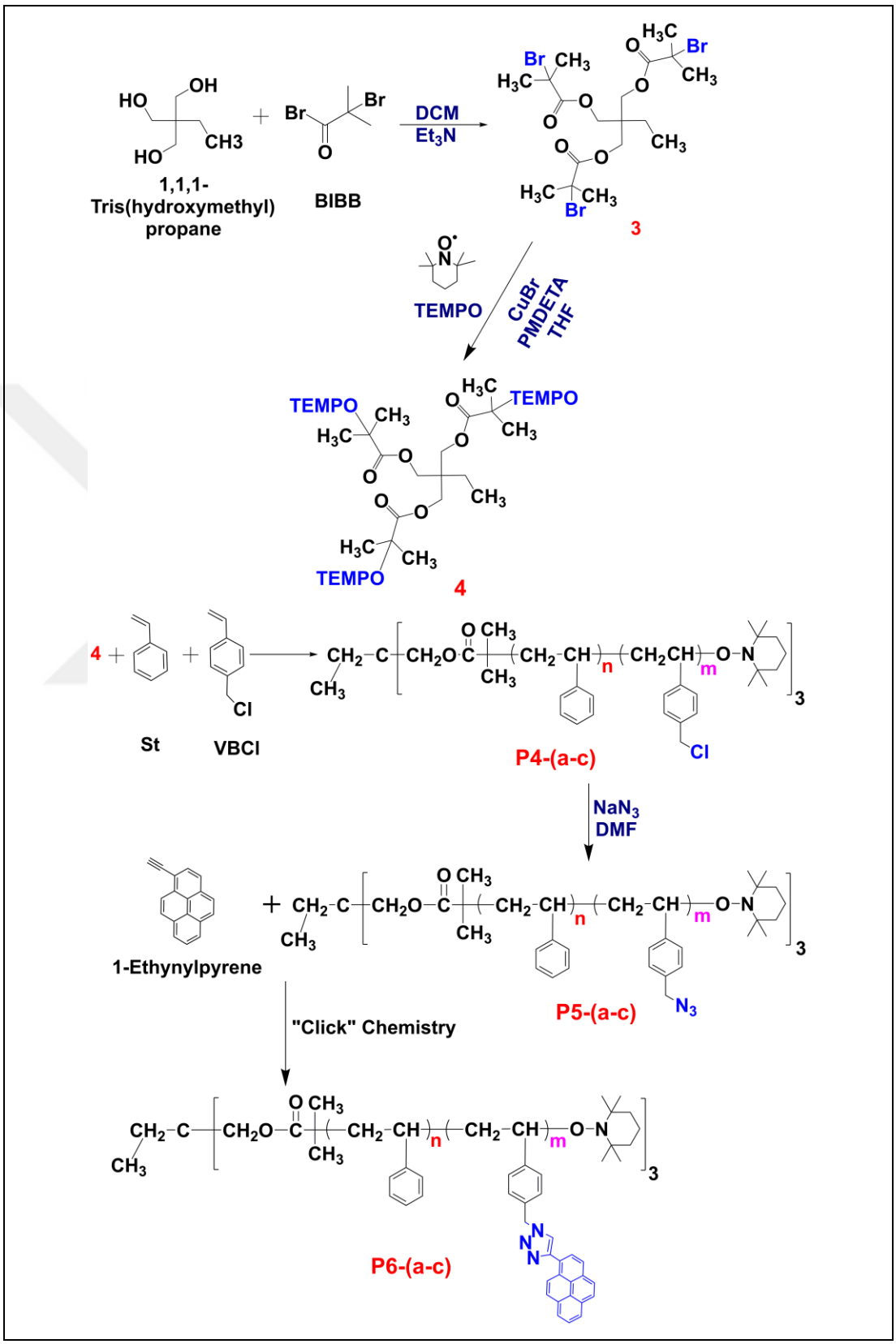

Figure 4.2: Synthetic procedure for the preparation of tri-armed poly **P6-(a-c)**.

4.3.1.1. Synthesis of Trifunctional Initiators (3 and 4)

4.3.1.1.1. Synthesis of Tribromo-Functionalized Initiator (3)

Tribromo-functionalized initiator (**3**) was synthesized according to the literature with minor modifications [73]. 1,1,1-Tris(hydroxyl methyl propane) (1 g, 7.45 mmol 1 eq.) and Et_3N (2.41 g, 23.85 mmol, 3.2 eq.) were dissolved in DCM (10 mL) under argon atmosphere and the mixture was cooled to 0 °C with ice-salt mixture. BIBB (5.31 g, 23.11 mmol, 3.1 eq) dissolved in DCM (5 mL) was added dropwise in 30 minutes and then the mixture was left stirring for 12 h at room temperature. The obtained solution was transferred to separatory flask and washed with a 20 mL Na_2CO_3 (%10, w/v) aqueous solution. The organic phase was dried over anhydrous $MgSO_4$ and the solvent was evaporated to give crude product. Finally, compound **3** was obtained after recrystallization with methanol.

Yield: 3 g (70%). m.p: 55-57 °C. HRMS (ESI, m/z): 602.94 $[M + Na]^+$, MW_{theo}: 579.95 g mol^{-1}. FTIR (ATR, cm^{-1}): 3000 and 2850 (-CH), 1729 (C=O). ^{1}H NMR (400 MHz, $CDCl_3$, δ, ppm): 4.18 (s, 6H; -C-(C***H***$_2$O)$_3$), 1.93 (s, 18H; (C***H***$_3$)$_2$CBr), 1.63 ppm (2H, CH_3-C***H***$_2$-C-), 0.97 (t, 3H, C***H***$_3$-CH_2-C-). ^{13}C NMR (100 MHz, $CDCl_3$, δ, ppm): 30.81 (s, (***C***H_3)$_2$-C-Br), 42.09 (s, CH_3-***C***-$CH_2O)_3$), 55.55 (s, ***C***-$(CH_3)_2$), 64.87 (s, -***C***H_2O), 23.23 (s, -***C***H_2-CH_3), 7.58 (s, -CH_2-***C***H_3), 171.30 (s, ***C***=O).

4.3.1.1.2. Synthesis of Three TEMPO-Capped Alkoxyamine/NMP Initiator (4)

Compound **3** (0.9 g, 1.23 mmol, 1 eq.) and TEMPO (1.74 g, 11.15 mmol, 7.2 eq.) was dissolved in THF (20 mL) in a 50 mL one-necked round bottom flask under argon atmosphere. Then, CuBr (0.69 g, 4.80 mmol, 3.1 eq.) was added and the mixture was deaerated with three freeze-pump-thaw cycles. After the addition of PMDETA (1.66 g, 9.60 mmol, 6.2 eq.), the color of the solution turned to dark green and the reaction mixture was left stirring at room temperature for 48 h. Upon completing the reaction, solvent was removed via rotary evaporator, the crude product was dissolved in DCM and purified by precipitating into cold methanol:water mixture (1:4). Compound **4** was collected by filtering through a sintered glass filter (G4) and dried under vacuum at room temperature. The final product was a white powder.

Yield: 0.63 (50%). m.p: 133-135 °C. HRMS (ESI, m/z): 810.59 $[M+H]^+$, M_{Wtheo}: 809.61 g/mol. FTIR (ATR, cm^{-1}): 3000 and 2850 (-CH), 1730 (C=O), 1360 (N-O), 1130 (C-O). ^{1}H NMR (400 MHz, $CDCl_3$, δ, ppm): 1.00 and 1.14 (s, 36H; C***H***$_3$ (TEMPO)), 1.46 (s, 18H; CC***H***$_3$), 1.40-1.70 (m, 20H; C***H***$_2$), 4.08 (s, 6H; OC***H***$_2$). ^{13}C NMR (100 MHz, $CDCl_3$, δ, ppm): 7.25 (s, CH_2-***C***H_3), 17.06 (s, CH_2***C***HCH_2), 20.47 and 24.60 (s, C***H***$_3$ (TEMPO)), 22.52 (s, -***C***H_2-CH_3), 33.49 (s, OC***C***H_3), 40.51 (s, ***C***H_2CH_2***C***H_2), 41.05 (s, -CH_2-***C***-$CH_2O)_3$), 59.58 (s, -**C**H_2O), 63.76 (s, N-***C***-$(CH_3)_2$), 81.24 (s, ***C***-$(CH_3)_2$), 175.80 (s, ***C***=O).

4.3.1.2. Synthesis of Chloride Side-Functional Styrenic Star Copolymers (P4)

Chloride side tri-functional styrenic star copolymers (**P4-a**, **P4-b**, and **P4-c**) were synthesized in the same manner via unimolecular nitroxide-mediated radical polymerization (NMP) of styrene (St) and 4-vinylbenzyl chloride (VBCl) at different monomer feed ratios. Therefore, the synthesis of **P1-a** was given as the representative for the chloride side-functional styrenic star copolymers (Please see Table 4.5 for the synthesis of **P4-b** and **P4-c**).

TEMPO-capped NMP Initiator, compound **3,** (0.048 g, 0.06 mmol), St (1.87 g, 17.74 mmol), VBCl (0.14 g, 0.89 mmol), and TEMPO (0.083 g, 0.53 mmol) were placed into a 25 mL Schlenk flask under argon and freeze-thaw degassed three times. The flask was dipped into an oil-bath, which was thermostated at 120 °C, the reaction mixture was stirred for 48 h and then polymerization was quenched by fast cooling in a water-ice bath. The obtained crude polymerization product was dissolved in DCM (20 mL) and purified by precipitating twice in cold methanol. **P4-a** was separated on a sintered glass filter (G4) by vacuum filtration and dried under reduced pressure at 35 °C until constant weight was attained.

Yield: 1.5 g (74%). $M_{n,\ GPC}$: 12 100 g/mol; M_w/M_n: 1.51. FTIR (cm^{-1}): 3026−3080 (CH stretching, aromatic); 2840−2920 (CH stretching, aliphatic); 1601, 1493 and 1452 (C=C stretching, aromatic). ^{1}H NMR (400 MHz, $CDCl_3$, δ, ppm): 6.47−7.11 (C_6***H***$_4$ and C_6***H***$_5$); 4.54 (C_6H_4C***H***$_2$Cl); 1.44−2.08 (polymer backbone).

Tablo 4.5: P4-(a-c) Polymers Experimental Data.

Polymer	Feed Ratio (St:VBCl)	Initiator (2)(mmol)	Styrene (mmol)	VBCl (mmol)	TEMPO (mmol)	Yield (%)	$Mn_{,GPC}$	PDI
P4-a	100:5	0.09	17.94	0.89	0.53	74	12100	1.51
P4-b	100:10	0.09	17,94	1.77	0.53	68	11500	1.44
P4-c	100:15	0.09	17.94	2.69	0.53	54	11200	1.44

4.3.1.3. Synthesis of Azide Side-Functional Styrenic Star Copolymers (P5)

The synthesis of **P5-a** was given as the representative for the azide side-functional styrenic star copolymers (Please see Table 4.6 for the synthesis of **P5-b** and **P5-c**).

P4-a (0.8 g, $M_{n,NMR}$: 13 348 g/mol, contains 0.35 mmol of Cl units) was dissolved in anhydrous DMF (40 mL) in a single-necked round bottom flask under argon. NaN_3 (0.23 g, 3.50 mmol) was added in one portion, the mixture was purged gently with Ar for 5 min and left stirring for two days at 60 °C. After the reaction was completed, the raw polymerization product was transferred to a separating funnel with DCM (100 mL), and the organic layer was washed with brine (2x50 mL) and deionized water (50 mL). The solvent was evaporated to ~5 mL and azide functional star-shaped styrene copolymer was precipitated in cold methanol. **P5-a** was dried under reduced pressure at 40 °C for until constant weight was attained.

Yield: 0.82 g (99%). $M_{n,GPC}$: 12 300 g/mol; Mw/Mn: 1.51. FTIR (cm^{-1}): 3026−3080 (CH stretching, aromatic); 2848−2920 (CH stretching, aliphatic); 2095 (-N=N=N-); 1601, 1493 and 1452 (C=C stretching, aromatic). ^{1}H NMR (400 MHz, $CDCl_3$, δ, ppm): 6.47− 7.11 ($C_6\boldsymbol{H}_4$ and $C_6\boldsymbol{H}_5$); 4.23 ($C_6H_4C\boldsymbol{H}_2N_3$); 1.44−2.05 (polymer backbone).

Table 4.6: P5-(a-c) Polymers Experimental Data.

Polymer	Precursor Polymer	Pre. Polymer (-Cl / mmol)	NaN_3 (mmol)	Yield (%)	$Mn_{,GPC}$	PDI
P5-a	P4-a	0.35	3.5	99	12300	1.51
P5-b	P4-b	0.65	6.5	98	11750	1.46
P5-c	P4-c	0.81	8.1	98	11350	1.46

4.3.1.4. Synthesis of Pyrene Side-Functional Styrenic Star Copolymers (P6)

The synthesis of **P6-a** was given as the representative for the pyrene side-functional styrenic star copolymers (Please see Table 4.7 for the synthesis of **P6-b** and **P6-c**).

P5-a (0.4 g, contains 0.45 mmol of N_3 unit), 1-ethynylpyrene (00.19 g, 0.86 mmol), and PMDETA (0.7 g, 4.0 mmol) were dissolved in DMF (20 mL) and the resulting solution was degassed by gently purging argon for 5 min. After the addition of CuBr (0.58 g, 4.0 mmol) in one portion, the mixture was degassed again with argon for 5 min and left stirring at room temperature for 48 h. Then, the solvent was removed by rotary evaporator, the residue was dissolved in DCM (100 mL) and washed with water (2 × 100 mL). The obtained organic phases were dried over $MgSO_4$, concentrated to 10 mL by a rotary evaporator, and then **P6-a** was purified by precipitating in cold methanol. **P6-a** was collected on a sintered glass filter (G4) by vacuum filtration as a yellow product and dried under reduced pressure at ambient temperature until constant weight was attained.

Yield: 0.36 g (77%). $M_{n,GPC}$: 12 600 g/mol; M_w/M_n: 1.44. FTIR (cm^{-1}): 3026−3080 (CH stretching, aromatic); 2848−2920 (CH stretching, aliphatic); 1601, 1493 and 1452 (C=C stretching, aromatic). ^{1}H NMR (400 MHz, $CDCl_3$, δ, ppm): 8.68 (C***H***, triazole ring); 7.70− 8.18 (C***H***, pyrene); 6.51− 7.11 (C_6***H***$_4$ and C_6***H***$_5$); 5.53 (C_6H_4C***H***$_2$Pyr); 1.44−2.05 (polymer backbone).

Table 4.7: P6-(a-c) Polymers Experimental Data.

Polymer	**Precursor Polymer**	**Pre. Polymer (-N_3 / mmol)**	**Ethynyl Pyr. (mmol)**	**Yield (%)**	**Mn,GPC**	**PDI**
P6-a	P5-a	0.45	1.35	77	12600	1.44
P6-b	P5-b	0.80	2.41	70	12200	1.34
P6-c	P5-c	1.02	3.06	70	11700	1.35

4.4.1. Synthesis of Pyrene Functional Linear Styrene Copolymers (P9-(a-c))

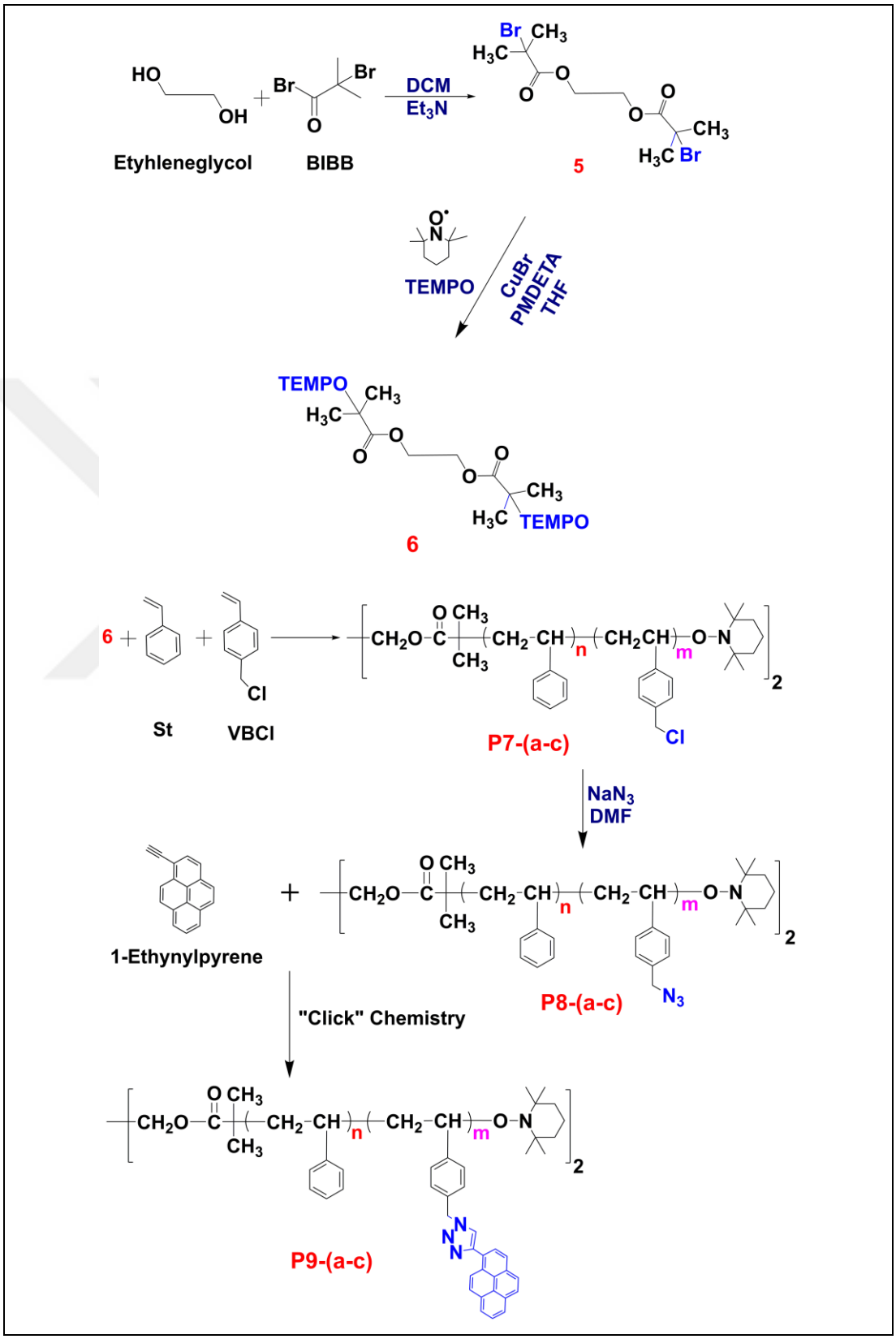

Figure 4.3: Synthetic procedure for the preparation of linear poly **P9-(a-c)**.

4.4.1.1. Synthesis of Bifunctional Initiators (5 and 6)

4.4.1.1.1. Synthesis of Dibromo-Functionalized Initiator (5)

Ethylene glycol (1.11 g, 17.93 mmol, 1 eq.) and Et_3N (3.99 g, 39.45 mmol, 2.2 eq.) were dissolved DCM (10 mL) and was cooled to 0 °C. The 5 mL DCM solution of 2-bromoisobutrylbromide (8.66 g, 37.66 mmol, 2.1 eq) was then added dropwise to the mix in 30 min with stirring and the mixture was stirred for 12 h at room temperature. The mix was washed with a 20 mL Na_2CO_3 (%10, w/v) aq. solution. The organic phase was dried over anhydrous $MgSO_4$ and the solvent was evaporated to give crude product. Finally, the product (**5**) was obtained after recrystallization with methanol.

Yield: 4.52 g (70%). m.p: 42-46 °C. HRMS (ESI, m/z): 382.93 $[M + Na]^+$, MW_{theo}: 359.94 g mol^{-1}. **FTIR** (ATR, cm^{-1}): 3000 and 2850 (-CH), 1729 (C=O). **^{1}H NMR** ($CDCl_3$, 400 MHz), δ (ppm): 4.45 (s, 4H, RO-(C***H***$_2$)$_2$-OR) and 1.95 (s, 12H, -(C***H***$_3$)$_2$). **^{13}C NMR** ($CDCl_3$, 400 MHz), δ (ppm): 171.42 (***C***=O), 63.19 (-(***C***H_2)$_2$), 55.34 (-***C***-) and 30.69 (-(***C***H_3)$_2$).

4.4.1.1.2. Synthesis of Two TEMPO-Capped Alkoxyamine/NMP Initiator (6)

Ethane-1,2-diyl bis(2-bromo-2-methylpropanoate) (**5**) (1.52 g, 4.22 mmol, 1 eq.), 2,2,6,6-Tetramethylpiperidine-1-oxyl (TEMPO) (3.16 g, 20.25 mmol, 4.8 eq.) and CuBr (1.27 g, 8.86 mmol, 2.1 eq.) were dissolved in THF (20 mL) in a 100 mL flask, and the solution was deaerated with three cycles of freezing-pump-thawing. Then PMDETA (3.07 g, 17.72 mmol, 4.2 eq.) was added into the flask and the solution turned to dark green in color. The mixture was kept at room temperature for 48 h and was precipitated twice in 500 mL H_2O:MeOH (1:9) solvent mix. with vigorous stirring. Then filtered, washed with same solvents and kept under vacuum overnight. Finally, the product (**6**) was obtained in 60% yield.

Yield: 1.30 (60%). m.p: 90-94 °C. HRMS (ESI, m/z): 513.38 $[M+H]^+$, M_{Wtheo}: 512.38 g/mol. **FTIR** (ATR, cm^{-1}): 3000 and 2850 (-CH), 1730 (C=O), 1360 (N-O), 1130 (C-O). **^{1}H NMR** (400 MHz, $CDCl_3$, δ, ppm): 1.01 and 1.61 (s, 24H; C***H***$_3$ (TEMPO)), 1.49 (s, 12H; OCC***H***$_3$), 1.40-1.80 (m, 12H; C***H***$_2$), 4.35 (s, 4H; OC***H***$_2$). ^{13}C

NMR (100 MHz, $CDCl_3$, δ, ppm): 17.07 (s, $CH_2\boldsymbol{C}HCH_2$), 20.49 and 24.47 (s, $C\boldsymbol{H}_3$ (TEMPO)), 33.49 (s, $OC\boldsymbol{C}H_3$), 40.58 (s, $\boldsymbol{C}H_2CH_2\boldsymbol{C}H_2$), 59.57 (s, N-$\boldsymbol{C}$-$(CH_3)_2$), 62.68 (s, -O$\boldsymbol{C}H_2$), 81.11 (s, O**C**-$(CH_3)_2$), 175.81 (s, $\boldsymbol{C}$=O).

4.4.1.2. Synthesis of Chloride Side-Functional Styrenic Linear Copolymers (P7)

Chloride side-functional linear copolymer (**P7-a**) were synthesized in the same manner with star shaped copolymers (**P1-a and P4-a**) via unimolecular NMP of styrene (St) and 4-vinylbenzyl chloride (VBCl).

Compound **6** (0.046 g, 0.09 mmol), St (1.87 g, 17.94 mmol), VBCl (0.14 g, 0.89 mmol), and TEMPO (0.084 g, 0.54 mmol) were placed into a 25 mL Schlenk flask under argon and freeze-thaw degassed three times. The flask was dipped into an oil-bath, which was thermostated at 120 °C, the reaction mixture was stirred for 48 h and then polymerization was quenched by fast cooling in a water-ice bath. The obtained crude polymerization product was dissolved in DCM (20 mL) and purified by precipitating twice in cold methanol. **P7-a** was separated on a sintered glass filter (G4) by vacuum filtration and dried under reduced pressure at 35 °C until constant weight was attained.

Yield: 0.99 g (48%). $M_{n,\ GPC}$: 8 200 g/mol; M_w/M_n: 1.29. **FTIR** (cm^{-1}): 3026−3080 (CH stretching, aromatic); 2840−2920 (CH stretching, aliphatic); 1601, 1493 and 1452 (C=C stretching, aromatic). **^{1}H NMR** (400 MHz, $CDCl_3$, δ, ppm): 6.47− 7.11 ($C_6\boldsymbol{H}_4$ and $C_6\boldsymbol{H}_5$); 4.52 ($C_6H_4C\boldsymbol{H}_2Cl$); 1.44−2.02 (polymer backbone).

Tablo 4.8: P7-(a-c) Polymers Experimental Data.

Polymer	Feed Ratio (St:VBCl)	Initiator (2)(mmol)	Styrene (mmol)	VBCl (mmol)	TEMPO (mmol)	Yield (%)	$Mn_{,GPC}$	PDI
P7-a	100:5	0.09	17.94	0.89	0.53	48	8200	1.29
P7-b	100:10	0.09	17.94	1.77	0.53	47	7700	1.31
P7-c	100:15	0.09	17.94	2.69	0.53	62	7400	1.35

4.4.1.3. Synthesis of Azide Side-Functional Styrenic Linear Copolymers (P8)

Azide (-N_3) side-functional linear copolymer (**P8-a**) were synthesized in the same manner with star shaped copolymers (**P2-a and P5-a**).

P7-a (0.66 g, $M_{n,NMR}$: 29.895 g/mol, contains 0.29 mmol of Cl units) was dissolved in anhydrous DMF (40 mL) in a single-necked round bottom flask under argon. NaN_3 (0.19 g, 2.9 mmol) was added in one portion, the mixture was purged gently with Ar for 5 min and left stirring for two days at 60 °C. After the reaction was completed, the raw polymerization product was transferred to a separating funnel with DCM (100 mL), and the organic layer was washed with brine (2x50 mL) and deionized water (50 mL). The solvent was evaporated to ~5 mL and azide functional linear styrene copolymer was precipitated in cold methanol. **P8-a** was dried under reduced pressure at 40 °C for 24 h.

Yield: 0.60 g (90.9%). $M_{n,GPC}$: 8 300 g/mol; Mw/Mn: 1.29. **FTIR** (cm^{-1}): 3026−3080 (CH stretching, aromatic); 2848−2920 (CH stretching, aliphatic); 2095 (-N=N=N-); 1601, 1493 and 1452 (C=C stretching, aromatic). **^{1}H NMR** (400 MHz, $CDCl_3$, δ, ppm): 6.47− 7.11 ($C_6\boldsymbol{H}_4$ and $C_6\boldsymbol{H}_5$); 4.23 ($C_6H_4C\boldsymbol{H}_2N_3$); 1.44−2.05 (polymer backbone).

Table 4.9: P8-(a-c) Polymers Experimental Data.

Polymer	Precursor Polymer	Pre. Polymer (-Cl / mmol)	NaN_3 (mmol)	Yield (%)	$Mn_{,GPC}$	PDI
P8-a	P7-a	0.29	2.9	90.9	8300	1.29
P8-b	P7-b	0.53	5.3	84.4	7850	1.31
P8-c	P7-c	0.83	8.3	87.2	7600	1.35

4.4.1.4. Synthesis of Pyrene Side-Functional Styrenic Linear Copolymers (P9)

Pyrene (-Pyr) side-functional linear copolymer (**P9-a**) were synthesized in the same manner with star shaped copolymers (**P3-a and P6-a**).

P8-a (0.3 g, $M_{n,NMR}$: 30 080 g/mol, contains 0.26 mmol of N_3 unit), 1-ethynylpyrene (0.19 g, 0.86 mmol), and PMDETA (0.15 g, 0.86 mmol) were dissolved

in DMF (20 mL) and the resulting solution was degassed by gently purging argon for 5 min. After the addition of CuBr (0.12 g, 0.86 mmol) in one portion, the mixture was degassed again with argon for 5 min and left stirring at room temperature for 48 h. Then, the solvent was removed by rotary evaporator, the residue was dissolved in DCM (100 mL) and washed with water (2 × 100 mL). The obtained organic phases were dried over $MgSO_4$, concentrated to 10 mL by a rotary evaporator, and then **P9-a** was purified by precipitating in cold methanol. **P9-a** was collected on a sintered glass filter (G4) by vacuum filtration as a yellow product and dried under reduced pressure at ambient temperature until constant weight was attained.

Yield: 0.26 g (71%). $M_{n,GPC}$: 8 400 g/mol; M_w/M_n: 1.29. **FTIR** (cm^{-1}): 3026−3080 (CH stretching, aromatic); 2848−2920 (CH stretching, aliphatic); 1601, 1493 and 1452 (C=C stretching, aromatic). **^{1}H NMR** (400 MHz, $CDCl_3$, δ, ppm): 8.68 (C***H***, triazole ring); 7.70− 8.18 (C***H***, pyrene); 6.51− 7.11 (C_6***H***$_4$ and C_6***H***$_5$); 5.53 (C_6H_4C***H***$_2N_3$); 1.44−2.05 (polymer backbone).

Table 4.10: P9-(a-c) Polymers Experimental Data.

Polymer	**Precursor Polymer**	**Pre. Polymer (-N_3 / mmol)**	**Ethynyl Pyr. (mmol)**	**Yield (%)**	**$Mn_{,GPC}$**	**PDI**
P9-a	P8-a	0.26	0.86	71	8400	1.29
P9-b	P8-b	0.42	1.26	70	8000	1.25
P9-c	P8-c	0.47	1.41	68	7700	1.29

5. RESULTS and DISCUSSION

5.1. Characterization of Pyrene Functional Tetra-Armed Star-Shaped Styrene Copolymers (P3-(a-c))

Pyrene functional tetra-Armed star-shaped styrene copolymers (**P3-(a-c)**) were prepared using styrene (St) and 4-vinylbenzylchloride (VBCl) as the monomer at different molar ratios (St:VBCl; 100:5, 100:10 and 100:15 per arm). Chemical structures of the synthesized small molecular compounds and star-shaped styrenic copolymers were determined by FTIR and ^{1}H NMR spectroscopies. Also used GPC, DSC and TGA characterization techniques for chemical structure determination.

The tetra-armed star-shaped styrenic copolymers having pyrene side-groups (**P3-(a-c)**) were prepared using core-first approach (Figure 4.1), by which the number of arms of the star polymer could be clearly defined and would be equal to the number of the functional units on the polymerization-initiating compound [74-75]. Besides, this method provides good control on the macromolecular architecture [76]. The tetra-functional initiator (**2**) was synthesized via facile esterification and atom transfer radical addition (ATRA) reactions. Firstly, pentaerythritol was reacted with 2-bromoisobutyryl bromide and the product (**1**) was purified easily by crystallization. Then, compound **1** was used to produce transient carbon centered radicals in the presence of CuBr/PMDETA catalyst system, which readily reacted with 2,2,6,6-tetramethyl-1-piperidinyloxy (TEMPO) to yield a novel tetra-TEMPO functional alkoxyamine unimolecular initiator compound (**2**). Unimolecular alkoxyamine initiators generate a stable free nitroxide radical (TEMPO) and a carbon-centered radical on the initiator (small molecule or macroinitiator) at considerably high temperatures. Carbon-centered radicals initiate the polymerization by attacking double bonds of monomers whereas TEMPO can only mediate the reaction by capping and de-capping the growing chain ends of the polymer. Besides, unimolecular alkoxyamine initiators allow preparation of star macroinitiators. Then, the unimolecular initiator (**2**) was employed in the nitroxide mediated radical polymerization (NMP) of St and VBC at different monomer feed ratios to produce a tetra-armed styrenic star copolymers with chloride side-functional units (**P1-(a-c)**). NMP method is a prominent technique among controlled living radical polymerization

(CLRP) techniques since it does not require metal catalysts which are very difficult to get rid of. Besides, it is tolerant to variety of functional groups and allows easy purification of the polymerization products. Then, the reaction of chloride side-groups of (**P1-(a-c)**) with sodium azide in DMF in mild reaction conditions straightforwardly gave azide-functional star-shaped styrenic copolymers (**P2-(a-c)**). In the final step, we took the advantage of Cu(I)-catalyzed 1,3-dipolar cycloaddition (click) reaction to attach fluorescent-active pyrene moieties to the pendant groups of the polymer arms. In this manner, azide functional units of (**P2-(a-c)**) were reacted with alkyne unit of 1-ethynylpyrene, providing pyrene-functional styrenic star copolymers (**P3-(a-c)**). Click reactions have considerably high compatibility to various functional units and solvents and give regiospecific 1,3-cycloaddition products with near quantitative yields under mild reaction conditions.

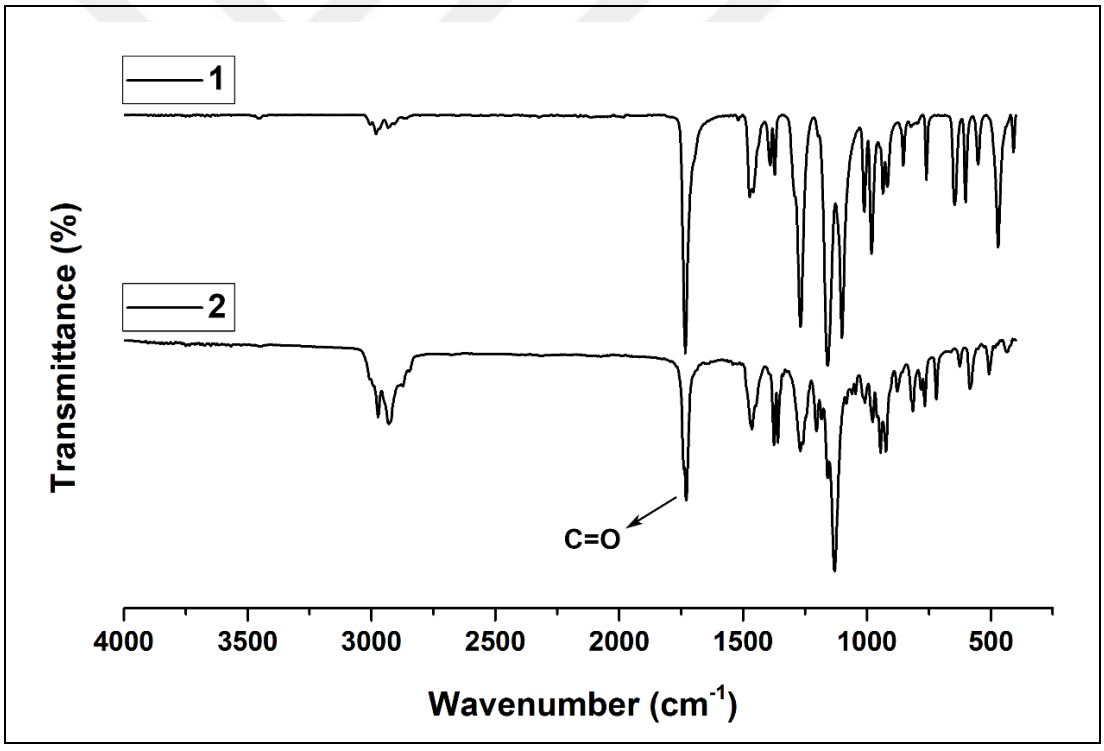

Figure 5.1: FTIR spectra of compound **1**, **2**.

Chemical structures of the synthesized small molecular compounds and star-shaped styrenic copolymers were determined by FTIR and ^{1}H NMR spectroscopies. In the FTIR spectra of compound **1** and **2** (Figure 5.1), aliphatic CH and C=O stretching signals were observed around 2850-3000 and 1730 cm^{-1}, respectively.

Besides, NO stretching frequencies of compound **2** were overlapped by those of geminal CH_3 deformations of TEMPO unit.

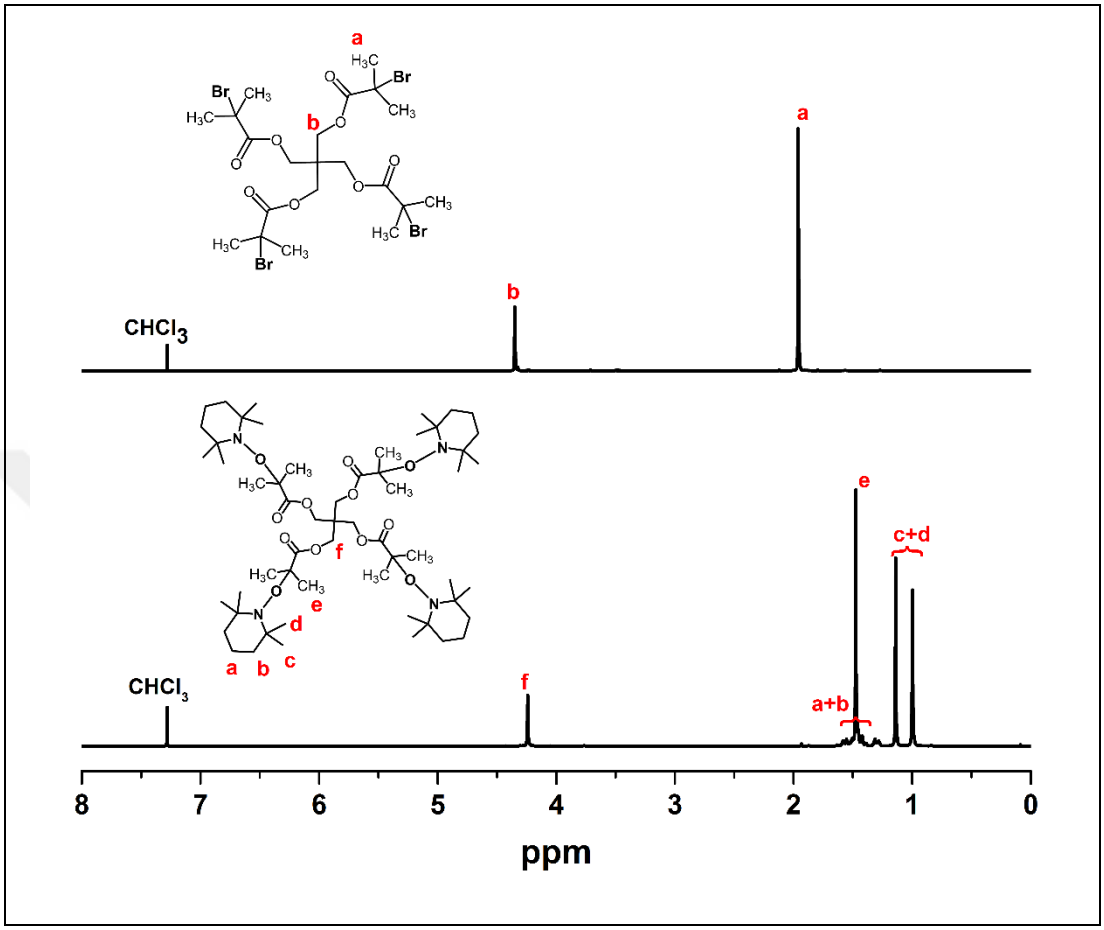

Figure 5.2: ^{1}H NMR spectra of compound **1**, **2**.

The most meaningful information on the success of the synthesis of compound **1** and **2** came from their ^{1}H NMR spectra (Figure 5.2). The methylene (C***H***$_2$OC=O) and terminal C***H***$_3$ protons of **1** resonated at 4.35 and 1.96 ppm, respectively. Upon ATRA reaction of compound **1** with TEMPO, the signals of these protons shifted to higher magnetic field and were observed at 4.24 and 1.47 ppm, respectively, indicating completeness of the reaction. Besides, some new peaks were also observed at 1.00-1.14 and 1.40-1.70 ppm, which were attributed to methyl and methylene protons of TEMPO moiety.

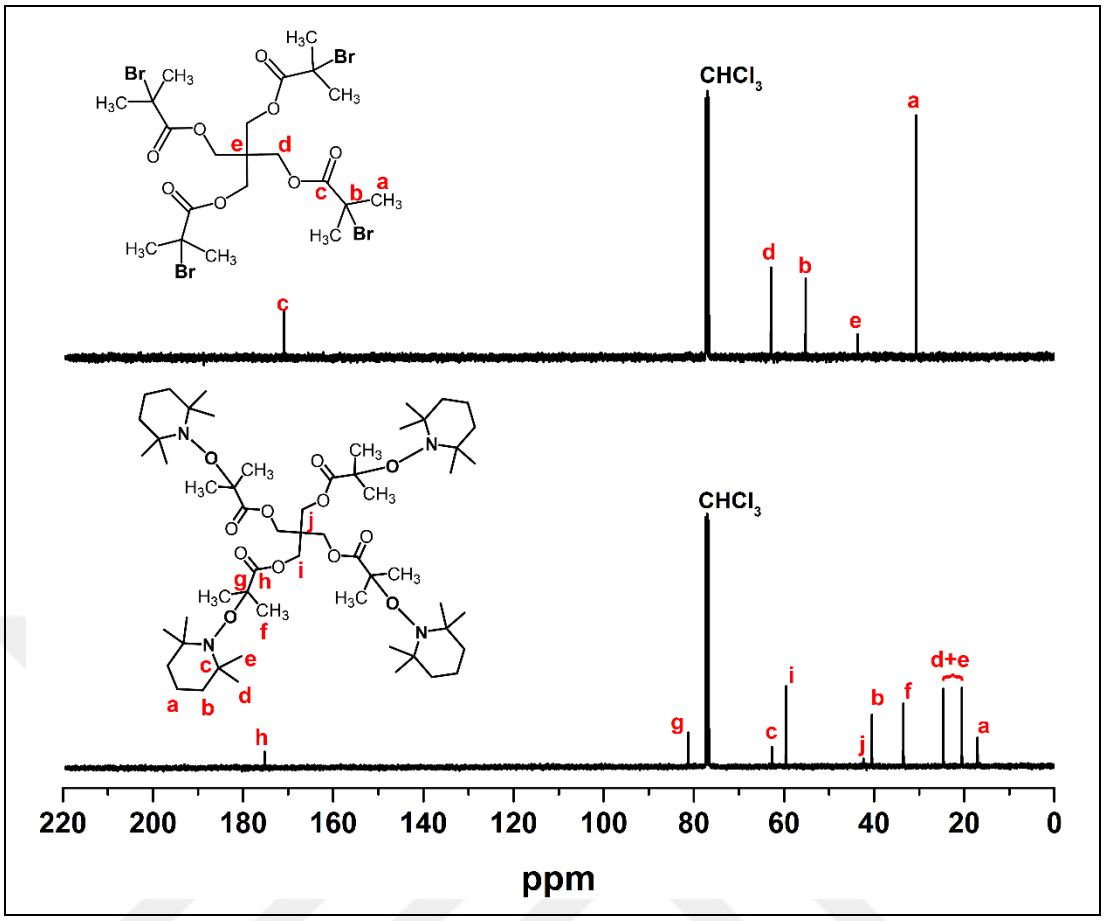

Figure 5.3: ^{13}C NMR spectra of compound **1**, **2**.

The structure of initiator **1** and **2** was also confirmed by ^{13}C NMR spectroscopy (Figure 5.3). The peak (a) of eight methyl carbon atoms of **1** was presented as a sharp peak at 30.64 ppm in the spectrum. Quaternary carbon atoms (b and e) gave resonance at 43.67 and 55.19 ppm, relatively. The methlyene carbon signal (d) is at 62.90 ppm. Carbonyl carbons (c) gave resonance at 170.91. The methylene and methyl carbon atoms in the TEMPO ring of the compound **2** (labeled as a, b, c, d, e) are clearly seen at 17.04, 40.50, 62.68, 20.52 and 24.63 ppm in the spectrum, relatively. The peak (f) of eight methyl carbon atoms was also presented as a one peak at 33.51 ppm in the spectrum. Quaternary carbon atoms (g and j) gave resonance at 81.26 and 42.39 ppm, relatively. The methlyene carbon signals (i) is at 59.60 ppm. Carbonyl carbons (h) gave resonance at 175.23.

In the mass spectra of initiators **1 and 2** obtained in the positive ion mode. The experimental results (*m/z*= 732.8 (M+1)) was very close to the theoretically expected one (*m/z*=731.8). Threotical mass of initiator (**2**), m/z: 1036.77. The found m/z value

is 1037.76 (M+1) in the spectrum (Appendix A). Thus, all the above results confirmed the successful synthesis of initiators **1** and **2**.

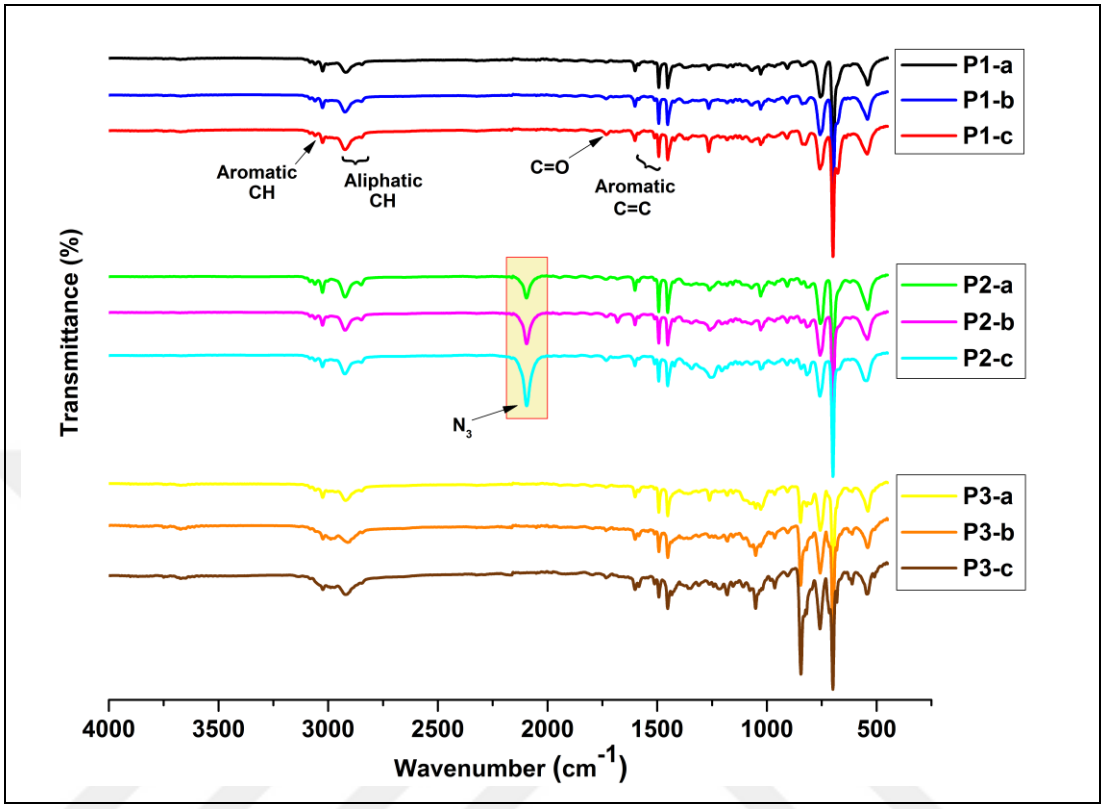

Figure 5.4: FTIR spectra of **P1**, **P2**, **P3** series polymers.

FTIR spectra of tetra armed styrenic star copolymers were demonstrated in Figure 5.4. In these spectra, aromatic and aliphatic CH stretching signals of the star copolymers were observed around 3026−3080 and 2848−2920 cm^{-1}, respectively. The peaks seen at 1601, 1493 and 1452 cm^{-1} were assigned to aromatic C=C stretching frequencies in the phenyl rings. On the other hand, C=O stretching signal of the initiator was hardly seen at 1730 cm^{-1} due to dilution of this residue in the polymer structure. Upon the reaction of the chloride functional styrenic star polymers (**P1-(a-c)**) with sodium azide, emergence of a new signal emerged at 2098 cm^{-1} in the the FTIR spectrum of **P2-(a-c)** is a qualitative indication for the presence of azide functional unit in the chemical structure of the yielded polymer (**P2-(a-c)**). Then, after the Cu(I)-catalyzed 1,3-dipolar cycloaddition reaction between **P2-(a-c)** and 1-ethynylpyrene, the complete disappearance of this signal indicated that azide-functional units were quantitively converted to pyrene groups, yielding **P3-(a-c)**.

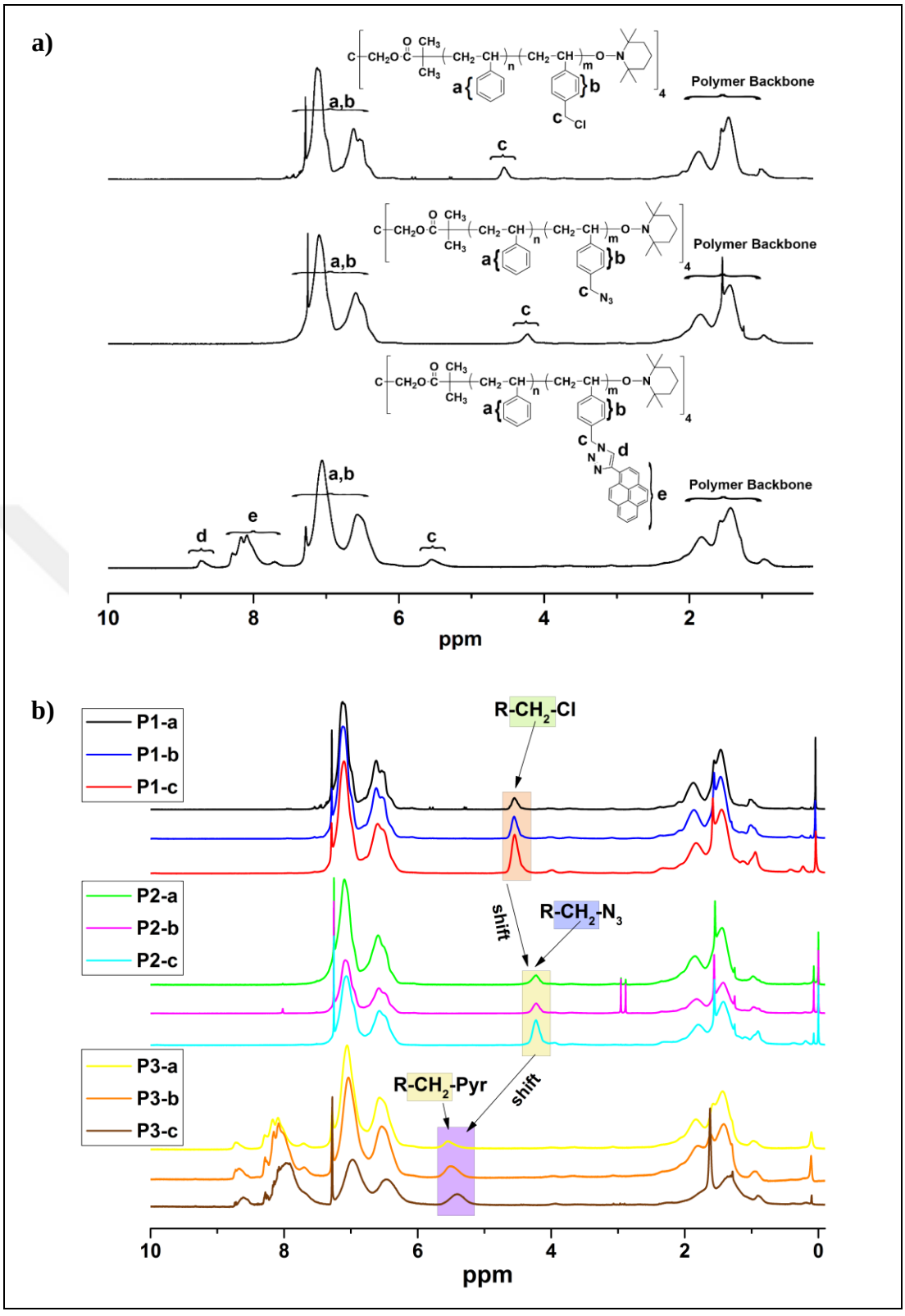

Figure 5.5: a) ^{1}H NMR spectra of **P1-a**, **P2-a**, **P3-a**, b) **P1**, **P2**, **P3** series polymers.

^{1}H NMR spectra of the styrenic star copolymers were given in Figure 5.5. In these spectra, the polymer backbone protons gave signals between 1.44 and 2.02 ppm,

while aromatic C***H*** protons ($H_{a,b}$) in styrene and vinylbenzyl repeating units produced resonances between 6.47− 7.11 ppm. In the ^{1}H NMR spectrum of **P1-(a-c)** (Figure 5.5b), the signal of the methylene protons (H_c) adjacent to the benzene ring was observed at 4.52 ppm, and shifted slightly to higher magnetic field (4.21 ppm) as a result of azidification. After 1,3-dipolar cycloaddiditon (click) reaction between **P2-(a-c)** with 1-ethynylpyrene, these signals moved to downfield and gave resonances at 5.47 ppm. The clear shift of H_c protons on azidification and click reactions further proves the success of the reactions. Besides, some new proton resonance signals were seen in the ^{1}H NMR spectrum of **P3-(a-c)** and they were attributed to triazole methine protons (H_d, 8.70 ppm) and aromatic C***H*** protons of pendant pyrene units (H_e, 7.68-8.68 ppm).

Average molecular weights (M_n and M_w) and polydispersity indexes (PDIs) of the obtained star-shaped styrenic polymers were determined via gel permeation chromatography (GPC) analysis. The star polymers demonstrated monodisperse chromatogram curves with reasonably low PDI values between 1.38 and 1.58, pointing out that either polymerization products or post-modified polymers contained only the targeted ones. On the other hand, the values obtained through GPC experiments are only estimated results based on linear polystyrene standards. Unfortunately, these calibration standards have different hydrodynamic volumes from the synthesized star-shaped polymers with different functional units. Therefore, average molecular weights obtained from conventional GPC experiments have limited reliability with respect to those obtained via NMR calculations [30]. In the ^{1}H NMR spectra of the prepared star polymers, any discernable signal belonging to terminal TEMPO and initiating core residues were not observed since they are overlapped by those of the repeating units or diluted by those of long polymer chains. On the other hand, m/n ratios for the monomeric residues (see Figure 4.1) were calculated from ratios of integral peak areas aromatic phenyl ($C_6\boldsymbol{H}_5$ plus $C_6\boldsymbol{H}_4$-CH_2-) and methylene protons next to the benzene ring (C_6H_4−C$\boldsymbol{H}_2$) and were summarized in Table 5.1. Thus, the molar mass of the polymer fragments having single functional grup (-Cl or -N_3) were computed with the equation (m/n) × M_w of styrene + M_w of chloride or azide functional repeating units [61].

Table 5.1: Results of the star-shaped styrenic copolymers with different side-functional groups.

Polymers	Feeds	Composition [a] (n/m)	$M_{n,\ NMR}$	$M_{n,\ GPC}$ [b]	M_w/M_n [b]	Functional Groups
P1-a	100:5	10	36400	15300	1.46	
P1-b	100:10	5.2	28800	14800	1.57	-Cl
P1-c	100:15	2.6	18000	13700	1.49	
P2-a	100:5	10	36600	15600	1.46	
P2-b	100:10	5.2	29000	15000	1.58	$-N_3$
P2-c	100:15	2.6	17800	14100	1.57	
P3-a	100:5	10	43300	15900	1.45	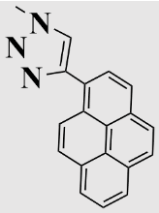
P3-b	100:10	5.2	38200	15300	1.49	
P3-c	100:15	2.6	27300	14400	1.38	

[a] See Figure 4:1 for "n" and "m". It was calculated from ratios of integral peak areas aromatic phenyl ($C_6\boldsymbol{H}_5$ plus $C_6\boldsymbol{H}_4$-CH_2-) and methylene protons next to the benzene ring (C_6H_4–$C\boldsymbol{H}_2$) in related ^{1}H NMR spectra.

[b] $M_{n,GPC}$ and M_w/M_n were determined via GPC analysis using linear polystyrene calibration standards with narrow molecular weight distributions.

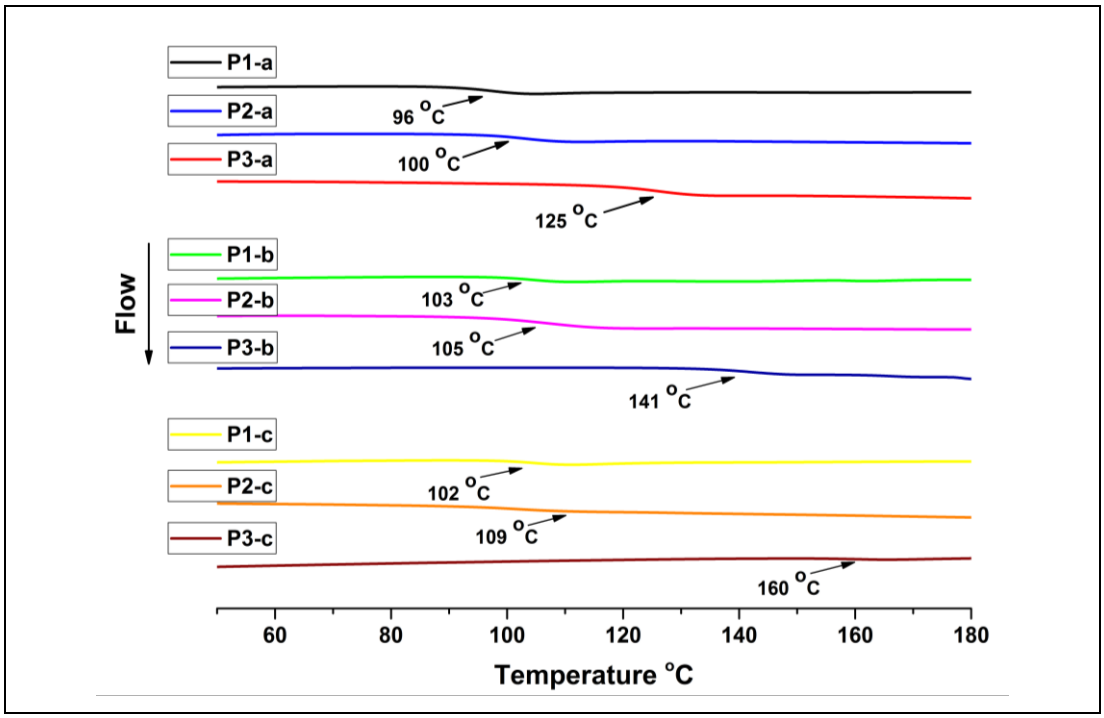

Figure 5.6: DSC curves of **P1**, **P2**, **P3** series polymers.

Differential scanning calorimetry (DSC) experiments were conducted to determine thermal phase transitions of the prepared styrenic star copolymers. The midpoint of the heat capacity change was taken as glass transition temperature (T_g) and the relevant data were presented in Table 5.2. DSC thermograms of **P1-P3** series copolymers were demonstrated in Figure 5.6. In these thermograms, T_g of chloride-functional tetra-armed star shaped (**P1-(a-c)**) were found to be close to each other. Upon incorporation and increase in the number of azide-functional units, only slight enhancement was observed in the T_g values of the copolymers (**P2-(a-c)**). On the other hand, binding of pendant bulky pyrene groups raised substantially the T_g of **P1-c** by 25 °C and increase in T_g values of the pyrene-functional copolymers were getting more pronounced for **P2-c** (36 °C) and **P3-c** (51 °C) as their pyrene contents were increased. These results were attributed to the increase in the rigidity of the pyrene-functional star copolymers due to π-stacking interaction between pyrene side-units, as well as their bulky structure [30].

Table 5.2: Thermal properties of star-shaped styrenic copolymers with different functional groups.

Polymers	T_g **(°C)** [a]	T_{onset} **°C)** [b]	T_{max} **(°C)** [c]	**Char Yield (%)** [d]
P1-a	96	286	405	4
P2-a	100	271	394	6
P3-a	125	328	401	15
P1-b	103	287	417	8
P2-b	105	235	392	8
P3-b	141	336	387	23
P1-c	102	264	402	12
P2-c	109	218	385	14
P3-c	160	306	409	28

Table: 5.2. Continuation of the table.

[a] T_g is the glass transition temperature (The midpoint of the heat capacity change was taken) of the polymers in DSC experiments.
[b] T_{onset} is the onset decomposition temperature (3% mass fraction loss) of the polymers in TGA experiments.
[c] T_{max} is the temperature corresponding to the maximum rate of weight loss in TGA experiments.
[d] The percent of the mass remained at 700 °C in TGA experiments.

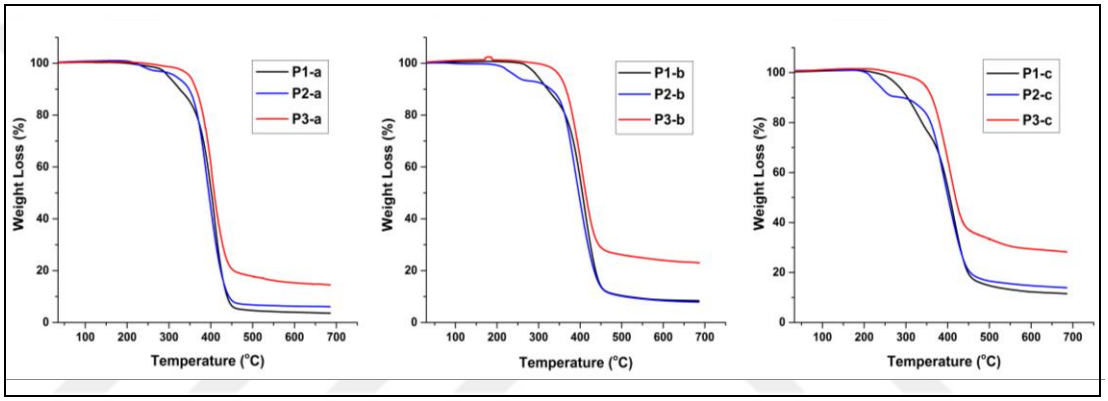

Figure 5.7: TGA thermograms of **P1**, **P2**, **P3** series polymers.

Thermal stabilities of the synthesized tetra-armed star-shaped copolymers were studied via TGA experiments under inert nitrogen atmosphere. Percent weight loss/temperature curves of the **P1-P3** series star-shaped copolymers were demonstrated in Figure 5.7. The data related to their initial (T_{onset}) and maximum (T_{max}) decomposition temperatures as well as their percent char yields were summarized in Table 5.2. In these thermograms, chloride-functional star copolymers decomposed in a single step starting around 264-287 °C, whereas azide-functional copolymers showed two-step decomposition profiles due to evolution of nitrogen gas above 200 °C [77-78]. Besides, the amount of decomposition in the first step and decrease in the T_{onset} values of the star copolymers became more remarkable as the azide content of the copolymers was increased. On the other hand, incorporation of pyrene-functional units considerably enhanced T_{onset} values of the star copolymers as well as their char yields.

5.2. Characterization of Pyrene Functional Three-Armed Star-Shaped Styrene Copolymers (P6-(a-c))

Tri-Pyrene Functional Star-Shaped Styrene Copolymers (**P6-(a-c)**) were prepared using styrene (St) and 4-vinylbenzylchloride (VBCl) as the monomer at different molar ratios (St:VBCl; 100:5, 100:10 and 100:15 per arm). Chemical structures of the synthesized small molecular compounds and star-shaped styrenic copolymers were determined by FTIR and ^{1}H NMR spectroscopies. Also used GPC, DSC and TGA characterization techniques for chemical structure determination. Finally, nitroaromatic sensing applications of pyrene functional polystyrene copolymers were performed via fluorescence spectroscopy.

The synthesis of pyrene-functional star-shaped styrenic copolymers (**P6-(a-c)**) were started with the preparation of the tri-bromo functional compound (**3**) through esterification of pentaerythritol and 2-bromoisobutyryl bromide. Then, an atom transfer radical addition (ATRA) reaction between bromide functional groups of **3** and 2,2,6,6-tetramethyl-1-piperidinyloxy (TEMPO) in the presence of CuBr/PMDETA catalyst system produced a novel tri-TEMPO functional alkoxyamine compound (**4**). Subsequently, compound **4** was employed a unimolecular initiator in the NMP of St and VBC at different monomer feed ratios to produce a tri-armed styrenic star copolymers with chloride side-functional units (**P4-(a-c)**). Then, chloride side-groups of (**P4-(a-c)**) were reacted with sodium azide in DMF, yielding azide-functional star-shaped styrenic copolymers (**P5-(a-c)**). Finally, pyrene-functional styrenic star copolymers (**P6-(a-c)**) were obtained quantitatively through 1,3-dipolar cycloaddition (click) reaction between azide-functional groups of (**P5-(a-c)**) and 1-ethynylpyrene.

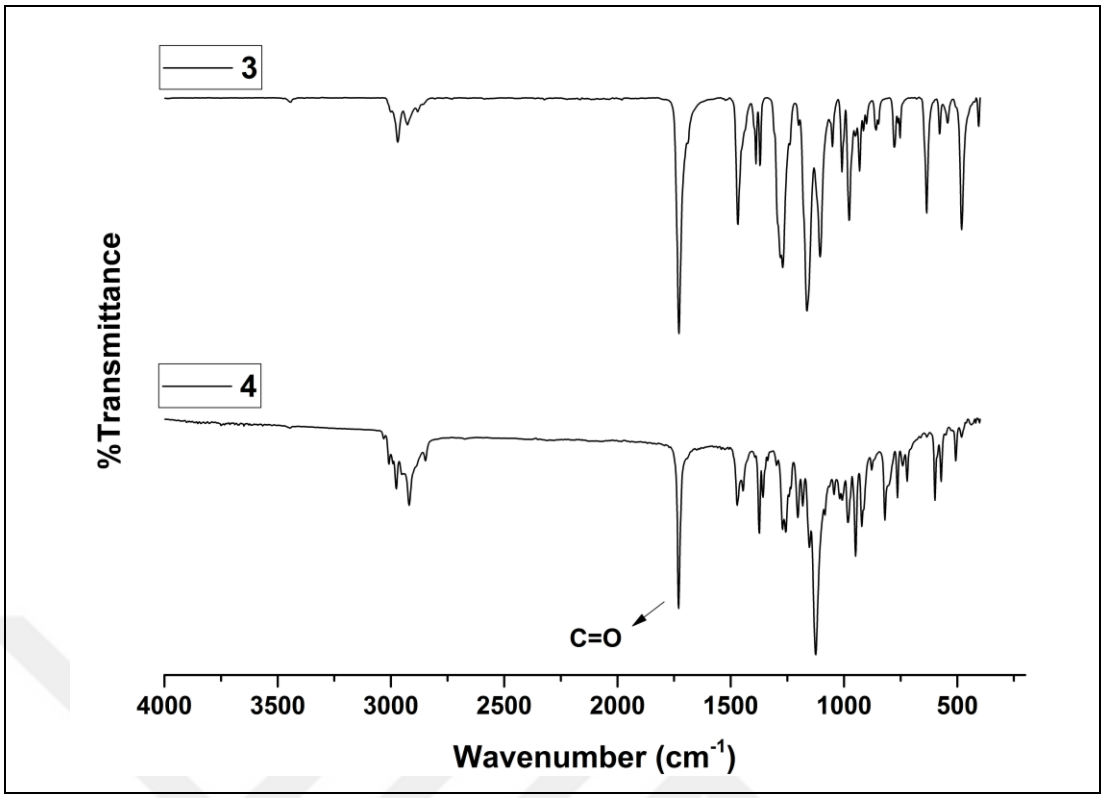

Figure 5.8: FTIR spectra of compound **3**, **4**.

Chemical structures of the synthesized small molecular compounds and star-shaped styrenic copolymers were determined by FTIR and ^{1}H NMR spectroscopies. In the FTIR spectra of compound **3** and **4** (Figure 5.8), aliphatic CH and C=O stretching signals were observed around 2800-3000 and 1730 cm^{-1}, respectively. Besides, NO stretching frequencies of compound **4** were overlapped by those of geminal CH_3 deformations of TEMPO unit.

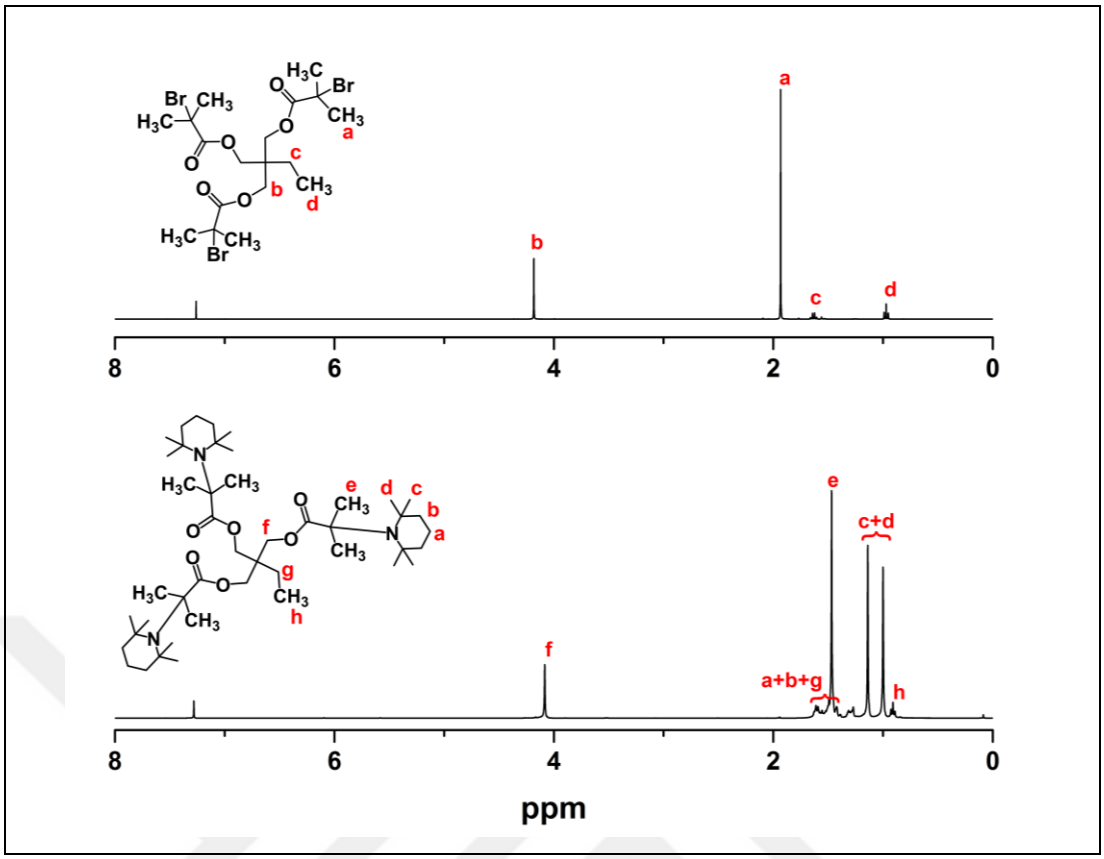

Figure 5.9: ^{1}H NMR spectra of compound **3**, **4**.

The most meaningful information on the success of the synthesis of compound **3** and **4** came from their ^{1}H NMR spectra (Figure 5.9). The methylene (H_b, C***H***$_2$OC=O), (H_c, C***H***$_2$-CH_3) and terminal C***H***$_3$ protons (H_a and H_d) of **3** resonated at 4.35, 1.63, 1.96 and 0.97 ppm, respectively. Upon ATRA reaction of compound **3** with TEMPO, the signals of these protons (H_b, H_a and H_d) shifted to higher magnetic field and were observed at 4.08, 1.46 and 0.91 ppm, respectively, indicating completeness of the reaction. Besides, some new peaks were also observed at 1.00-1.14 and 1.40-1.70 ppm, which were attributed to methyl and methylene protons of TEMPO moiety.

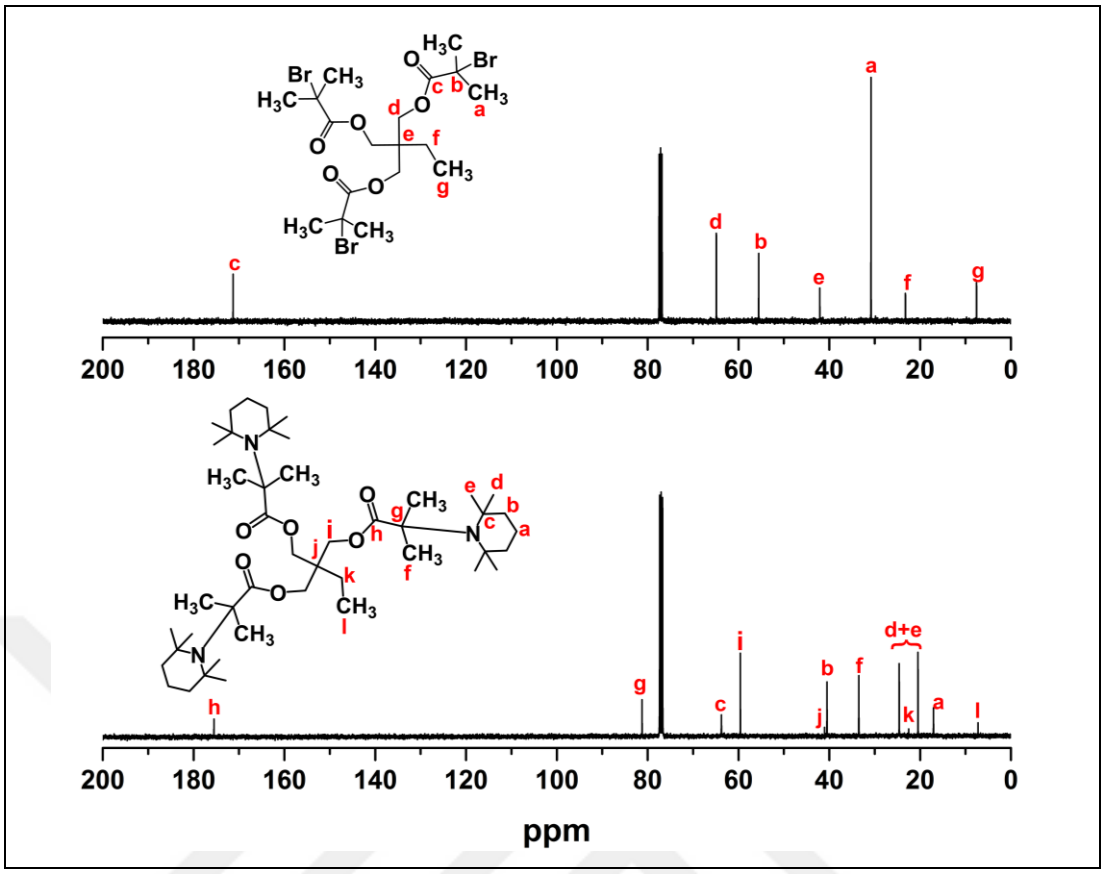

Figure 5.10: ^{13}C NMR spectra of compound **3**, **4**.

The structure of initiator **3** and **4** was also confirmed by ^{13}C NMR spectroscopy (Figure5.10). The terminal methyl carbon atom (g) gave resonance at 7.58 ppm. The peak (a) of six methyl carbon atoms of **3** was presented as a sharp peak at 30.81 ppm in the spectrum. Quaternary carbon atoms (b and e) gave resonance at 55.55 and 42.09 ppm, relatively. The methlyene carbon signals (d) and (f) are at 64.87 and 23.23 ppm, respectively. Carbonyl carbons (c) gave resonance at 171.30. The methylene and methyl and quaternary carbon atoms in the TEMPO rings of **4** (labeled as a, b, c, d, e) are clearly seen at 17.06, 40.51, 63.76, 24.67 and 20.47 ppm in the spectrum, relatively. The peak (f) of six methyl carbon atoms was also presented as a one peak at 33.49 ppm in the spectrum. Quaternary carbon atoms (g and j) gave resonance at 81.24 and 41.05 ppm, relatively. The methlyene carbon signals (i and k) were at 59.58 and 22.52 ppm, respectively. Carbonyl carbons (h) gave resonance at 175.50 (lowest field). Besides, the terminal -CH_3 carbon atom (l) was shown at highest field (7.25 ppm).

In the mass spectra of initiators **3 and 4** obtained in the positive ion mode. The experimental results (*m/z*= 601.4 (M+Na)) was very close to the theoretically expected

one (*m/z*=577.9). Threotical mass of initiator (**2**), m/z: 809.61. The found m/z value is 810.59 (M+1) in the spectrum (Appendix A). Thus, all the above results confirmed the successful synthesis of initiators **3** and **4**.

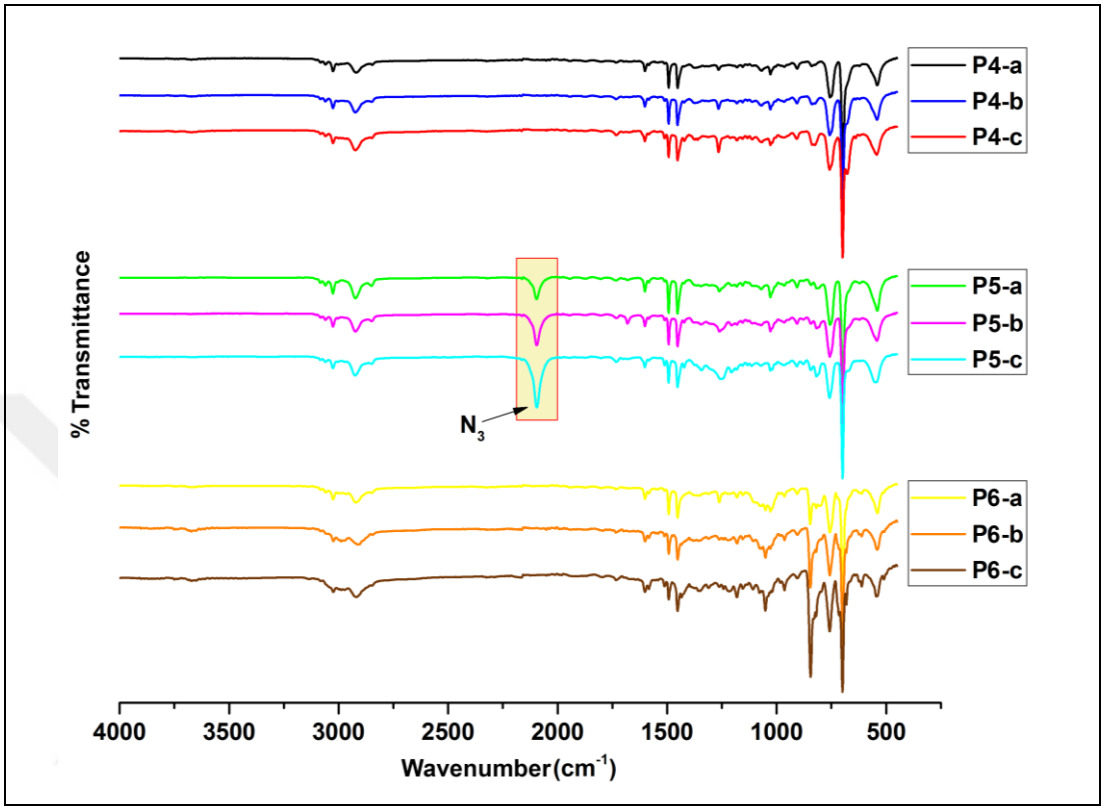

Figure 5.11: FTIR spectra of **P4**, **P5**, **P6** series polymers.

FTIR spectra of styrenic tri-functional star copolymers were demonstrated in Figure 5.11. In these spectra, aromatic and aliphatic CH stretching signals of the tri-functional star copolymers were observed around 3026−3080 and 2840−2920 cm^{-1}, respectively. The peaks seen at 1601, 1493 and 1452 cm^{-1} were assigned to aromatic C=C stretching frequencies in the phenyl rings. On the other hand, C=O stretching signal of the initiator was hardly seen at 1730 cm^{-1} due to dilution of this residue in the polymer structure. Upon the reaction of the chloride functional styrenic star polymers (**P4-(a-c)**) with sodium azide, emergence of a new signal emerged at 2095 cm^{-1} in the the FTIR spectrum of **P5-(a-c)** is a qualitative indication for the presence of azide functional unit in the chemical structure of the yielded polymers (**P5-(a-c)**). Then, after the Cu(I)-catalyzed 1,3-dipolar cycloaddition reaction between **P5-(a-c)** and 1-ethynylpyrene, the complete disappearance of this signal indicated that azide-functional units were quantitively converted to pyrene groups, yielding **P6-(a-c)**.

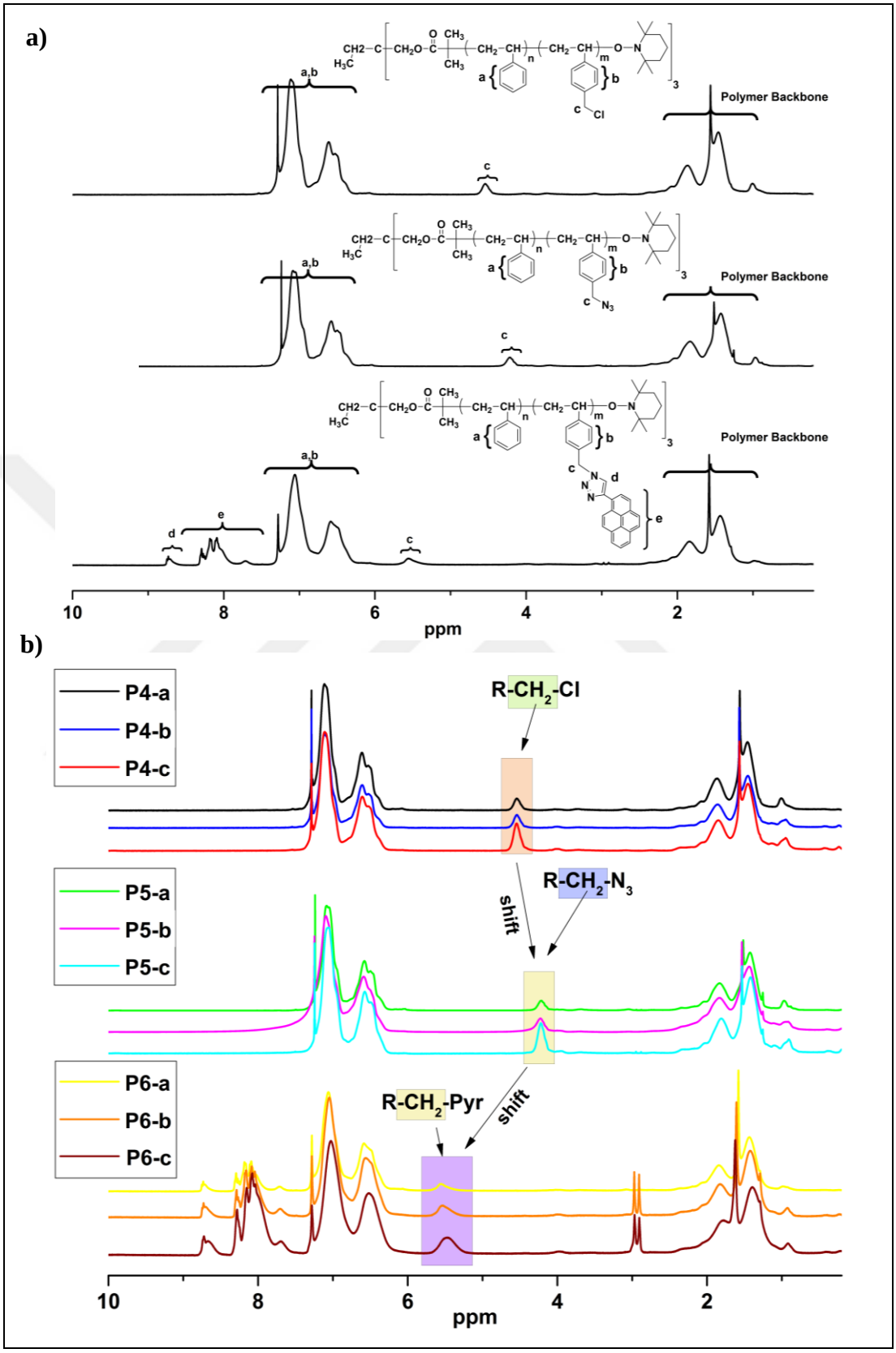

Figure 5.12: a) ^{1}H NMR spectra of **P4-a**, **P5-a**, **P6-a**, b) **P4**, **P5**, **P6** series polymers.

^{1}H NMR spectra of the styrenic tri-functional star copolymers were given in Figure 5.12. In these spectra, the polymer backbone protons gave signals between 1.44 and 2.02 ppm, while aromatic C***H*** protons ($H_{a,b}$) in styrene and vinylbenzyl repeating units produced resonances between 6.47− 7.11 ppm. In the ^{1}H NMR spectrum of **P4-(a-c)** (Figure 5.12b), the signal of the methylene protons (H_c) adjacent to the benzene ring was observed at 4.52 ppm, and shifted slightly to higher magnetic field (4.21 ppm) as a result of azidification. After 1,3-dipolar cycloaddiditon (click) reaction between **P5-(a-c)** with 1-ethynylpyrene, these signals moved to downfield and gave resonances at 5.47 ppm. The clear shift of H_c protons on azidification and click reactions further proves the success of the reactions. Besides, some new proton resonance signals were seen in the ^{1}H NMR spectrum of **P6-(a-c)** and they were attributed to triazole methine protons (H_d, 8.70 ppm) and aromatic C***H*** protons of pendant pyrene units (H_e, 7.68-8.68 ppm).

Average molecular weights (M_n and M_w) and polydispersity indexes (PDIs) of the obtained star-shaped styrenic polymers were determined via gel permeation chromatography (GPC) analysis. The star polymers demonstrated monodisperse chromatogram curves with reasonably low PDI values between 1.34 and 1.51, pointing out that either polymerization products or post-modified polymers contained only the targeted ones. On the other hand, the values obtained through GPC experiments are only estimated results based on linear polystyrene standards. Unfortunately, these calibration standards have different hydrodynamic volumes from the synthesized star-shaped polymers with different functional units. Therefore, average molecular weights obtained from conventional GPC experiments have limited reliability with respect to those obtained via NMR calculations [30]. In the ^{1}H NMR spectra of the prepared star polymers, any discernable signal belonging to terminal TEMPO and initiating core residues were not observed since they are overlapped by those of the repeating units or diluted by those of long polymer chains. On the other hand, m/n ratios for the monomeric residues (see Figure 4.2) were calculated from ratios of integral peak areas aromatic phenyl ($C_6\boldsymbol{H}_5$ plus $C_6\boldsymbol{H}_4$-CH_2-) and methylene protons next to the benzene ring (C_6H_4−C$\boldsymbol{H}_2$) and were summarized in Table 5.3. Thus, the molar mass of the polymer fragments having single functional grup (-Cl or -N_3) were computed with the equation (m/n) × M_w of styrene + M_w of chloride or azide functional repeating units [61].

Table 5.3: Results of the tri-armed star-shaped styrenic copolymers with different side-functional groups.

Polymers	Feeds	Composition [a] (n/m)	$M_{n,\,NMR}$	$M_{n,\,GPC}$ [b]	M_w/M_n [b]	Functional Groups
P4-a	100:5	10.1	13400	12100	1.51	
P4-b	100:10	6.7	14900	11500	1.44	**-Cl**
P4-c	100:15	3.9	17600	11200	1.44	
P5-a	100:5	10.1	13500	12300	1.51	
P5-b	100:10	6.7	15000	11750	1.46	**$-N_3$**
P5-c	100:15	3.9	17800	11350	1.46	
P6-a	100:5	10.1	15800	12600	1.44	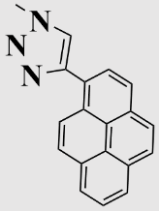
P6-b	100:10	6.7	18700	12200	1.34	
P6-c	100:15	3.9	24600	11700	1.35	

[a] See Figure 4:2 for "n" and "m". It was calculated from ratios of integral peak areas aromatic phenyl ($C_6\boldsymbol{H}_5$ plus $C_6\boldsymbol{H}_4$-CH_2-) and methylene protons next to the benzene ring (C_6H_4–$C\boldsymbol{H}_2$) in related ^{1}H NMR spectra.

[b] $M_{n,GPC}$ and M_w/M_n were determined via GPC analysis using linear polystyrene calibration standards with narrow molecular weight distributions.

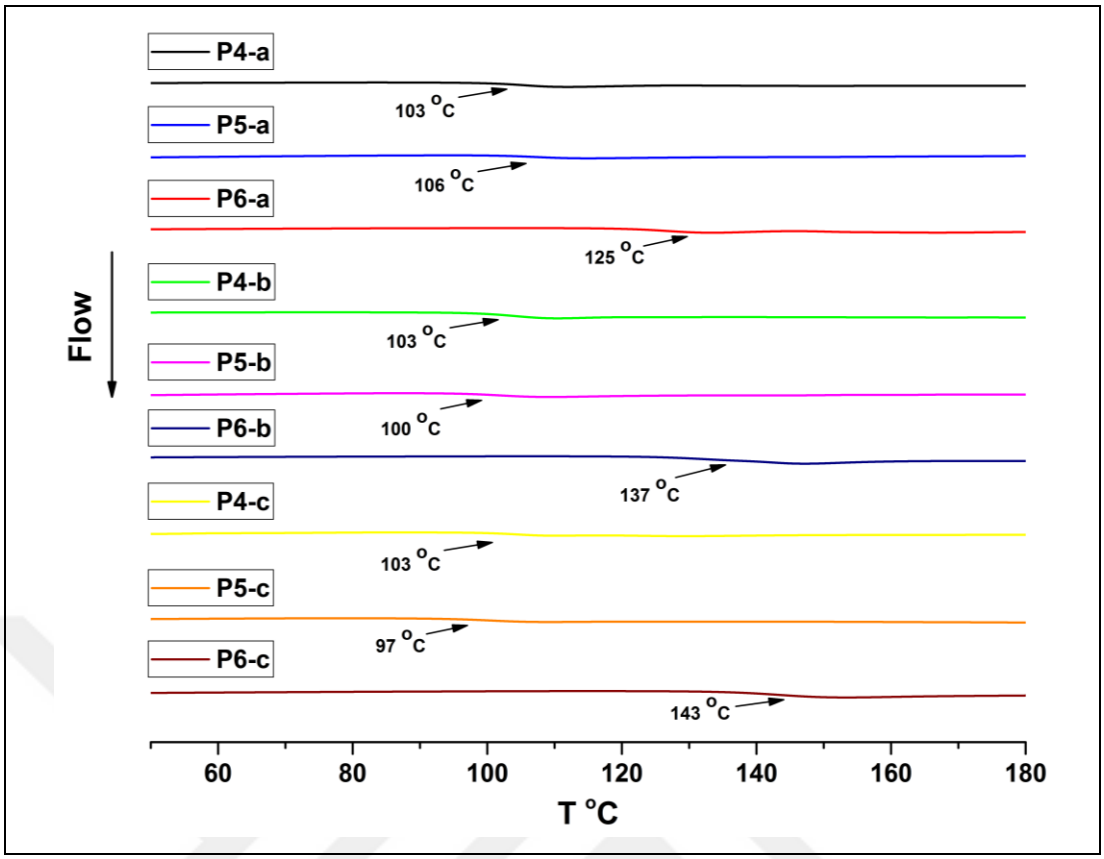

Figure 5.13: DSC curves of **P4**, **P5**, **P6** series polymers.

Differential scanning calorimetry (DSC) experiments were conducted to determine thermal phase transitions of the prepared styrenic tri-armed star copolymers. The midpoint of the heat capacity change was taken as glass transition temperature (T_g) and the relevant data were presented in Table 5.4. DSC thermograms of **P4-P6** series copolymers were demonstrated in Figure 5.13. In these thermograms, T_g of chloride-functional tetra-armed star shaped (**P4-(a-c)**) were found to be close to each other. Upon incorporation and increase in the number of azide-functional units, only slight enhancement was observed in the T_g values of the copolymers (**P5-(a-c)**). On the other hand, binding of pendant bulky pyrene groups raised substantially the T_g of **P4-c** by 25 °C and increase in T_g values of the pyrene-functional copolymers were getting more pronounced for **P5-c** (36 °C) and **P6-c** (51 °C) as their pyrene contents were increased. These results were attributed to the increase in the rigidity of the pyrene-functional star copolymers due to π-stacking interaction between pyrene side-units, as well as their bulky structure [30].

Table 5.4: Thermal properties of tri-armed star-shaped styrenic copolymers with different functional groups.

Polymers	T_g (°C) [a]	T_{onset} °C) [b]	T_{max} (°C) [c]	Char Yield (%) [d]
P4-a	103	290	403	3
P5-a	106	262	401	4
P6-a	125	338	397	10
P4-b	103	267	406	3
P5-b	100	235	390	3
P6-b	137	340	381	17
P4-c	103	281	409	6
P5-c	97	224	382	6
P6-c	143	340	386	22

[a] T_g is the glass transition temperature (The midpoint of the heat capacity change was taken) of the polymers in DSC experiments.

[b] T_{onset} is the onset decomposition temperature (3% mass fraction loss) of the polymers in TGA experiments.

[c] T_{max} is the temperature corresponding to the maximum rate of weight loss in TGA experiments.

[d] The percent of the mass remained at 700 °C in TGA experiments.

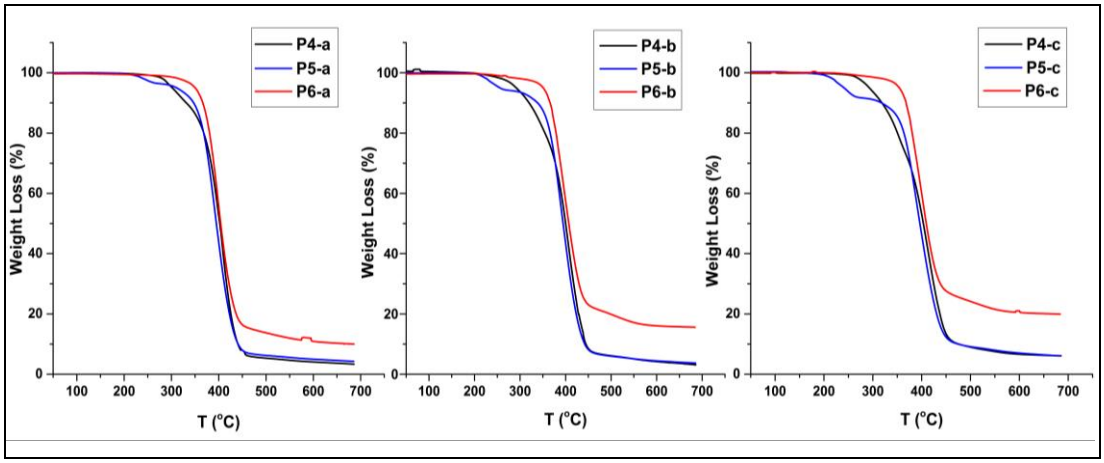

Figure 5.14: TGA thermograms of **P4**, **P5**, **P6** series polymers.

Thermal stabilities of the synthesized tri-armed star-shaped copolymers were studied via TGA experiments under inert nitrogen atmosphere. Percent weight loss/temperature curves of the **P4-P6** series star-shaped copolymers were demonstrated in Figure 5.14. The data related to their initial (T_{onset}) and maximum (T_{max}) decomposition temperatures as well as their percent char yields were summarized in Table 5.4. In these thermograms, chloride-functional star copolymers decomposed in a single step starting around 267-290 °C, whereas azide-functional copolymers showed two-step decomposition profiles due to evolution of nitrogen gas above 220 °C [77-78]. Besides, the amount of decomposition in the first step and decrease in the T_{onset} values of the star copolymers became more remarkable as the azide content of the copolymers was increased. On the other hand, incorporation of pyrene-functional units considerably enhanced T_{onset} values of the star copolymers as well as their char yields.

5.3. Characterization of Pyrene Functional Linear Styrene Copolymers (P9-(a-c))

Pyrene Functional Linear Styrene Copolymers (P9-(a-c)) were prepared using styrene (St) and 4-vinylbenzylchloride (VBCl) as the monomer at different molar ratios (St:VBCl; 100:5, 100:10 and 100:15 per arm). Chemical structures of the synthesized small molecular compounds linear styrenic copolymers were determined by FTIR and ^{1}H NMR spectroscopies. Also used GPC, DSC and TGA characterization techniques for chemical structure determination. Finally, nitroaromatic sensing applications of pyrene functional polystyrene copolymers were performed via fluorescence spectroscopy.

The synthesis of pyrene-functional linear styrenic copolymers (**P9-(a-c)**) were started with the preparation of the di-bromo functional compound (**5**) through esterification of ethyleneglycol and 2-bromoisobutyryl bromide. Then, an atom transfer radical addition (ATRA) reaction between bromide functional groups of **5** and 2,2,6,6-tetramethyl-1-piperidinyloxy (TEMPO) in the presence of CuBr/PMDETA catalyst system produced a novel TEMPO functional alkoxyamine compound (**6**). Subsequently, compound **6** was employed a unimolecular initiator in the NMP of St and VBC at different monomer feed ratios to produce linear copolymers with chloride side-functional units (**P7-(a-c)**). Then, chloride side-groups of (**P7-(a-c)**) were reacted

with sodium azide in DMF, yielding azide-functional linear styrenic copolymers (**P8-(a-c)**). Finally, pyrene-functional styrenic linear copolymers (**P9-(a-c)**) were obtained quantitatively through 1,3-dipolar cycloaddition (click) reaction between azide-functional groups of (**P8-(a-c)**) and 1-ethynylpyrene.

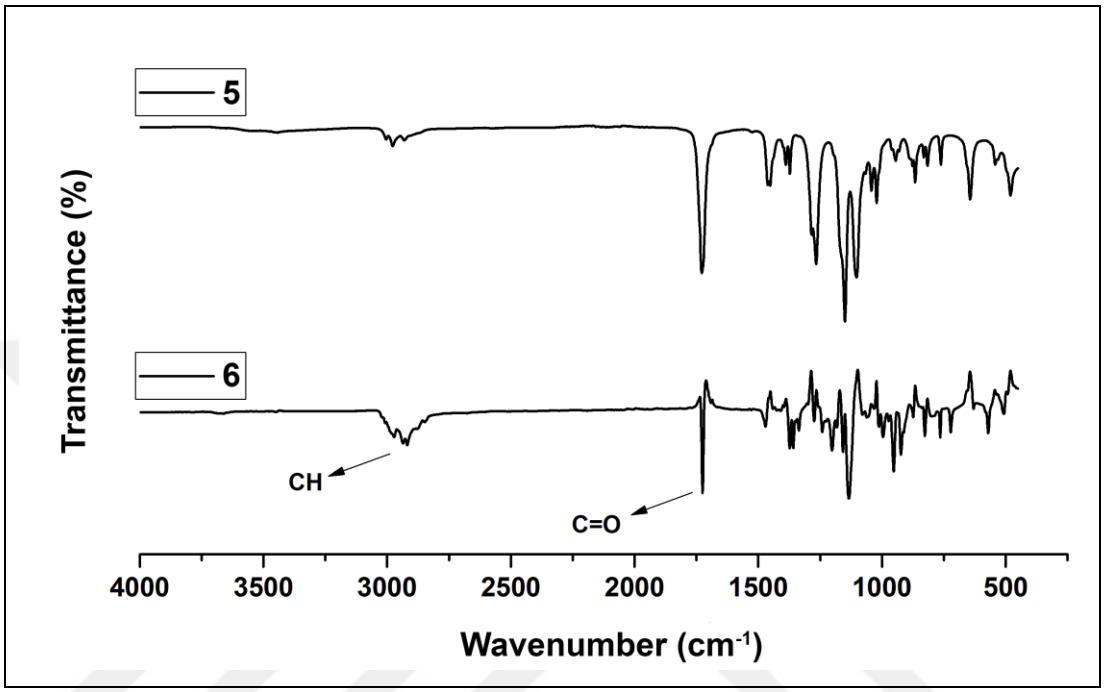

Figure 5.15: FTIR spectra of compound **5**, **6**.

Chemical structures of the synthesized small molecular compounds and linear styrenic copolymers were determined by FTIR and ^{1}H NMR spectroscopies. In the FTIR spectra of compound **5** and **6** (Figure 5.15), aliphatic CH and C=O stretching signals were observed around 2850-3000 and 1730 cm^{-1}, respectively. Besides, NO stretching frequencies of compound **6** were overlapped by those of geminal CH_3 deformations of TEMPO unit.

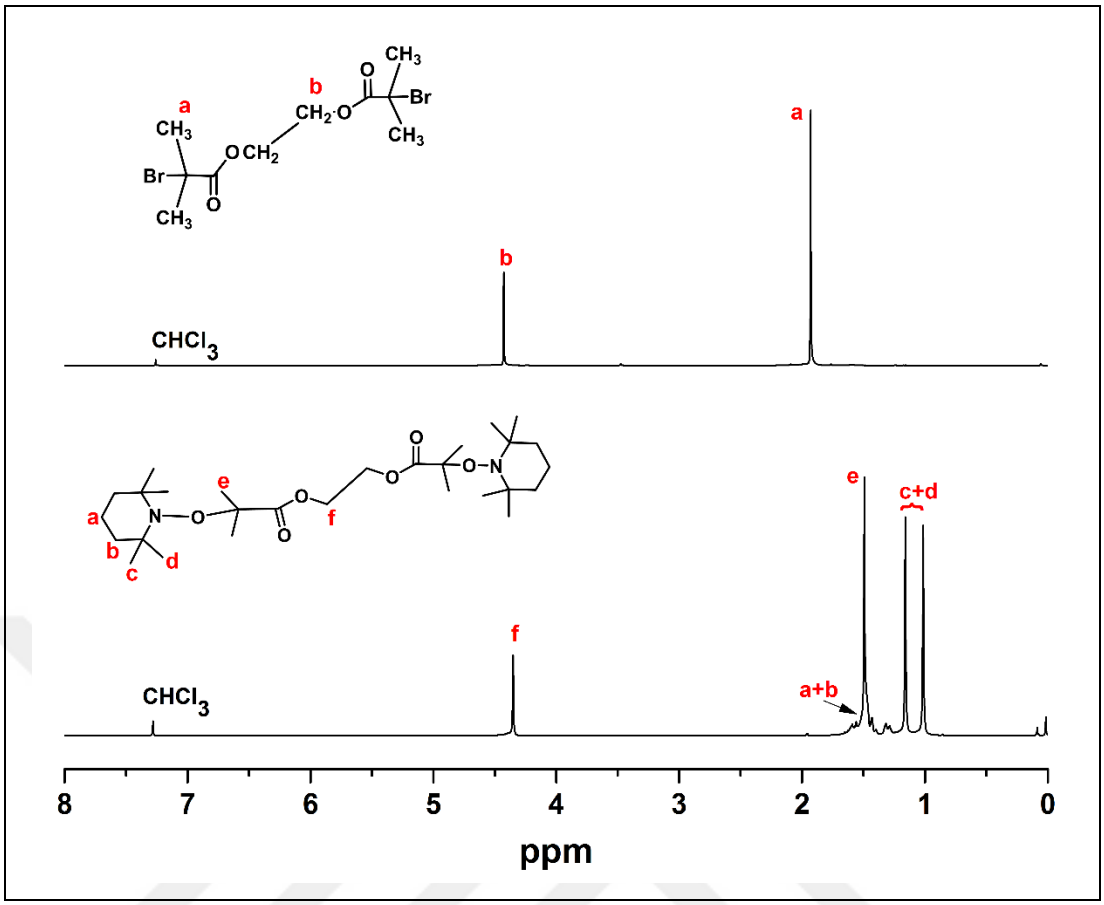

Figure 5.16: ^{1}H NMR spectra of compound **5**, **6**.

The most meaningful information on the success of the synthesis of compound **5** and **6** came from their ^{1}H NMR spectra (Figure 5.16). The methylene (C***H***$_2$OC=O) and terminal C***H***$_3$ (a) protons of **5** resonated at 4.45 and 1.95 ppm, respectively. Upon ATRA reaction of compound **5** with TEMPO, the signals of these protons shifted to higher magnetic field and were observed at 4.35 and 1.49 ppm, respectively, indicating completeness of the reaction. Besides, some new peaks were also observed at 1.01-1.61 and 1.40-1.80 ppm, which were attributed to methyl and methylene protons of TEMPO moiety.

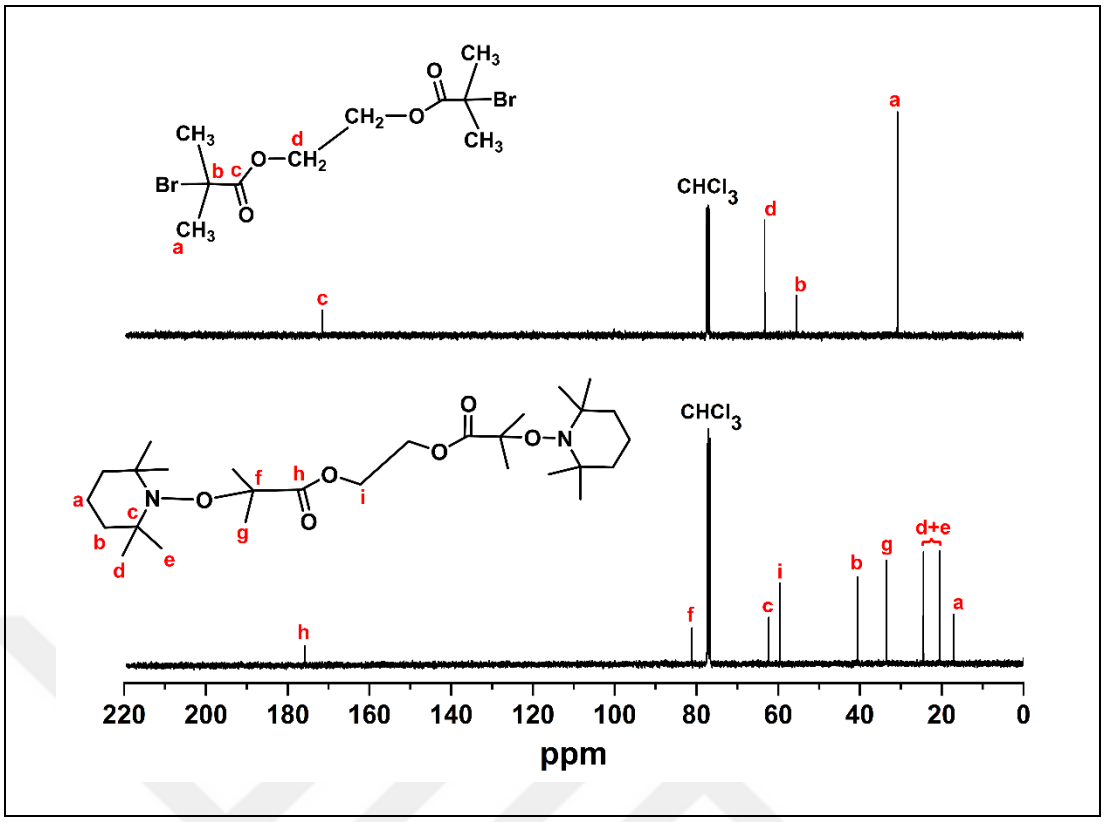

Figure 5.17: ^{13}C NMR spectra of compound **5**, **6**.

The structure of initiator compounds **5** and **6** was also confirmed by ^{13}C NMR spectroscopy (Figure 5.17). The peak (a) of four methyl carbon atoms of **5** was presented as a sharp peak at 30.69 ppm in the spectrum. Quaternary carbon atom (b) gave resonance at 55.34 ppm. The methlyene carbon signal (d) is at 63.19 ppm. Carbonyl carbons (c) gave resonance at 171.42. The methylene and methyl carbon atoms in the TEMPO ring of the compound **6** (labeled as a, b, c, d, e) are clearly seen at 17.07, 40.58, 62.68, 20.49 and 24.47 ppm in the spectrum, relatively. Quaternary carbon atom (f) gave resonance at 81.11 ppm. The peak (g) of four methyl carbon atoms was also presented as a one peak at 33.49 ppm in the spectrum. The methlyene carbon signals (i) is at 59.57 ppm. Carbonyl carbons (h) gave resonance at 175.81.

In the mass spectra of initiator **6** obtained in the positive ion mode, the experimental result (*m/z*= 513.4 (M+1)) was very close to the theoretically expected one (*m/z*=512.4). (Appendix A).

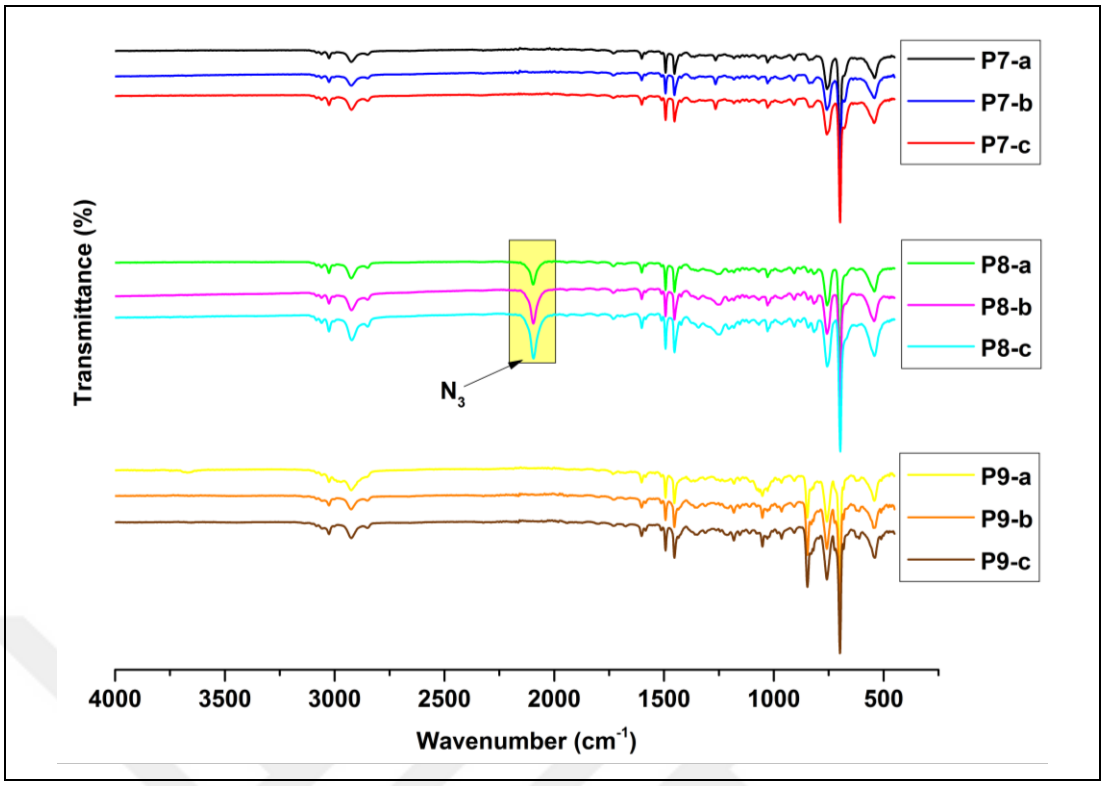

Figure 5.18: FTIR spectra of **P7**, **P8**, **P9** series polymers.

FTIR spectra of linear copolymers were depicted in Figure 5.18. In these spectra, aromatic and aliphatic CH stretching signals of the linear copolymers were observed around 3026−3080 and 2840−2920 cm^{-1}, respectively. The peaks seen at 1601, 1493 and 1452 cm^{-1} were assigned to aromatic C=C stretching frequencies in the phenyl rings. On the other hand, C=O stretching signal of the initiator was hardly seen at 1730 cm^{-1} due to dilution of this residue in the polymer structure. Upon the reaction of the chloride functional styrenic linear polymers (**P7-(a-c)**) with sodium azide, emergence of a new signal emerged at 2095 cm^{-1} in the the FTIR spectrum of **P8-(a-c)** is a qualitative indication for the presence of azide functional unit in the chemical structure of the yielded polymer (**P8-(a-c)**). Then, after the Cu(I)-catalyzed 1,3-dipolar cycloaddition reaction between **P8-(a-c)** and 1-ethynylpyrene, the complete disappearance of this signal indicated that azide-functional units were quantitively converted to pyrene groups, yielding **P9-(a-c)**.

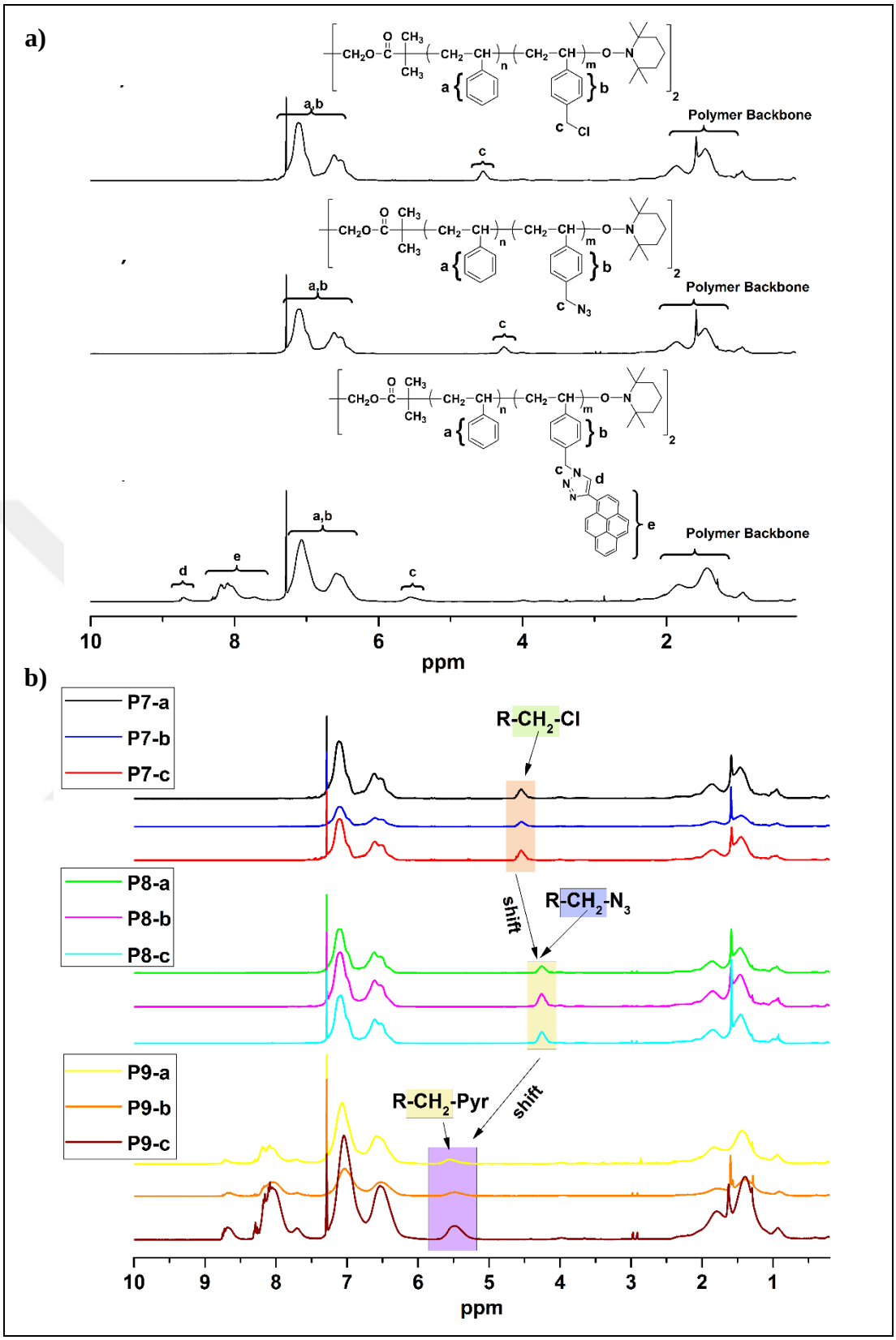

Figure 5.19: a) ^{1}H NMR spectra of **P7-a**, **P8-a**, **P9-a**, b) **P7**, **P8**, **P9** series polymers.

^{1}H NMR spectra of the styrenic linear copolymers were given in Figure 5.19. In these spectra, the polymer main chain protons gave signals between 1.44 and 2.05 ppm, while aromatic C***H*** protons ($H_{a,b}$) in styrene and vinylbenzyl repeating units produced resonances between 6.47− 7.11 ppm. In the ^{1}H NMR spectrum of **P7-(a-c)** (Figure 5.19b), the signal of the methylene protons (H_c) adjacent to the benzene ring was observed at 4.52 ppm, and shifted slightly to higher magnetic field (4.23 ppm) as a result of azidification. After 1,3-dipolar cycloaddiditon (click) reaction between **P8-(a-c)** with 1-ethynylpyrene, these signals moved to downfield and gave resonances at 5.53 ppm. The clear shift of H_c protons on azidification and click reactions further proves the success of the reactions. Besides, some new proton resonance signals were seen in the ^{1}H NMR spectrum of **P9-(a-c)** and they were attributed to triazole methine protons (H_d, 8.68 ppm) and aromatic C***H*** protons of pendant pyrene units (H_e, 7.70-8.18 ppm).

Average molecular weights (M_n and M_w) and polydispersity indexes (PDIs) of the obtained linear styrenic polymers were determined via gel permeation chromatography (GPC) analysis. The polymers demonstrated monodisperse chromatograms with reasonably low PDI values between 1.25 and 1.35, pointing out that either polymerization products or post-modified polymers contained only the targeted ones. Moreover, the values obtained through GPC experiments are only estimated results based on linear polystyrene standards. Unfortunately, these calibration standards have different hydrodynamic volumes from the synthesized linear polymers with different functional units. Therefore, average molecular weights obtained from conventional GPC experiments have limited reliability with respect to those obtained via NMR calculations.[30] In the ^{1}H NMR spectra of the synthesized polymers, any discernable signal belonging to terminal TEMPO and initiating core residues were not observed since they are overlapped by those of the repeating units or diluted by those of long polymer chains. On the other hand, m/n ratios for the monomeric residues (see Figure 4.3) were calculated from ratios of integral peak areas aromatic phenyl (C_6***H***$_5$ plus C_6***H***$_4$-CH_2-) and methylene protons next to the benzene ring (C_6H_4−C***H***$_2$) and were summarized in Table 5.5. Thus, the molar mass of the polymer fragments having single functional grup (-Cl or -N_3) were computed with the equation (m/n) × M_W of St + M_W of chloride or azide functional repeating units.[61]

Table 5.5: Results of the linear styrenic copolymers with different side-functional groups.

Polymers	Feeds	Composition [a] (n/m)	$M_{n,\,NMR}$	$M_{n,\,GPC}$ [b]	M_w/M_n [b]	Functional Groups
P7-a	100:5	8.4	29900	8200	1.29	
P7-b	100:10	4.8	37800	7700	1.31	**-Cl**
P7-c	100:15	3.7	25000	7400	1.35	
P8-a	100:5	8.4	30100	8300	1.29	
P8-b	100:10	4.8	38000	850	1.31	**-N_3**
P8-c	100:15	3.7	25200	7600	1.35	
P9-a	100:5	8.4	36600	8400	1.29	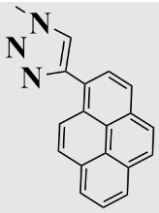
P9-b	100:10	4.8	51200	8000	1.25	
P9-c	100:15	3.7	33500	7700	1.29	

[a] See Figure 4:3 for "n" and "m". It was calculated from ratios of integral peak areas aromatic phenyl ($C_6\boldsymbol{H}_5$ plus $C_6\boldsymbol{H}_4$-CH_2-) and methylene protons next to the benzene ring (C_6H_4–$C\boldsymbol{H}_2$) in related ^{1}H NMR spectra.

[b] $M_{n,GPC}$ and M_w/M_n were determined via GPC analysis using linear polystyrene calibration standards with narrow molecular weight distributions.

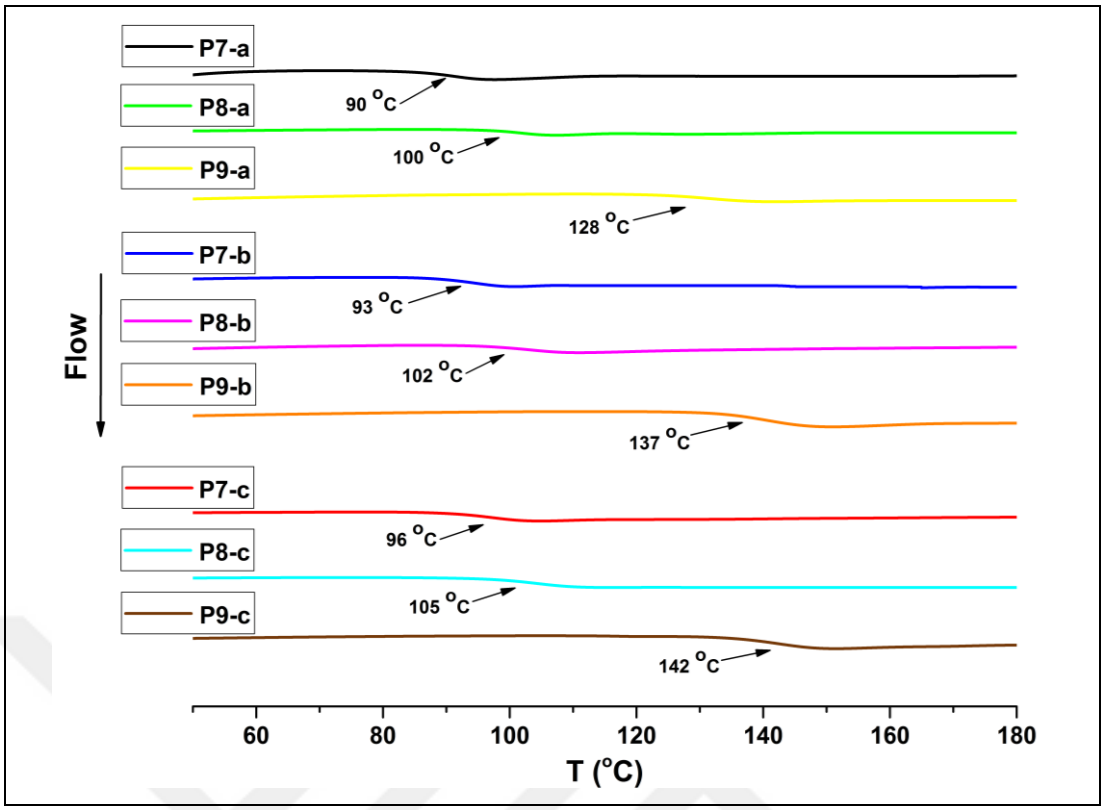

Figure 5.20: DSC curves of **P4**, **P5**, **P6** series polymers.

Table 5.6: Thermal properties of linear styrenic copolymers with different functional groups.

Polymers	T_g (°C) [a]	T_{onset} °C) [b]	T_{max} (°C) [c]	**Char Yield (%)** [d]
P7-a	90	260	403	4
P8-a	100	222	400	6
P9-a	128	301	413	10
P7-b	93	272	399	4
P8-b	102	229	383	6
P9-b	137	283	397	12
P7-c	96	274	407	5
P8-c	105	230	386	7
P9-c	142	330	393	14

Table: 5.6: Continuation of the table.

[a] T_g is the glass transition temperature (The midpoint of the heat capacity change was taken) of the polymers in DSC experiments.
[b] T_{onset} is the onset decomposition temperature (3% mass fraction loss) of the polymers in TGA experiments.
[c] T_{max} is the temperature corresponding to the maximum rate of weight loss in TGA experiments.
[d] The percent of the mass remained at 700 °C in TGA experiments.

Differential scanning calorimetry (DSC) experiments were conducted to determine thermal phase transitions of the prepared styrenic linear copolymers. The midpoint of the heat capacity change was taken as T_g and the related data were presented in Table 5.6. DSC thermograms of **P7-P9** series copolymers were demonstrated in Figure 5.20. In these thermograms, T_g of chloride-functional linear polymers (**P7-(a-c)**) were found to be close to each other. Upon incorporation and increase in the number of azide-functional units, only slight enhancement was observed in the T_g values of the copolymers (**P8-(a-c)**). On the other hand, binding of pendant bulky pyrene groups raised substantially the T_g of **P9-a** by 28 °C and increase in T_g values of the pyrene-functional copolymers were getting more pronounced for **P9-b** (35 °C) and **P9-c** (37 °C) as their pyrene contents were increased. These results were attributed to the increase in the rigidity of the pyrene-functional linear copolymers due to π-stacking interaction between pyrene side-units, as well as their bulky structure [30].

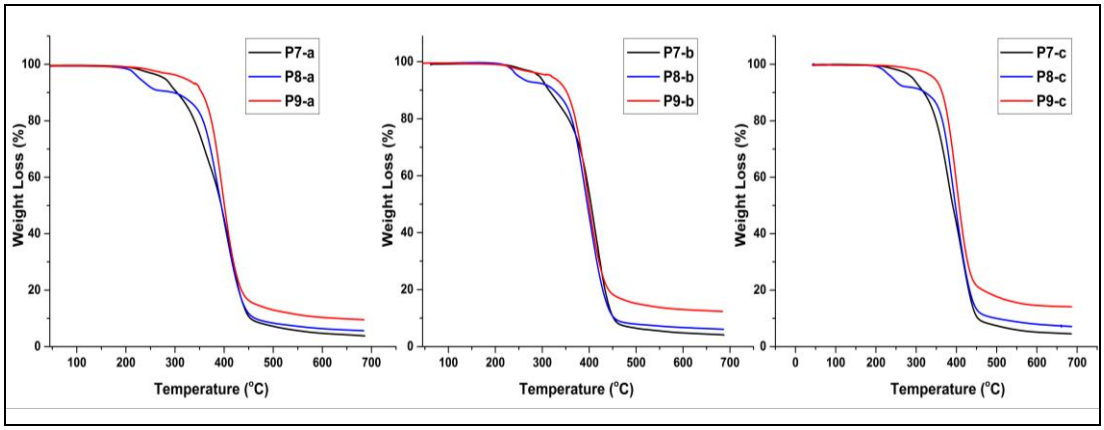

Figure 5.21: TGA thermograms of **P4**, **P5**, **P6** series polymers.

Thermal stabilities of the synthesized linear copolymers were studied via TGA experiments under inert nitrogen (N_2) gas atmosphere. TGA thermograms of the **P7-P9** series copolymers were demonstrated in Figure 5.21. The data related to their initial (T_{onset}) and maximum (T_{max}) decomposition temperatures as well as their percent char yields were summarized in Table 5.6. In these thermograms, chloride-functional copolymers decomposed in a single step starting around 260-274 °C, whereas azide-functional copolymers showed two-step decomposition profiles due to evolution of nitrogen gas above 220 °C [77-78]. Incorporation of pyrene-functional units considerably enhanced T_{onset} values of the polymers as well as their char yields.

5.4. Spectrophotometric Measurements and Nitroaromatic Sensing Applications of Pyrene-Functional Styrenic Copolymers

The presence of pyrene moieties in **P3-a**, **P3-b**, **P3-c**, **P6-a** and **P9-a** were further confirmed by absorption and fluorescence spectroscopy experiments and their UV-vis spectra in DMF were demonstrated in Figure 5.22(a), along with 1-ethynylpyrene for comparison purposes. In these spectra, all of the pyrene side-functional copolymers demonstrated typical pyrene absorption bands with strong broadening above 300 nm, regardless of their topologies. This peak broadening indicated ground state pyrene-pyrene association [42,79] induced by increased local concentration of pyrene units on the polymer skeleton [80]. **P3-a**, **P3-b**, **P3-c** and **P6-a** showed featureless broad bands between 390 and 450 nm and their absorptions in this spectral range were much stronger than that of the linear copolymer (**P9-a**). Whereas, 1-ethynylpyrene, as an analogous compound to pyrene, did not make any absorption in this range. These results were thought to indicate that the emergence of broad band in the UV-vis spectra of pyrene-pendant copolymers were resulted from $\pi - \pi^*$ electron transitions induced by close proximity of the pyrene pendant groups on the polymer chains [81].

The fluorescence spectra of pyrene **P3-a**, **P3-b**, **P3-c, P6-a** and **P9-a** along with that of 1-ethynylpyrene were demonstrated in Figure 5.22(b). As seen from the Figure 5.22(b), 1-ethynylpyrene depicted characteristic pyrene monomer emission bands with maxima at 391 and 405 nm. On the other hand, there observed broad excimer emission bands with a maximum around 485 nm as well as well-structured pyrene monomer emission signals in the emission spectrum of the pyrene-pendant star and linear

copolymers. The monomer emission intensity of the linear **P9-a** polymer was stronger than those of the pyrene-pendant star copolymers. Besides, as the pyrene contents of the tetra-armed star copolymers were increased from **P3-a** to **P3-b**, intensities of their monomer emission bands considerably weakened with respect to the excimer emission bands due to increased local concentration of pendant pyrene units in the polymer arms [80,82]. The intensity of the monomer emission of tri-functional star-shaped polymer **P6-a** appears to be close to the monomer intensity value of **P3-a.**

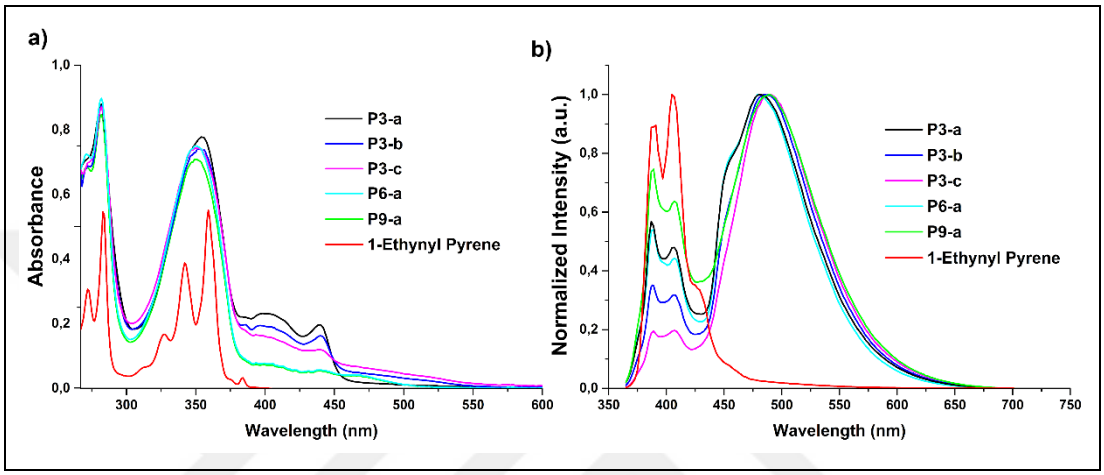

Figure 5.22: a) Absorption and b) emission spectra of 1-ethynylpyrene ($1.33x10^{-5}$ M), **P3-a** ($2.56x10^{-5}$ M), **P3-b** ($2.78x10^{-5}$ M), **P3-c** ($3.22x10^{-5}$ M), **P6-a** ($2.47x10^{-5}$ M), **P9-a** ($2.93x10^{-5}$ M) in DMF at room temperature.

Pyrene and its derivatives in solid or solution phase have been widely used in the fluorometric determination nitroaromatic compounds. Pyrene itself gives monomer emissions in various solvents at dilute concentrations and it needs to be concentrated to millimolar or higher concentrations to produce excimer emissions [83]. Since, excimer emissions of pyrene are prone to be affected by the polarity of the environment [40,46] and have been commonly used in turn-off fluorescence detection of various quencher molecules.

The potential of pyrene functional polystyrene copolymers as fluorescent probes towards nitroaromatic compounds were evaluated in DMF at 350 nm excitation wavelength (λ_{ext}) at room temperature. The Figure 5.23 depicts fluorescence emission spectra of **P3-a** before and after titration with different concentrations of picric acid (PA) from 1 to 25 equivalents (to number of moles of pyrene units). These spectra explicitly show significant and gradual changes in the emission intensity of **P3-a** upon the addition of increasing amounts of PA. The quenching efficiency (QE) of PA was calculated using the following formula: $QE=((I_0 - I)/I_0)x100$, where I_0 and I are the

emission intensities before and after the addition of PA, respectively. According to Figure 5.23(b), **P3-a** lost 31.5% of its initial fluorescence emission intensity after the addition of 1 equivalent of PA, it showed very strong quenching (around 75%) at a slightly higher concentration (5 equivalent), and finally full quenching was observed when PA concentration reached 25 equivalents ratio. On the other hand, Figure 5.23(c) provides visual proof for the quenching phenomenon of **P3-a** with PA. The photographic images from left to right belong to **P3-a** solutions in quartz cuvettes before and after the addition of 5, 10, 15, 20, and 25 equivalent of PA under UV light (λ_{ext}-254 nm) at room temperature. The image clearly shows gradual decrease in the fluorescence emission intensity of **P3-a** up to complete quenching as the concentration of PA in the media increases.

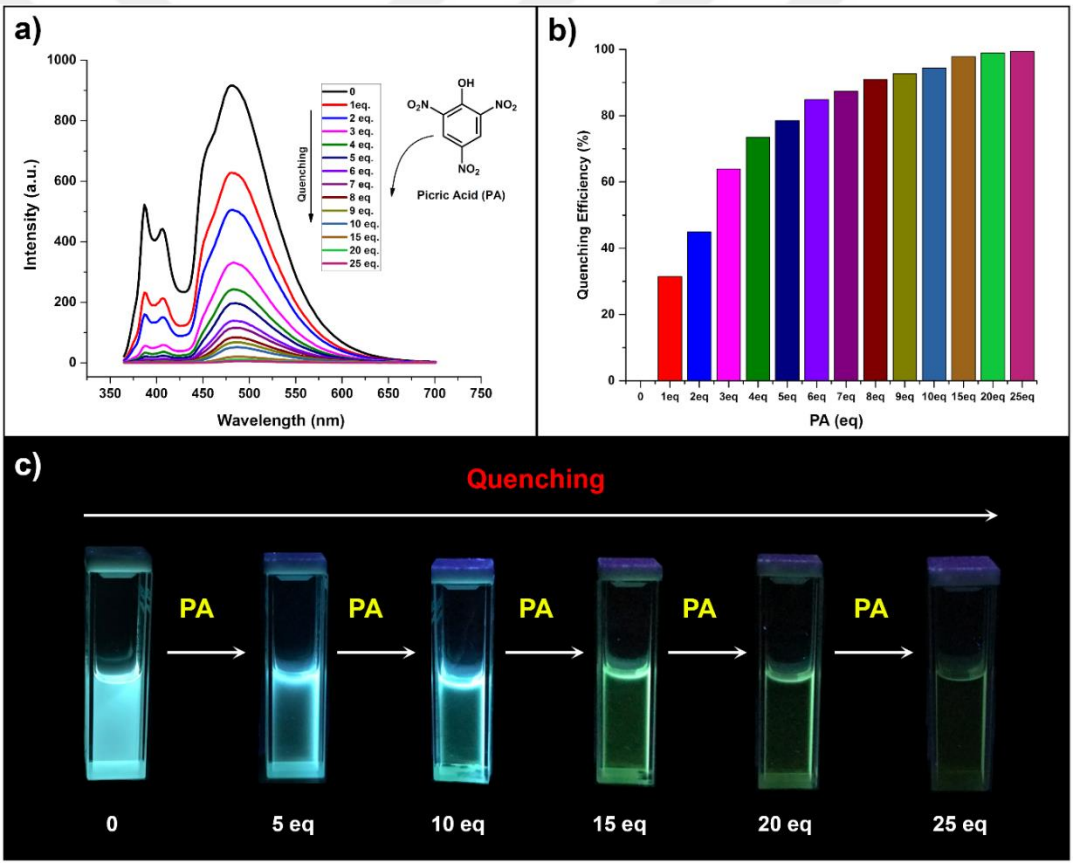

Figure 5.23: a) Fluorescence emission spectra and b) quenching ratios of **P3-a** in the presence of increasing concentrations of PA. c) The photographic images of **P3-a** solutions in quartz cuvettes under UV light at room temperature before and after the addition of 25 eq. of PA.

Fluorescence emission quenching ratios of pyrene-functional star-shaped polymers (**P3-a**, **P3-b**, **P3-c**, **P6-a**) and the linear polymer (**P9-a**) in the presence of 25

equivalents of PA were shown in Figure 5.24 As it is seen from the figure that all of the star-shaped and linear polymers gave very similar responses to the presence of PA. Besides, as the pyrene content of the tetra-armed polymers increased from **P3-a** to **P3-c,** there observed only very slight and insignificant enhancement in their quenching ratios, due to increased probability of pyrene groups to approach PA molecules in proper orientations. Shortly, the obtained results showed that the differences in the topology of these pyrene-functional polymers did not much affect their fluorescence emission behaviors and quenching ratios in the presence PA. Fluorescence emission quenching ratios of all synthesized polymers in the presence of increasing concentrations of NACs presented in Appendix B.

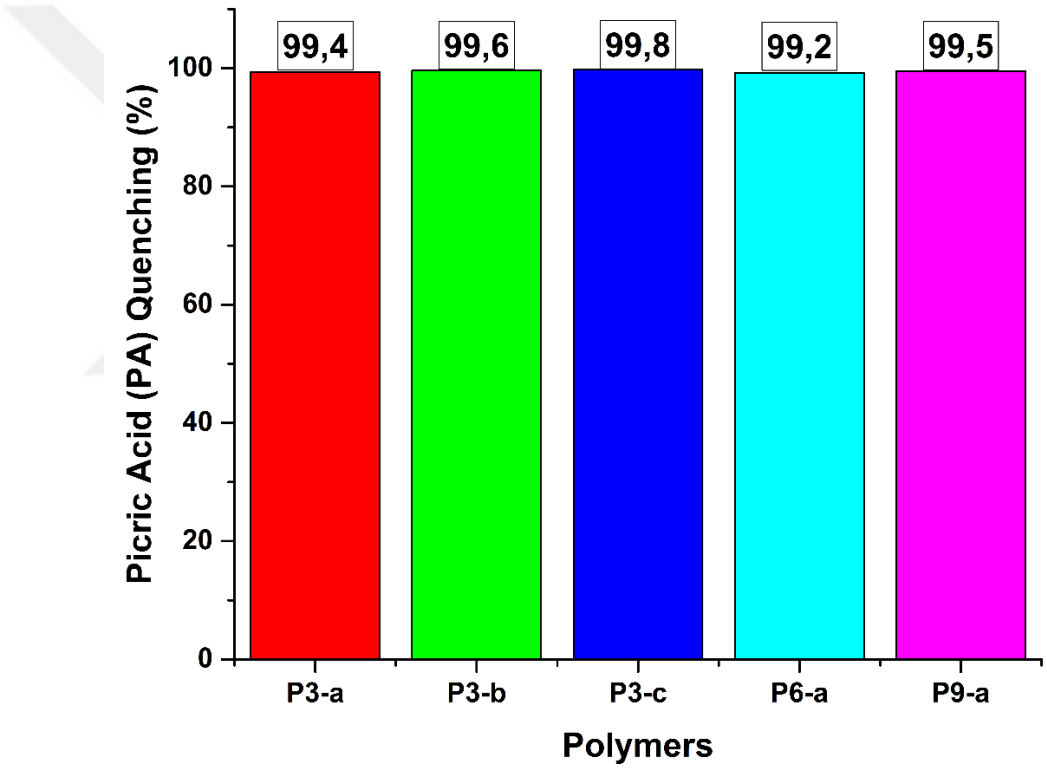

Figure 5.24: Quenching ratios of **P3-a**, **P3-b**, **P3-c**, **P6-a**, **P9-a** in the presence of 25 equivalents of picric acid.

Selectivity is a key parameter for a sensing material to be used in real-life applications, thus, the interference of other widespread nitroaromatics was investigated. Fluorescence emission spectra of **P3-a** before and after addition of 25 equivalents of different nitroaromatic compounds were depicted in Figure 5.25. It is notable that the presence of 25 eq. of 2,4-dinitrophenol (DNP) and 4-nitrophenol (NP) effectively decreased fluorescence emission intensity of **P3-a** by 84.2% and 82.6%,

respectively. In other respects, 2,4,6-trinitrotoluene (TNT), 2,4-dinitrotolunene (DNT), and 4-nitrotoluene (NT) were found to quench the emission intensity only by 44.0%, 32.6%, and 28.8%, respectively. It is remarkable that increase in the number of nitro groups on the aromatic rings of nitrophenols or nitrotoluenes enhanced their quenching efficiencies towards **P3-a** and the highest quenching efficiency was obtained with PA (99.4%). Curiously, 4-nitrophenol (NP) had more quenching effect (almost two-fold) than 2,4,6-trinitrotoluene (TNT) on **P3-a** and this higher quenching efficiency of NP may be attributed to its stronger binding affinity to **P3-a**. Pyrene units are attached to the polymer chains through triazole bridges and these connecting units include three highly electronegative nitrogen atoms which makes the triazole C^5-H bonds strongly polarized [84]. These C^5-H hydrogen atoms can make effective hydrogen bonding with nitroaromatic compounds [85] and it appears to be as a clear explanation for the sensitivity of the pyrene-functional polymers in this study. On the other hand, nitrophenols have strongly polarized O-H bonds and they behave as weak acids [86-87]; therefore, they have the ability to form strong complexes through C-H and N-N=N parts of triazole group. These charactestics of nitrophenols make them superior quenchers for the pyrene-functional polymers in this thesis project.

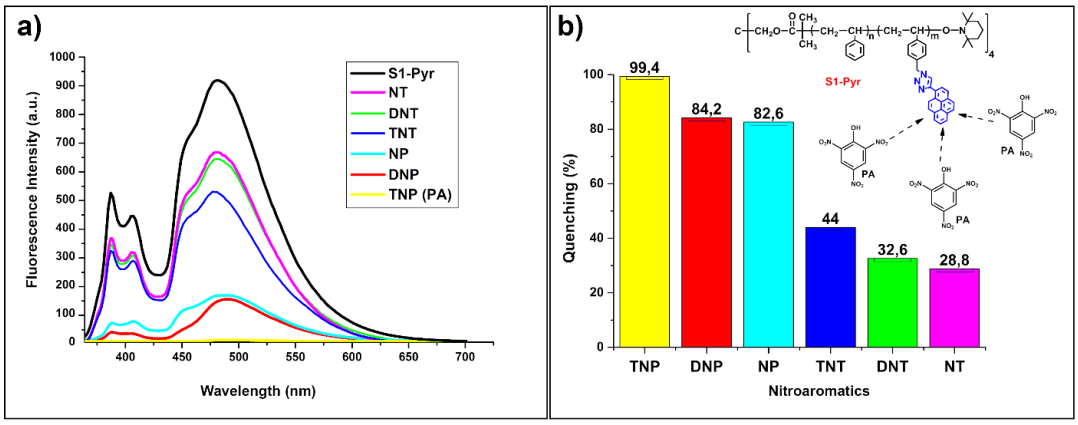

Figure 5.25: a) Fluorescence intensities of **P3-a** with adding NACs, b) Fluorescence quenching ratios of **P3-a** (λext: 350 nm) with 25 equivalents of NT, DNT, TNT, NP, DNP, TNP (PA).

6. CONCLUSION

Fluorescence active polymers are one of the best alternative materials for selective and sensitive detection of nitroaromatic compounds (NACs). Pyrene is a very important PAH compound and have been the most frequently used fluorophore to prepare fluorescently labeled polymers. Pyrene-containing polymers were mainly used as fluorescence probes against nitroaromatic compounds. Star-shaped polymers have been known to have several advantages over their linear analogues of the same molecular weight, such as higher solubilities, lower solution and melt viscosities as they have less chain entanglements due to their compact and branched molecular structures. Whereas, the scientific papers and thesis studies reporting star-shaped polymers having pyrene functional groups for fluorescence applications are rare. The effect of polymer topology on fluorescence detection of NACs has been investigated as extensively as it is in this thesis.

Within the scope of this dissertation study, novel tri-, tetra-armed star-shaped and linear styrenic nine different copolymers having pyrene side-groups were designed, successfully synthesized. The attained polymers were employed as fluorescence sensing probe for fast and sensitive determination of nitroaromatic compounds. The synthesis of the copolymers started with NMP of St and VBC in the presence of Br- (**1**, **3** and **5**) and novel TEMPO end-capped unimolecular NMP (**2, 4 and 6**) initiator compounds to yield chloride-functional linear and star copolymers (**P1-(a-c)**, **P4-(a-c)** and **P7-(a-c)**). Subsequent to the modification of chlorides to azide groups (**P2-(a-c)**, **P5-(a-c)** and **P8-(a-c)**), quantitative attachment of pyrene units was succeeded via 1,3-dipolar cycloaddition reaction between 1-ethynylpyrene and azide-functional groups of the copolymers (**P2-(a-c)**, **P5-(a-c)** and **P8-(a-c)**), yield pyrene-functional (**P3-(a-c)**, **P6-(a-c)** and **P9-(a-c)**). The success and completeness of the reactions for the synthesis of the small compounds and the copolymers were confirmed via FTIR and ^{1}H NMR spectroscopic measurements. Besides, monodisperse chromatogram curves of these copolymers and as well as their reasonably low PDI values obtained from GPC analysis provided further proofs for the effectiveness of the synthetic procedure to produce targeted linear and star copolymers. The presence of pyrene units in the styrenic copolymers were further confirmed by absorption and fluorescence spectroscopy measurements. These pyrene-containing copolymers

depicted typical pyrene absorption bands with strong broadening above 300 nm, indicating ground state pyrene-pyrene association, due to increased local concentration of pendant pyrene units on the polymer chains. In the fluorescence experiments, they gave characteristic pyrene monomer emission signals with maxima at 391 and 405 nm as well as broad excimer bands centered around 485 nm. The monomer emission intensity of the linear analogue polymers was stronger than those of star-shaped ones and these signals of the star copolymers weakened with respect to their excimer emission bands as their pyrene contents increased from **P3-a** to **P3-c** due to increased close proximity of the pyrene groups. **P3-(a-c)** gave very sensitive responses to the presence of nitroaromatic compounds and it was attributed to the hydrogen binding interaction of the polymers through their triazole linkers with considerably high dipole moment. The highest quenching efficiency was observed for PA (99.4%) followed by DNP (84.2%), NP (82.6%), TNT (44.0%), DNT (32.6%), and NT (28.8%). High quenching ability of nitrophenolic compounds was attributed to their strong binding affinity for **P3-(a-c)** due to the acidity of phenolic hydroxyl units. On the other hand, quenching ratios of **P3-(a-c)**, **P6-a-c** and **P9-a** in the presence of 25 equivalents of PA were observed to be very close to each other. These results indicated that **P3-(a-c)**, **P6-a** and **P9-a** are promising polymers to be used as selective and sensitive probes for the fluorescence detection of phenolic nitroaromatic compounds, especially picric acid.

REFERENCES

[1] Altintas O., Yilmaz I., Hizal G., Tunca U., (2006). "Synthesis of poly(methyl methacrylate)-b-polystyrene containing a crown ether unit at the junction point via combination of atom transfer radical polymerization and nitroxide mediated radical polymerization routes", Journal of Polymer Science Part A: Polymer Chemistry, 44, 3242-3249.

[2] Bartholome C., Beyou E., Bourgeat-Lami E., Chaumont P., Lefebvre F., Zydowicz N., (2005). "Nitroxide-Mediated Polymerization of Styrene Initiated from the Surface of Silica Nanoparticles. In Situ Generation and Grafting of Alkoxyamine Initiators", Macromolecules, 38, 1099-1106.

[3] Celik C., Hizal G., Tunca U., (2003). "Synthesis of miktoarm star and miktoarm star block copolymers via a combination of atom transfer radical polymerization and stable free-radical polymerization", Journal of Polymer Science Part A: Polymer Chemistry, 41, 2542-2548.

[4] Delplace V., Harrisson S., Tardy A., Gigmes D., Guillaneuf Y., Nicolas J., (2014). "Nitroxide-Mediated Radical Ring-Opening Copolymerization: Chain-End Investigation and Block Copolymer Synthesis", Macromolecular Rapid Communications, 35, 484-491.

[5] Durmaz H., Karatas F., Tunca U., Hizal G., (2006). "Preparation of ABC miktoarm star terpolymer containing poly(ethylene glycol), polystyrene, and poly(tert-butylacrylate) arms by combining diels–alder reaction, atom transfer radical, and stable free radical polymerization routes", Journal of Polymer Science Part A: Polymer Chemistry, 44, 499-509.

[6] Gozgen A., Dag A., Durmaz H., Sirkecioglu O., Hizal G., Tunca U., (2009). "ROMP-NMP-ATRP combination for the preparation of 3-miktoarm star terpolymer via click chemistry", Journal of Polymer Science Part A: Polymer Chemistry, 47, 497-504.

[7] Grubbs R.B., (2011). "Nitroxide-Mediated Radical Polymerization: Limitations and Versatility", Polymer Reviews, 51, 104-137.

[8] Hawker C.J., Barclay G.G., Orellana A., Dao J., Devonport W., (1996). "Initiating Systems for Nitroxide-Mediated “Living” Free Radical Polymerizations: Synthesis and Evaluation", Macromolecules, 29, 5245-5254.

[9] Nicolas J., Guillaneuf Y., Lefay C., Bertin D., Gigmes D., Charleux B., (2013). "Nitroxide-mediated polymerization", Progress in Polymer Science, 38, 63-235.

[10] Sciannamea V., Jérôme R., Detrembleur C., (2008). "In-Situ Nitroxide-Mediated Radical Polymerization (NMP) Processes: Their Understanding and Optimization", Chemical Reviews, 108, 1104-1126.

[11] Tunca U., Ozyurek Z., Erdogan T., Hizal G., (2004). "Novel miktofunctional initiator for the preparation of an ABC-type miktoarm star polymer via a combination of controlled polymerization techniques", Journal of Polymer Science Part A: Polymer Chemistry, 42, 4228-4236.

[12] Zhou M., McManus N.T., Vivaldo-Lima E., Lona L.M.F., Penlidis A., (2010). "Kinetics of Nitroxide Mediated Radical Polymerization of Styrene with Unimolecular Initiators", Macromolecular Symposia, 289, 95-107.

[13] Sang N., Zhan C., Cao D., (2015). "Highly sensitive and selective detection of 2,4,6-trinitrophenol using covalent-organic polymer luminescent probes", J. Mater. Chem. A, 3, 92-96.

[14] Dario A., Schroeder M., Nyanhongo G.S., Englmayer G., Guebitz G.M., (2010). "Development of a biodegradable ethylene glycol dinitrate-based explosive", Journal of Hazardous Materials, 176, 125-130.

[15] Sohn H., Sailor M.J., Magde D., Trogler W.C., (2003). "Detection of Nitroaromatic Explosives Based on Photoluminescent Polymers Containing Metalloles", Journal of the American Chemical Society, 125, 3821-3830.

[16] Duraimurugan K., Siva A., (2016). "Phenylene(vinylene) based fluorescent polymer for selective and sensitive detection of nitro-explosive picric acid", Journal of Polymer Science Part A: Polymer Chemistry, 54, 3800-3807.

[17] Long Y., Chen H., Wang H., Peng Z., Yang Y., Zhang G., Li N., Liu F., Pei J., (2012). "Highly sensitive detection of nitroaromatic explosives using an electrospun nanofibrous sensor based on a novel fluorescent conjugated polymer", Analytica Chimica Acta, 744, 82-91.

[18] Germain M.E., Knapp M.J., (2009). "Optical explosives detection: from color changes to fluorescence turn-on", Chemical Society Reviews, 38, 2543-2555.

[19] Chowdhury A., Mukherjee P.S., (2015). "Electron-Rich Triphenylamine-Based Sensors for Picric Acid Detection", The Journal of Organic Chemistry, 80, 4064-4075.

[20] Ponnuvel K., Banuppriya G., Padmini V., (2016). "Highly efficient and selective detection of picric acid among other nitroaromatics by NIR fluorescent organic fluorophores", Sensors and Actuators B: Chemical, 234, 34-45.

[21] Acharyya K., Mukherjee P.S., (2014). "A fluorescent organic cage for picric acid detection", Chemical Communications, 50, 15788-15791.

[22] Santra D.C., Bera M.K., Sukul P.K., Malik S., (2016). "Charge-Transfer-Induced Fluorescence Quenching of Anthracene Derivatives and Selective Detection of Picric Acid", Chemistry – A European Journal, 22, 2012-2019.

[23] Erande Y., Chemate S., More A., Sekar N., (2015). "PET governed fluorescence "Turn ON" BODIPY probe for selective detection of picric acid", RSC Advances, 5, 89482-89487.

[24] Shaligram S., Wadgaonkar P.P., Kharul U.K., (2014). "Fluorescent polymeric ionic liquids for the detection of nitroaromatic explosives", Journal of Materials Chemistry A, 2, 13983-13989.

[25] Xu Y., Wu X., Chen Y., Hang H., Tong H., Wang L., (2016). "Star-shaped triazatruxene derivatives for rapid fluorescence fiber-optic detection of nitroaromatic explosive vapors", RSC Advances, 6, 31915-31918.

[26] Lee Y.H., Liu H., Lee J.Y., Kim S.H., Kim S.K., Sessler J.L., Kim Y., Kim J.S., (2010). "Dipyrenylcalix[4]arene—A Fluorescence-Based Chemosensor for Trinitroaromatic Explosives", Chemistry – A European Journal, 16, 5895-5901.

[27] Reddy K.L., Kumar A.M., Dhir A., Krishnan V., (2016). "Selective and Sensitive Fluorescent Detection of Picric Acid by New Pyrene and Anthracene Based Copper Complexes", Journal of Fluorescence, 26, 2041-2046.

[28] Sang N., Zhan C., Cao D., (2015). "Highly sensitive and selective detection of 2,4,6-trinitrophenol using covalent-organic polymer luminescent probes", Journal of Materials Chemistry A, 3, 92-96.

[29] Toal S.J., Trogler W.C., (2006). "Polymer sensors for nitroaromatic explosives detection", Journal of Materials Chemistry, 16, 2871-2883.

[30] Karagollu O., Gorur M., Gode F., Sennik B., Yilmaz F., (2015). "Synthesis, Characterization, and Ion Sensing Application of Pyrene-Containing Chemical Probes", Macromolecular Chemistry and Physics, 216, 939-949.

[31] Lakowicz J.R., (1999). Principles of fluorescence spectroscopy, New York: Kluwer Academic/Plenum.

[32] Köz B., (2001). "Fluorescence Emission Studies With Energy Transfer Reactions", Dokuz Eylul University, Institute of Natural and Applied Sciences, 1-74.

[33] Dandan Doganci M., Bayir S., Doganci E., Gorur M., Yilmaz F., (2016). "Nitroaromatic Compound Sensing Application of Hexa-Armed Dansyl End-Capped Poly(Epsilon-Caprolactone) Star Polymer With Phosphazene Core", Journal of the Turkish Chemical Society, Section A: Chemistry, 3.

[34] Sun X., Wang Y., Lei Y., (2015). "Fluorescence based explosive detection: from mechanisms to sensory materials", Chemical Society Reviews, 44, 8019-8061.

[35] Gorur M., Doganci E., Yilmaz F., Isci U., (2015). "Synthesis, characterization, and Pb2+ ion sensing application of hexa-armed dansyl end-capped poly(ε-

caprolactone) star polymer with phosphazene core", Journal of Applied Polymer Science, 132, 42380.

[36] Kahya S.S., (2012). "Synthesis and Characterization Of Fluorescent Zinc Phthalocyanine Pigments and Its Combination Pigment With Mica Titania Pigment", Middle East Technical University, The Graduate School of Natural and Applied Sciences, 1-92.

[37] Braslavsky S.E., (2007). Glossary of terms used in photochemistry, 3rd edition (IUPAC Recommendations 2006). 293.

[38] Altundal Y., (2009). "Fluorescence Lifetime Images Of Dye Molecules", Boğaziçi University, Master of Science Thesis.

[39] Valeur B., Berberan-Santos M.N., (2012). Introduction, ed. Molecular Fluorescence. Wiley-VCH Verlag GmbH & Co. KGaA, 1-30.

[40] Figueira-Duarte T.M., Müllen K., (2011). "Pyrene-Based Materials for Organic Electronics", Chemical Reviews, 111, 7260-7314.

[41] Ding L., Fang Y., (2010). "Chemically assembled monolayers of fluorophores as chemical sensing materials", Chemical Society Reviews, 39, 4258-4273.

[42] Winnik F.M., (1993). "Photophysics of preassociated pyrenes in aqueous polymer solutions and in other organized media", Chemical Reviews, 93, 587-614.

[43] Ueno A., Suzuki I., Osa T., (1990). "Host-guest sensory systems for detecting organic compounds by pyrene excimer fluorescence", Analytical Chemistry, 62, 2461-2466.

[44] Yang R.-H., Chan W.-H., Lee A.W.M., Xia P.-F., Zhang H.-K., (2003). "A Ratiometric Fluorescent Sensor for AgI with High Selectivity and Sensitivity", Journal of the American Chemical Society, 125, 2884-2885.

[45] Demirel G.B., Daglar B., Bayindir M., (2013). "Extremely fast and highly selective detection of nitroaromatic explosive vapours using fluorescent polymer thin films", Chemical Communications, 49, 6140-6142.

[46] Kim J.H., Hwang A.-R., Chang S.-K., (2004). "Hg2+-selective fluoroionophore of p-tert-butylcalix[4]arene-diaza-crown ether having pyrenylacetamide subunits", Tetrahedron Letters, 45, 7557-7561.

[47] Birks J.B., (1975). "Excimers", Reports on Progress in Physics, 38, 903.

[48] Beyazkılıç P., (2013). "Formation of Pyrene Excimers in Mesoporous Organically Modified Silica Thin Films For Visual Detectıon Of Nitroaromatic Explosives", Bilkent University.

[49] Chopra R., Kaur P., Singh K., (2015). "Pyrene-based chemosensor detects picric acid upto attogram level through aggregation enhanced excimer emission", Analytica Chimica Acta, 864, 55-63.

[50] Burattini S., Colquhoun H.M., Greenland B.W., Hayes W., Wade M., (2009). "Pyrene-Functionalised, Alternating Copolyimide for Sensing Nitroaromatic Compounds", Macromolecular Rapid Communications, 30, 459-463.

[51] He G., Yan N., Yang J., Wang H., Ding L., Yin S., Fang Y., (2011). "Pyrene-Containing Conjugated Polymer-Based Fluorescent Films for Highly Sensitive and Selective Sensing of TNT in Aqueous Medium", Macromolecules, 44, 4759-4766.

[52] Wang Y., La A., Ding Y., Liu Y., Lei Y., (2012). "Novel Signal-Amplifying Fluorescent Nanofibers for Naked-Eye-Based Ultrasensitive Detection of Buried Explosives and Explosive Vapors", Advanced Functional Materials, 22, 3547-3555.

[53] Sun X., Liu Y., Shaw G., Carrier A., Dey S., Zhao J., Lei Y., (2015). "Fundamental Study of Electrospun Pyrene–Polyethersulfone Nanofibers Using Mixed Solvents for Sensitive and Selective Explosives Detection in Aqueous Solution", ACS Applied Materials & Interfaces, 7, 13189-13197.

[54] Kim J.S., Choi M.G., Song K.C., No K.T., Ahn S., Chang S.-K., (2007). "Ratiometric Determination of Hg2+ Ions Based on Simple Molecular Motifs of Pyrene and Dioxaoctanediamide", Organic Letters, 9, 1129-1132.

[55] Maeda H., Maeda T., Mizuno K., Fujimoto K., Shimizu H., Inouye M., (2006). "Alkynylpyrenes as Improved Pyrene-Based Biomolecular Probes with the Advantages of High Fluorescence Quantum Yields and Long Absorption/Emission Wavelengths", Chemistry – A European Journal, 12, 824-831.

[56] Gong Y., Zhan X., Li Q., Li Z., (2016). "Progress of pyrene-based organic semiconductor in organic field effect transistors", Science China Chemistry, 59, 1623-1631.

[57] Yuan W., Yuan J., Zhou M., Pan C., (2008). "Synthesis, characterization, and fluorescence of pyrene-containing eight-arm star-shaped dendrimer-like copolymer with pentaerythritol core", Journal of Polymer Science Part A: Polymer Chemistry, 46, 2788-2798.

[58] Beyazkilic P., Yildirim A., Bayindir M., (2014). "Formation of Pyrene Excimers in Mesoporous Ormosil Thin Films for Visual Detection of Nitro-explosives", ACS Applied Materials & Interfaces, 6, 4997-5004.

[59] Siu H., Duhamel J., (2005). "The Importance of Considering Nonfluorescent Pyrene Aggregates for the Study of Pyrene-Labeled Associative Thickeners by Fluorescence", Macromolecules, 38, 7184-7186.

[60] Kollár J., Hrdlovič P., Chmela Š., (2010). "Spectral properties of bichromophoric pyrene derivatives: Monomer vs. excimer fluorescence", Journal of Photochemistry and Photobiology A: Chemistry, 214, 33-39.

[61] Senthamizhan A., Celebioglu A., Bayir S., Gorur M., Doganci E., Yilmaz F., Uyar T., (2015). "Highly Fluorescent Pyrene-Functional Polystyrene Copolymer Nanofibers for Enhanced Sensing Performance of TNT", ACS Applied Materials & Interfaces, 7, 21038-21046.

[62] Deshmukh S.C., Rana S., Shinde S.V., Dhara B., Ballav N., Talukdar P., (2016). "Selective Sensing of Metal Ions and Nitro Explosives by Efficient Switching of Excimer-to-Monomer Emission of an Amphiphilic Pyrene Derivative", ACS Omega, 1, 371-377.

[63] Gacal B.N., Koz B., Gacal B., Kiskan B., Erdogan M., Yagci Y., (2009). "Pyrene functional poly(vinyl alcohol) by "click" chemistry", Journal of Polymer Science Part A: Polymer Chemistry, 47, 1317-1326.

[64] Tasdelen M.A., Yagci Y., Demirel A.L., Biedron T., Kubisa P., (2007). "Synthesis and Characterization of Block-Graft Copolymers [poly(epichlorohydrin-b-styrene)-g-poly(methyl methacrylate)] by Combination of Activated Monomer Polymerization, NMP and ATRP", Polymer Bulletin, 58, 653-663.

[65] Aydin M., Gorur M., Yilmaz F., (2016). "Phosphazene-cored star polymer bearing redox-active side groups as a cathode-active material in Li-ion batteries", Reactive and Functional Polymers, 102, 11-19.

[66] Tillman E.S., Contrella N.D., Leasure J.G., (2009). "Monitoring the Nitroxide-Mediated Polymerization of Styrene Using Gel Permeation Chromatography and Proton NMR", Journal of Chemical Education, 86, 1424.

[67] Mishra V., Kumar R., (2012). "Living radical polymerization: A review", Journal of Scientific research, 56, 141-176.

[68] Ayaz H., (2011). "Pirazabol Merkezli İki Kollu Polimetilmetakrilat'ın Hazırlanması ve Termal Davranışının İncelenmesi", Adıyaman Üniversitesi, Yüksek lisans Tezi.

[69] Binder W.H., Sachsenhofer R., (2007). "'Click' Chemistry in Polymer and Materials Science", Macromolecular Rapid Communications, 28, 15-54.

[70] Moses J.E., Moorhouse A.D., (2007). "The growing applications of click chemistry", Chemical Society Reviews, 36, 1249-1262.

[71] Haldon E., Nicasio M.C., Perez P.J., (2015). "Copper-catalysed azide-alkyne cycloadditions (CuAAC): an update", Organic & Biomolecular Chemistry, 13, 9528-9550.

[72] Halim A., Fu Q., Yong Q., Gurr P.A., Kentish S.E., Qiao G.G., (2014). "Soft polymeric nanoparticle additives for next generation gas separation membranes", Journal of Materials Chemistry A, 2, 4999.

[73] Tong Y., Chen L., He X., Chen Y., (2014). "Sequential effect and enhanced conductivity of star-shaped diblock liquid-crystalline copolymers for solid electrolytes", Journal of Power Sources, 247, 786-793.

[74] Gao H., Min K., Matyjaszewski K., (2007). "Synthesis of 3-Arm Star Block Copolymers by Combination of "Core-First" and "Coupling-Onto" Methods Using ATRP and Click Reactions", Macromolecular Chemistry and Physics, 208, 1370-1378.

[75] Robinson J.W., Zhou Y., Qu J., Erck R., Cosimbescu L., (2016). "Effects of star-shaped poly(alkyl methacrylate) arm uniformity on lubricant properties", Journal of Applied Polymer Science, 133, 43611.

[76] Wycisk A., Döring A., Schneider M., Schönhoff M., Kuckling D., (2015). "Synthesis of β-cyclodextrin-Based Star Block Copolymers with Thermo-Responsive Behavior", Polymers, 7, 921.

[77] Ervithayasuporn V., Wang X., Gacal B., Gacal B.N., Yagci Y., Kawakami Y., (2011). "Formation of trimethylsilylated open-cage oligomeric azidophenylsilsesquioxanes", Journal of Organometallic Chemistry, 696, 2193-2198.

[78] Eren O., Gorur M., Keskin B., Yilmaz F., (2013). "Synthesis and characterization of ferrocene end-capped poly(ε-caprolactone)s by a combination of ring-opening polymerization and "click" chemistry techniques", Reactive and Functional Polymers, 73, 244-253.

[79] Tanhuanpää K., Cheng K.H., Anttonen K., Virtanen J.A., Somerharju P., (2001). "Characteristics of Pyrene Phospholipid/γ-Cyclodextrin Complex", Biophysical Journal, 81, 1501-1510.

[80] Gorur M., Yilmaz F., Kilic A., Sahin Z.M., Demirci A., (2011). "Synthesis of pyrene end-capped A6 dendrimer and star polymer with phosphazene core via "click chemistry"", Journal of Polymer Science Part A: Polymer Chemistry, 49, 3193-3206.

[81] Zhu X., Lystrom L., Kilina S., Sun W., (2016). "Tuning the Photophysics and Reverse Saturable Absorption of Heteroleptic Cationic Iridium(III) Complexes via Substituents on the 6,6′-Bis(fluoren-2-yl)-2,2′-biquinoline Ligand", Inorganic Chemistry, 55, 11908-11919.

[82] Guler M.O., Claussen R.C., Stupp S.I., (2005). "Encapsulation of pyrene within self-assembled peptide amphiphile nanofibers", Journal of Materials Chemistry, 15, 4507-4512.

[83] Zagrobelny J., Betts T.A., Bright F.V., (1992). "Steady-state and time-resolved fluorescence investigations of pyrene excimer formation in supercritical CO2", Journal of the American Chemical Society, 114, 5249-5257.

[84] Romero T., Caballero A., Tárraga A., Molina P., (2009). "A Click-Generated Triazole Tethered Ferrocene−Pyrene Dyad for Dual-Mode Recognition of the Pyrophosphate Anion", Organic Letters, 11, 3466-3469.

[85] Sui B., Kim B., Zhang Y., Frazer A., Belfield K.D., (2013). "Highly Selective Fluorescence Turn-On Sensor for Fluoride Detection", ACS Applied Materials & Interfaces, 5, 2920-2923.

[86] Vishnoi P., Walawalkar M.G., Sen S., Datta A., Patwari G.N., Murugavel R., (2014). "Selective fluorescence sensing of polynitroaromatic explosives using triaminophenylbenzene scaffolds", Physical Chemistry Chemical Physics, 16, 10651-10658.

[87] Hussain S., Malik A.H., Afroz M.A., Iyer P.K., (2015). "Ultrasensitive detection of nitroexplosive - picric acid via a conjugated polyelectrolyte in aqueous media and solid support", Chemical Communications, 51, 7207-7210.

BIOGRAPHY

Enis TAŞCI was born in Devrek, Zonguldak, Turkey, in 1987. He graduated from Devrek Anatolian High School in 2005. In the following year, he was admitted to Giresun University, Department of Chemistry. After his graduation in 2010, he was accepted as a M.Sc. Student to Gebze Institute of Technology, Institute of Science, Department of Chemistry where he obtained M.Sc. degree in 2012. At the same year, he was registered as a Ph.D. student to Gebze Technical University, Graduate School of Natural and Applied Sciences, Depeartment of Chemistry. From 2012, he was a researcher in Giresun University Central Research Laboratory and Application and Research Center (GRUMLAB).

APPENDICES

Appendix A: Mass Spectra of Small Compounds

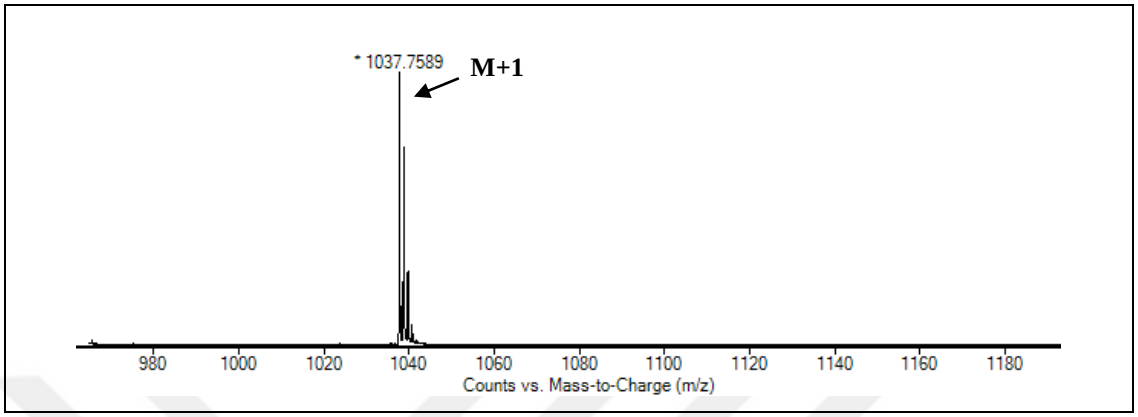

Figure A 1.1: Mass spectra of compound **2**.

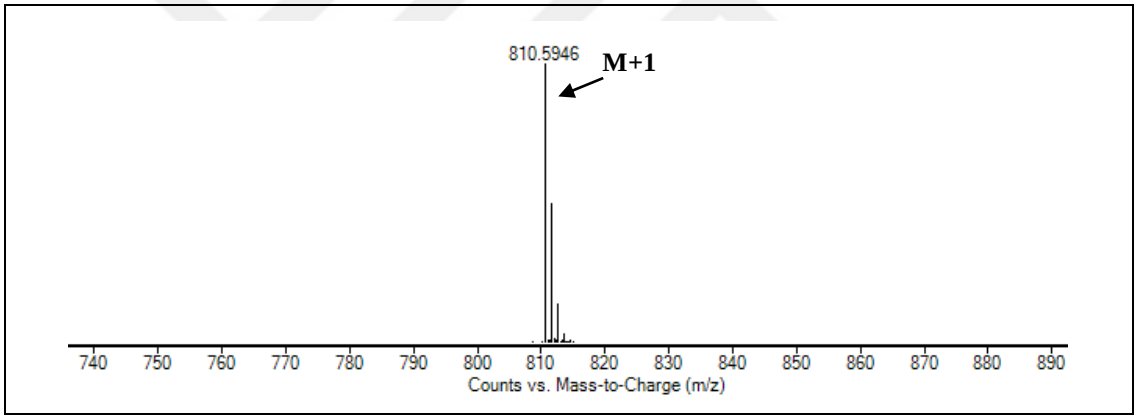

Figure A 1.2: Mass spectra of compound **4**.

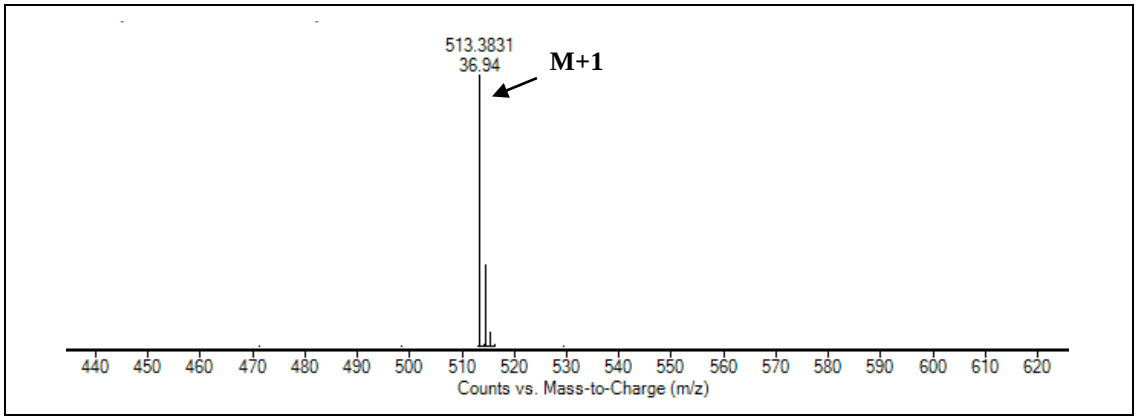

Figure A 1.3: Mass spectra of compound **6**.

Appendix B: Fluorescence Emission Quenching Spectra of Polymers

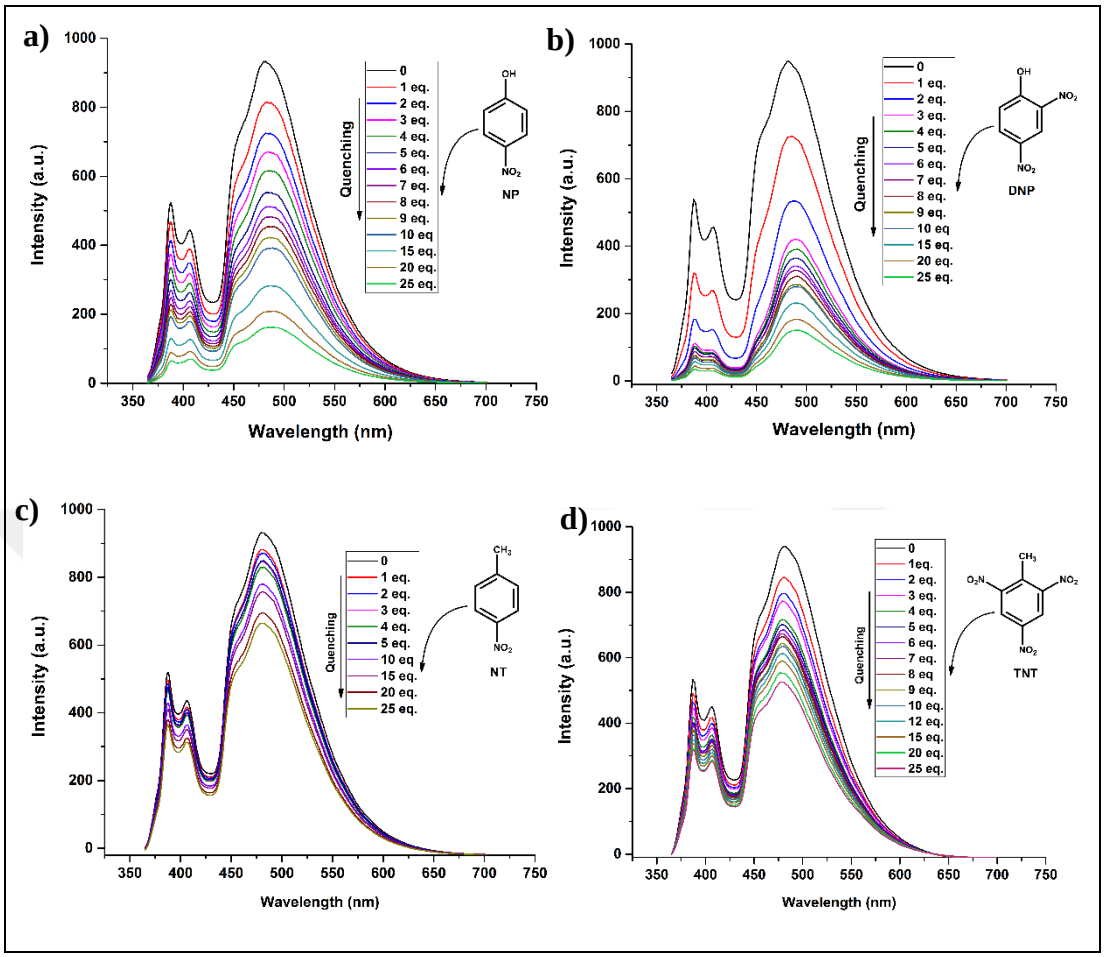

Figure B 1.1: Quenching ratios of **P3-a** in the presence of increasing concentrations of a) NP, b) DNP, c) NT, d) TNT in DMF at room temperature.

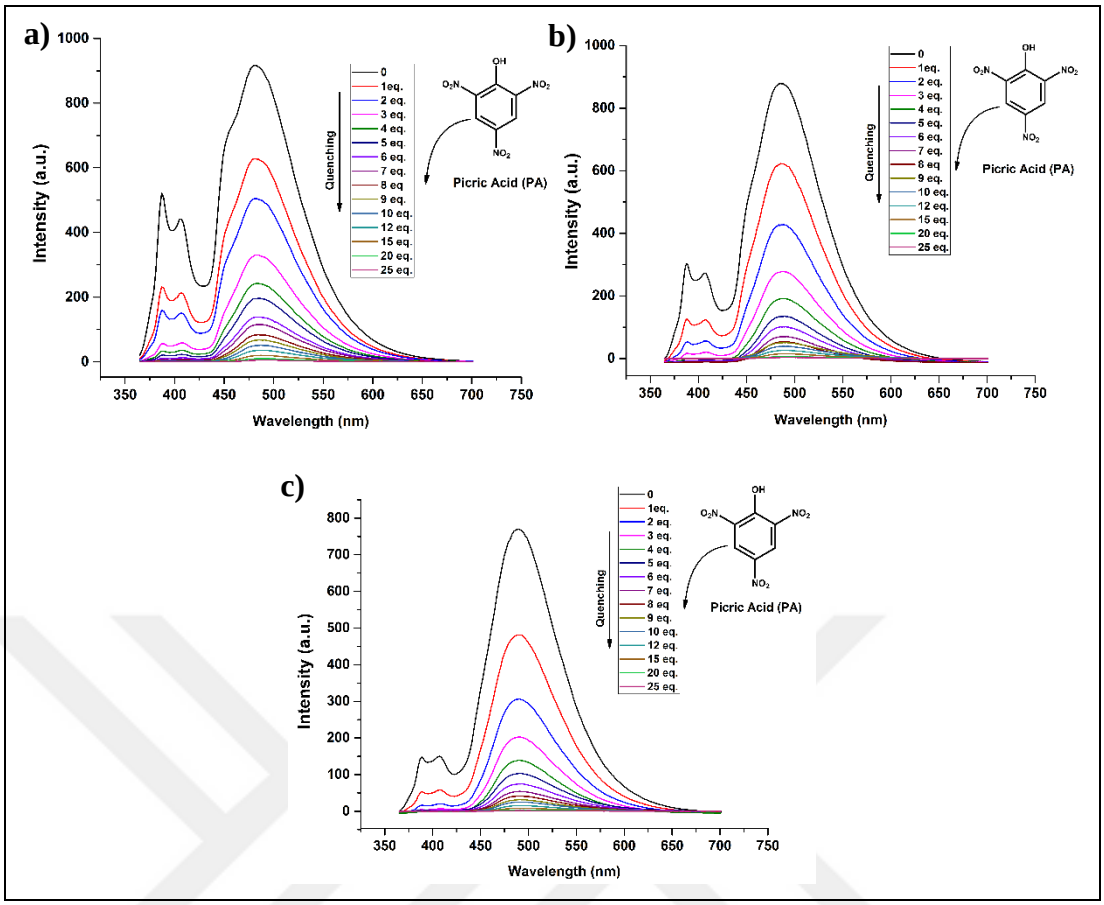

Figure B 1.2: Quenching ratios of a) **P3-a, b) P3-b,** c) **P3-c** in the presence of increasing concentrations of PA.

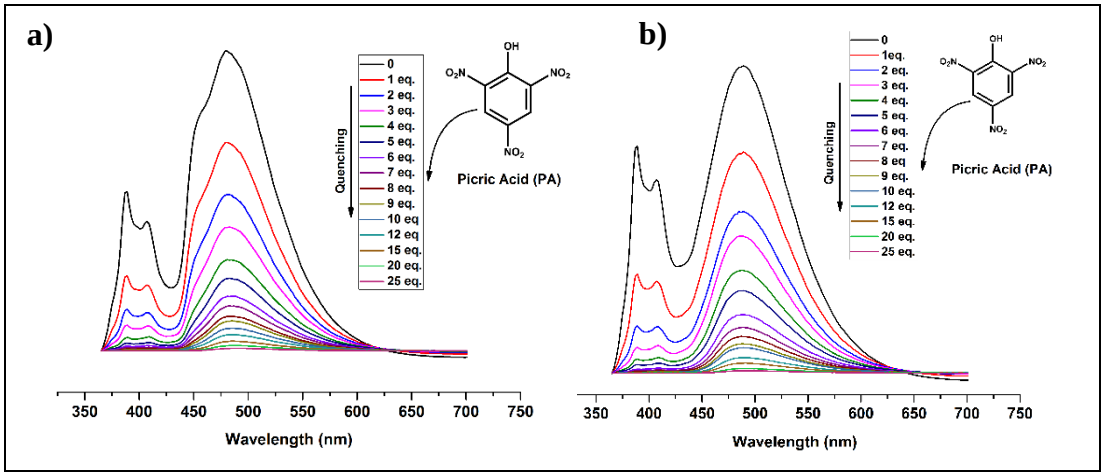

Figure B 1.3: Quenching ratios of a) **P6-a**, b) **P9-b** in the presence of increasing concentrations of PA.

Appendix C: Published Journals and Conference Presentations from Doctoral Thesis

Enis Tasci, Muhammet Aydin, Mesut Gorur, Ayşe Gül Gürek, Faruk Yilmaz, "Pyrene-Functional Star Polymers as Fluorescent Probes for Nitrophenolic Compounds" Journal of Applied Polymer Science, Accepted, Manuscript Number: app.20173042R1

Enis Tasci, Muhammet Aydin, (2016), "Piren Fonksiyonlu Yıldız-Şekilli Stiren Kopolimerlerinin Sentezi ve Nitroaromatik Bileşiklere Karşı Floresans Sensör Özelliklerinin İncelenmesi**"** III. Ulusal Organik Kimya Kongresi, Trabzon, Turkey 5-8 September.